THE FRACTURE TOUGHNESS OF LOW ALLOY STEEL

A Thesis Submitted at The University of Aston in Birmingham for the Degree of Doctor of Philosophy

Philip Terry B.Sc.

MARCH 1972

SUMMARY

The fracture resistance of pipeline steel in the as received condition and after welding is investigated using the crack opening displacement approach. The object of the work is firstly to examine the C.O.D. concept to determine its applicability as a measure of the toughness of a ductile material. If possible, the technique will then be used to assess the toughness of the parent plate and the weld heat affected zone in pipeline steel, in an attempt to provide information for the safe operation of natural gas pipelines.

The introduction contains a discussion on the natural gas pipeline system and of the types of steels used in its construction. The review of the literature surveys the development of fracture mechanics and the emergence of K_{Ic} as a toughness parameter, followed by the extension of fracture toughness testing into the regime of gross yielding using crack opening displacement.

The crack opening displacement approach is studied fully and modifications have been made to the technique. It is considered that these modifications make the technique more viable as applied to the particular steels under study. The modifications produce a pessimistic and probably uneconomic assessment of the material toughness in general, but it is shown that the results describe the specific case of gas pipelines very well.

The effect of a variation in angle between a moving crack and a weld is studied. Arising from this study a relationship is proposed between the opening mode C.O.D. and the shearing mode C.O.D.

Finally some estimates of critical defect size for pipe operation have been calculated.

CONTENTS

NOTATION

A	Mathematical constant
a,a'	crack lengths
B	Specimen thickness
b	distance from crack tip or atomic spacing
d	ligament depth in a specimen or heated width during welding
E	Young's Modulus
e	tensile strain
G	Strain energy release rate -(specified by subscript)
H	Rate of heat input during welding or half height of a C.T.S. specimen
K	Stress intensity factor -(specified by subscript)
n	plastic stress intensification factor or rotational constant of a bend specimen
P	Plastic work factor
Q	Flaw shape parameter
R	Radius of a pressure vessel
r	Co-ordinate from crack tip
r_y	Radius of plastic zone
S	Span of a bend specimen
T	Temperature ^{o}C
t	Plate thickness
v	Welding Velocity
W	Specimen depth
X, Y, Z	Three dimentional direction symbols
x, y	Mathematical constants
z	Distance from a specimen surface

α	thermal diffusivity
γ	Surface Energy
δ	Crack opening displacement (specified by subscript)
ϵ	Tensile strain
η	normal displacement within a slit
θ	Angle in radians
κ	Thermal Conductivity
μ	Shear modulus
ν	Poissons ratio
ρ	crack tip radius of curvature
σ	Tensile stress symbol (specified by subscript)
τ	Shear stress
( )	Figures in parenthesis refer to bibliography

1. INTRODUCTION

The discovery of commercial quantities of natural gas beneath the North Sea has revitalized the British gas industry but has however created some problems. The most important of these problems has been the distribution of the gas to the main centres of population and it has been decided that a large diameter high pressure grid (Figure 1) is the most economical under the circumstances.

The design of most engineering structures involves a compromise between several conflicting requirements and the ultimate design - philosophy reflects the combined views of the design engineer, metallurgist and accountant. High pressure, gas transmission pipelines are no exception to this, although, because of their special circumstances, particular emphasis must be placed on the safety aspects and this normally leads to some uneconomic penalties.

The introduction of grain refined, high yield strength steels has however resulted in both technical and financial gains. The benefits derive from the increase in the permissable operating stresses and the corresponding increased gas carrying capacity through the use of large diameter pipes and the use of the lines to store gas during periods of low consumption. The technical benefits derive from two sources, firstly the improvement in the inherent toughness and the weldability and secondly from the benefits to these properties of the use of thin walled pipes.

Figure 1

Natural Gas Transmission System

A large number of factors have to be considered in the design and construction of a high pressure gas pipeline, and three particularly important factors namely strength, toughness and weldability, are related to the properties of the steel selected. The question of toughness is at the moment the factor least understood and it is the purpose of this thesis to examine this property closely, both the factors which influence toughness and the accurate assessment of it.

United Kingdom pipeline is purchased to American Petroleum Institute (A.P.I.) 5LX specifications[1] which are based on minimum yield strength levels, their numerical designations 5LX 42, 5LX 46, 5LX 52 and 5LX 60 classify yield strength in thousands of pounds per square inch. The grades in use in the U.K. are in the main 5LX 52 and 5LX 60 which for brevity will be referred to as X52 and X60. These steels were selected because a great deal was already known about their properties.

Research work, on 5LX steels, was begun by the American Gas Association (A.G.A.) in the early 1950's they studied the fracture resistance of line pipe after a number of long breaks had occurred in a large diameter line during gas pressure test after construction. This work which was mainly concerned with the propagation of cracks in line pipe has been described by McClure et al[2]. Based on the findings of this work the

Gas Council feel that the possibility of long brittle failures has been eliminated by the introduction of the Drop Weight Tear Test (D.W.T.T.)[3] into the specification of U.K. gas pipelines. The propagation of shear fractures is at present under study by the A.G.A.[4] and the Gas Council[5] who are both working towards the introduction of a standard to prevent shear fracture propagation. The Gas Council will probably base their standard on the Charpy shear shelf energy since there appears[5] to be good correlation between this property and resistance to shear fracture propagation.

Even though the possibility of cleavage and shear cracks is being eliminated from pipeline materials it cannot necessarily be assumed that crack initiation in regions of low toughness is also eliminated. In practice failures have occurred in pre-service hydrostatic tests and the majority of these failures have been associated with the seam welds in longitudinally welded pipe and in particular with the heat affected zone (H.A.Z.) of these welds. Consequently a more intensive study of the problems of crack initiation and in particular crack initiation associated with weld H.A.Z.'s is required.

With this data it ought then be possible to calculate critical defect sizes for the most brittle part of a pipeline at operating stresses.

2. LITERATURE SURVEY

2.1 General

The most usual method of deriving the stress that can be supported by a component made in low strength steel (i.e. a steel with a yield stress of less than about 50 tons/sq.in.) is to apply a safety factor to the steel's strength as measured in the uniaxial tensile test. The main difficulty with this procedure, apart from the arbitrary nature of the safety factors, is that the working stress can only be raised by using a steel of greater uniaxial strength, which usually implies a reduction in uniaxial ductility and a large reduction in notch toughness. It is with this last factor that a designer is most concerned, because any component in service is bound to contain some sort of notch, whether external (design Keyway, fillet etc.) or internal (e.g. caused by the presence of inclusions).
Conventional methods for dealing with notch toughness rely on the measurement of the energy required to break a specimen in notched impact (e.g. Charpy or Izod test): values of energy are obtained over a range of temperatures, and steels are graded in terms of their transition temperatures. Thus, a steel with a low transition temperature is regarded as 'better' than a steel with a higher transition temperature.

This practice has two main disadvantages. Firstly, there is no reason for supposing that the conditions of high strain rate and moderate notch severity which are present in the notched impact test are even approximately equivalent to those existing at crack initiation in service where the strain rates are often low and the notch severity high. The order in which steels are graded, having regard to their impact transition temperatures, may not, therefore, be the same as that based on the steels' toughness under service conditions. Secondly, even if the orders were identical, an approach based on temperatures alone is of little use in calculating the applied stress that a notched body can tolerate without failure.

Although there is some merit in the use of a specific value of impact energy at some particular temperature to designate toughness (e.g. the B.S. 2742, ND1 acceptance standard of 20 ft. lb. at $0^{o}C$), this can only be used when substantial background information on a steel has been acquired. It is of less value for a newly developed steel, because there is no guarantee that previous empirical correlations between impact energy and service performance are still valid. Again, this approach can really only be used to grade steels, an impact energy value cannot be used directly in design

calculations. Design engineers need a value of a steels' toughness which is representative of its performance under the worst conditions that could exist in service, and which can be used in design calculations to determine the maximum applied stress that the component can tolerate without failure.

2.2 Fracture Toughness Theories

Tests designed to obtain toughness values of direct applicability to structures date from the classical work of Griffith[6] on the fracture of glass.

Griffith using the Inglis[7] solution for the stresses and strains around a crack, postulated that there is an energy balance between the stored elastic energy in a cracked body and the energy required to create new crack surfaces. The crack will spread if the decrease in the stored elastic energy is greater than the increase in surface energy. This gives rise to Griffiths' well known equation:

$$\sigma_a = \sqrt{\frac{2E\gamma}{\pi a}} \quad \ldots\ldots\ldots\ldots\ldots (1)$$

Where σ_a is the applied stress, E the elastic modulus, γ the surface energy per unit area and a the crack half length.

The crack can spread if the stress σ_a is exceeded so equation (1) gives the fracture stress σ_F in the presence of a crack.

The strength of a body containing a crack can also be treated directly in terms of the stresses[8] The highest tensile stress (which occurs at the end of the major axis) is given by:

$$\sigma_{max} = 2\,\sigma_a \left(\frac{a}{\rho}\right)^{\frac{1}{2}} \quad \ldots\ldots\ldots\ldots\ldots\ldots \quad (2)$$

Where ρ is the radius of curvature at the end of the crack[7]. The value of ρ for the sharpest crack will be of the order of the atomic spacing b. Substituting b for ρ in equation (2) the fracture strength can be shown to be:

$$\sigma_F = \left(\frac{E\gamma}{4b}\right)^{\frac{1}{2}} \quad \ldots\ldots\ldots\ldots\ldots\ldots \quad (3)$$

Comparison with the observed strength of glasses containing artificial defects is satisfactory. However when an attempt is made to use the Griffith theory on even the most brittle of metals the calculated values of strength for given defect lengths are in error by an order of magnitude.

Orowan [9] suggested that the Griffith equation could be made more compatible with brittle fracture in metals by the inclusion of a term P, expressing the plastic work required to create new surfaces, since observation had shown evidence of a thin layer of plastically deformed material when a metal which had fractured in a brittle manner was examined by X-ray diffraction. The relationship between fracture stress and crack length becoming:

$$\sigma_F = \frac{2E(\gamma + P)}{\pi a}^{\frac{1}{2}}$$

which since γ is approximately two order of magnitude less than P can be reduced to:

$$\sigma_F \simeq \left(\frac{EP}{a}\right)^{\frac{1}{2}} \quad \ldots\ldots\ldots\ldots\ldots\ldots \quad (4)$$

2.3 Linear Elastic Fracture Mechanics

In the Irwin[10] development of Griffith's theory the surface energy term is replaced by an experimentally determined "strain energy release rate" or "crack extension force" G, since the crack extension process requires a fixed rate of dissipation of energy. By definition G, measured in units of in. lb/in^2, is the quantity of stored elastic strain energy released from a cracking specimen as the result of the extension of an advancing crack by unit length. In these terms, the unstable propagation of a crack is associated with a critical value of G, such that the release of strain energy, as the crack extends, just exceeds the rate of energy dissipation needed for the creation of the new crack surface. The critical value, designated G_{Ic} or G_c according to whether the unstable condition is associated with plane strain or plane stress conditions, is known as the "fracture toughness". The subscript I refers to the opening mode of crack behaviour. It is convenient to describe three kinematic movements of crack surfaces relative to one another. These

displacement modes are illustrated in Figure 2 and a tearing mode III. These three modes are sufficient to describe all possible modes of crack behaviour. Any particular problem may be treated as one or a combination of these modes. The emphasis here shall be placed initially on the opening mode, which corresponds to the usual case of tensile loading and many others. Plane strain conditions apply to opening mode or cleavage-type fractures in which the fracture surface is flat and normal to the applied stress, while plane stress conditions are associated with an oblique shear mode of fracture, occurring predominantly in thin sheets. These conditions are shown schematically in Figure 3. In both cases the fracture toughness represents the work which is irreversibly absorbed in local plastic flow and cleavage in the creation of a unit area of fracture surface. For a crack of length 2a in an infinitely wide plate the relationship between the critical fracture stress and G_c is given by:

$$\sigma_F = \left(\frac{EG_c}{\pi a}\right)^{\frac{1}{2}} \quad \ldots\ldots\ldots\ldots\ldots\ldots \quad (5)$$

This is a simple relationship, but the concept of a fracture toughness in terms of a strain energy release rate has a number of drawbacks, principally because it is associated with the imperfectly understood "surface energy". The approach of linear

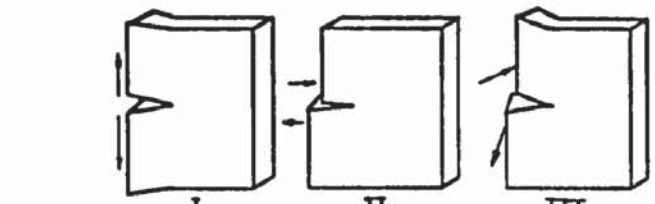

a) ELEMENTARY MODES OF CRACK TIP MOVEMENT DISPLACEMENT

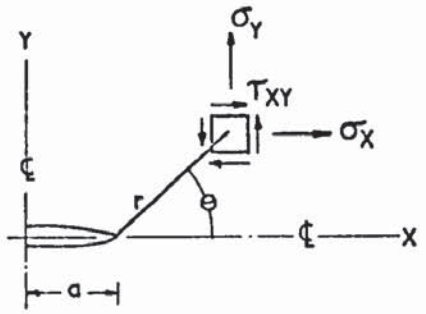

b) COORDINATES FOR ELEMENT NEAR CRACK TIP WITH SYMMETRICAL LOADING

$$\sigma_X = \frac{K}{\sqrt{2\pi r}} \cos\frac{\theta}{2}\left[1-\sin\frac{\theta}{2}\sin\frac{3\theta}{2}\right]$$

$$\sigma_Y = \frac{K}{\sqrt{2\pi r}} \cos\frac{\theta}{2}\left[1+\sin\frac{\theta}{2}\sin\frac{3\theta}{2}\right]$$

$$\tau_{XY} = \frac{K}{\sqrt{2\pi r}} \sin\frac{\theta}{2}\cos\frac{\theta}{2}\cos\frac{3\theta}{2}$$

PLANE STRESS $\tau_{XZ} = \tau_{YZ} = 0$
$\sigma_Z = 0$

PLANE STRAIN
$\varepsilon_Z = 0$
$\sigma_Z = \mu(\sigma_X + \sigma_Y)$

c) STRESS FIELD EQUATIONS - OPENING MODE I

Figure 2

Fundamentals of Linear Elastic Fracture Mechanics

elastic fracture mechanics (L.E.F.M.) is more attractive since it is based on the concept that the local stress field near the crack can be expressed in terms of a single stress field parameter, the stress intensity factor K, which for the fully linear elastic situation is simply related to the strain energy release rate G. The relationship being, for plane stress.

$$K^2 = EG \quad \ldots\ldots\ldots\ldots\ldots \quad (6)$$

and for plane strain

$$K^2 = \frac{EG}{(1-\nu^2)} \quad \ldots\ldots\ldots\ldots\ldots (7)$$

The attainment of a critical stress intensity factor is a necessary and sufficient condition for cracking and has the considerable advantage that if failure occurs under a critical stress, then a Griffith type relationship results without consideration of any energy dissipation processes involved. It also characterizes a stress field which can be used to estimate the size of the plastically deformed region ahead of the crack; furthermore, calibration equations, expressing K in terms of the applied load and the individual specimen geometry, can be determined.

Westergaard's[11] stress field equations are used to express the local stresses near the tip of the crack using a mathematical model of the crack as a flat, internal, free surface in a linear

Figure 3

Slant and Square Fractures as a Result of the State of Stress.

elastic solid. In these equation σ_Y is expressed in terms of the polar co-ordinate system as shown in Figure 2. The equation for the normal stress is:

$$\sigma_Y = \frac{[K \cos(\theta/2)][1 + \sin(\theta/2)\sin(3\theta/2)]}{(2\pi r)^{\frac{1}{2}}} \quad \ldots\ldots(8)$$

For a crack of length 2a in an infinitely wide plate:

$$K = \sigma (\pi a)^{\frac{1}{2}} \quad \ldots\ldots\ldots\ldots\ldots\ldots(9)$$

The subscript terminology for the stress intensity factor K is identical with that used for the strain energy release rate G. The critical value of K under plane stress conditions is designated K_c, the plane stress fracture toughness of the material, while the stress intensity factor under plane strain conditions is K_I, and at the onset of unstable fracture this is termed the plane strain fracture toughness K_{Ic}.

Since the plane strain fracture toughness represents the minimum value of the critical stress intensity, it is the more important quantity from the standpoint of brittle fracture in mild steels. There is however, no a priorimethod of anticipating the plane stress or plane strain fracture toughness from a given test although the recent A.S.T.M. recommendations [12] for K_{Ic} specimen geometry take this problem into account, and have reduced the

uncertainty by tabulating approximately valid K_{Ic} values for given yield stress levels. Figure 4 indicates schematically the fracture mode transition from plane stress to plane strain which results from increasing thickness, expressed in terms of a change from K_c to K_{Ic}. Plane strain conditions are favoured by increasing specimen size and are accompanied by a corresponding decrease in the size of the plastic zone. A formal representation of the plastic zone at the front of a through-thickness crack is shown in Figure 5 for a situation in which plane stress conditions apply at the surface and plane strain in the interior.

The presence of a plastic zone introduces an error into the determination of the stress intensity factor, the magnitude of the error being a function of the relative volumes of the plastic and elastic materials. In brittle materials the plastic volume is small, but in low strength structural steels such as X-52, the plastic volume could be very large. Such a large plastic zone nevertheless denotes desirable crack toughness and represents a conservative appreciation of the fracture situation since the fracture toughness is underestimated unless a plastic zone correction factor is employed.

The stress analysis becomes unacceptably inaccurate for applied stresses, σ_a, greater than about half the general yield stress σ_{GY} (defined as the stress at which plasticity has first completely

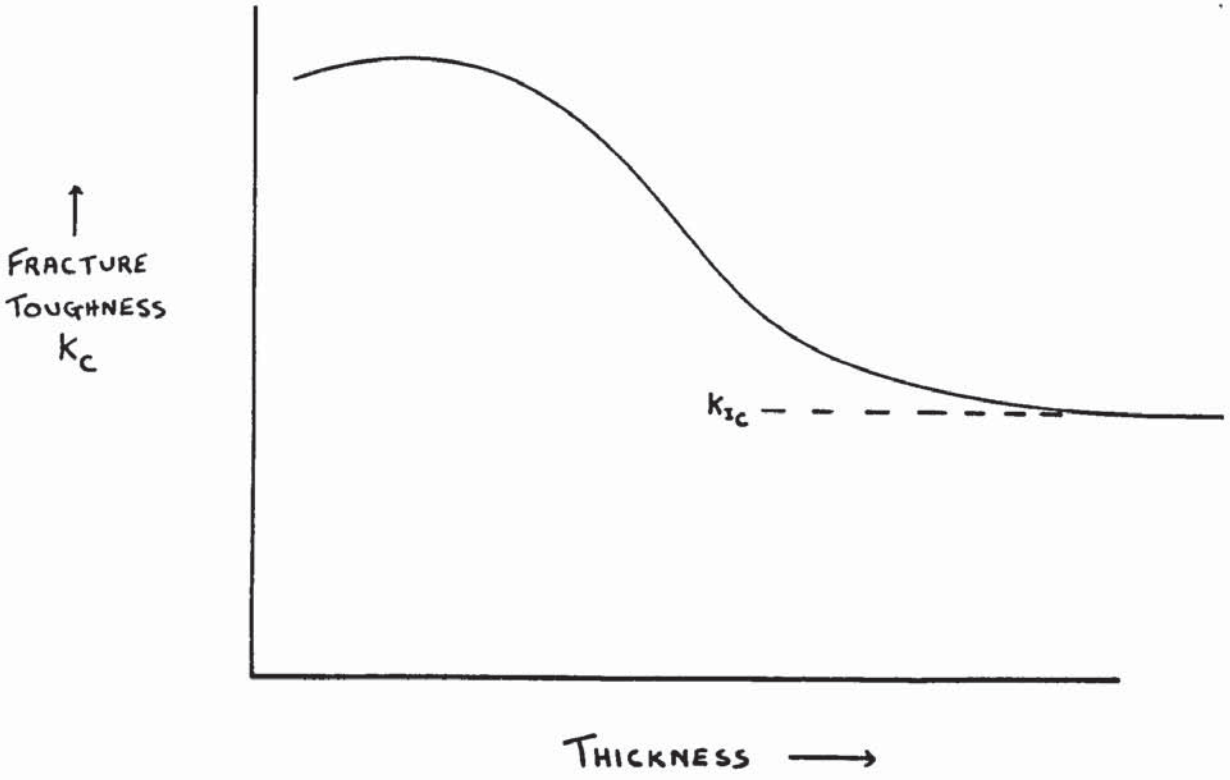

Figure 4

General Form of the Variation of Toughness with Thickness.

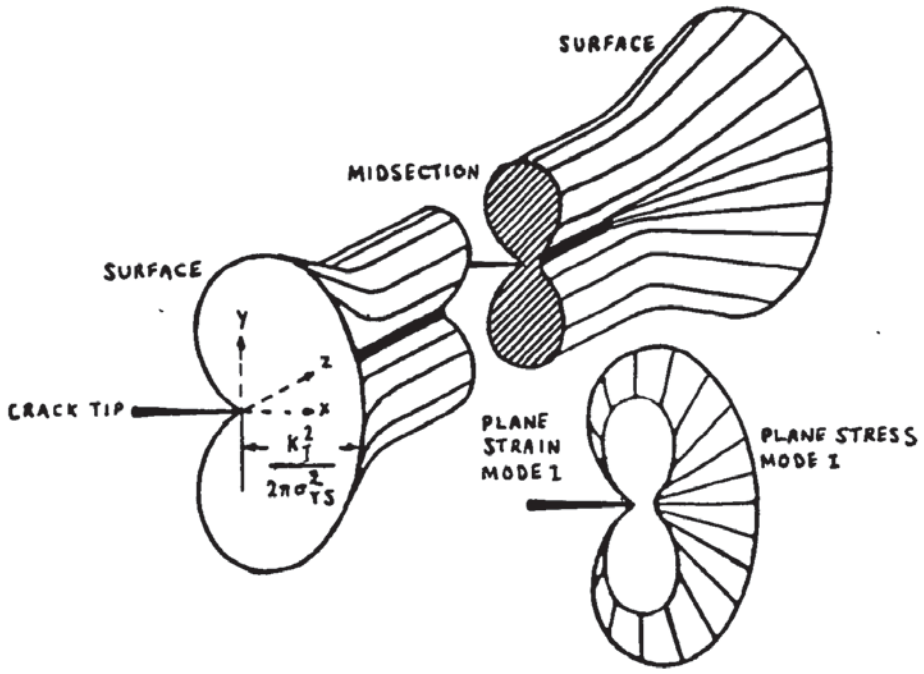

Figure 5

Schematic View of the Plastic Zone
Ahead of a Crack.

traversed the net section of the test piece). The stress analysis may be modified in the following way[13] to extend the range of applicability up to $\sigma_a/\sigma_{GY} \simeq 0.8$. Referring to Figure 6, consider a crack of length a subjected to an applied stress σ_a in mode I. The longitudinal stress across the cracking plane, σ_{YY}, is given by:

$$\sigma_{YY} = \frac{K}{(2\pi x)^{\frac{1}{2}}} \quad \ldots\ldots\ldots\ldots\ldots \quad (10)$$

(shown in Figure 6A). A simple model of the stress distribution when yielding is allowed to occur is shown in Figure 6B: $\sigma_{YY} = \sigma_y$ (the uniaxial yield stress) from $x = 0$ to $x = r_y$ (the extent of the plastic zone) and elastic values from $x > r_y$.

To determine r_y, suppose as in Figure 6A, that the point is found at which the elastic stress σ_{YY} equals the yield stress σ_y, i.e. putting $x = r_y$. Then:

$$\frac{K}{(2\pi r_y)^{\frac{1}{2}}} = \sigma_y$$

$$r_y = \frac{K^2}{2\pi\sigma_y^2} \quad \ldots\ldots\ldots\ldots\ldots \quad (11)$$

or from equation (9)

$$r_y = \frac{\sigma_a^2\, a}{2\,\sigma_y^2} \quad \ldots\ldots\ldots\ldots\ldots \quad (12)$$

However, the stress represented by the unshaded area in Figure 6A about the line $\sigma = \sigma_y$ and between the σ_{YY} line and the stress ordinate will produce further yielding. Since this area is equal to that of the shaded area below the line $\sigma = \sigma_y$ i.e.

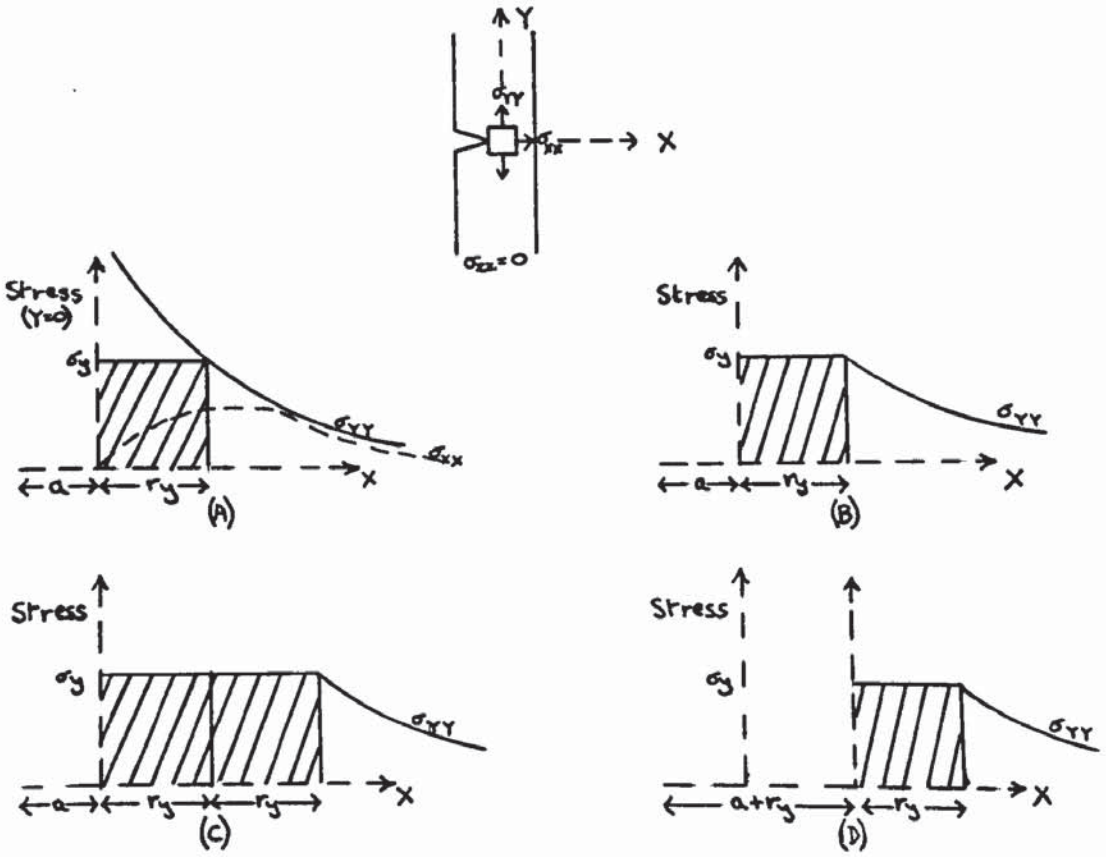

Figure 6

Derivation of Notional Crack Length $a' = a+r_y$.

$$\int_0^r \frac{K}{(2\pi x)^{\frac{1}{2}}}\,dx - \sigma_y r_y = \sigma_y r_y = \frac{K}{(2\pi r_y)^{\frac{1}{2}}}$$

the size of the plastic zone required to support all the load is given by $2r_y$ where r_y is defined as in equations (11) or (12) and this can be seen in Figure 6C. To represent the required stress distribution indicated in Figure 6B, use is made of the "notional" crack of length $a' = a + r_y$ as in Figure 6D. Equation (5) then becomes:

$$\sigma_F = \left(\frac{EG_c}{\pi a'}\right)^{\frac{1}{2}} = \left(\frac{EG_c}{\pi a(1+\sigma_F^2/2\sigma_y^2)}\right)^{\frac{1}{2}} \quad \ldots\ldots \quad (13)$$

Even with this correction for local plasticity around the crack tip, the maximum value of σ_F/σ_{GY} for which the fracture toughness approach is applicable is only about 0.8. This has restricted its use to fairly brittle materials, where fracture can be obtained well before general yield in a test specimen of moderate size. For ductile, low strength materials, such as X-52, the problem is more complex. Here, a relationship between applied stress and toughness for the case of fracture before general yield is required so that rational design of large structures can be achieved, but the appropriate toughness value must be deduced from measurements made on test specimens of convenient size, which will of necessity break after general yield, since the material is ductile. Since measurements of applied stress have

little meaning when fracture occurs after general yield, an alternative measure must be sought. The most attractive parameter available seems to be the crack opening displacement (C.O.D.)

2.4 General Yield Fracture Mechanics Crack Opening Displacement

The concept of C.O.D., suggested independently by Wells[13] and Cottrell[14], relies on the principle that the amount by which a sharp crack opens prior to fracture depends only on the local fracture ductility of the material, and does not depend on whether the fracture occurs before or after general yield. The only limitation is that the constraint, i.e. the hydrostatic component of stress, is the same in both cases. This opening, the C.O.D. is therefore as fundamental a material property as, for example, yield stress.

Bilby et al[15] have considered the approach theoretically. For mathematical simplicity they chose the case of a two dimensional slit in an infinite body subjected to an overall shear stress of σ, which produces yield zones spreading symmetrically outwards in its own plane. Although much simpler geometrically than the kinds of notches and yield zones encountered in service, it was expected that this would nevertheless indicate what is expected to happen in these cases.

Letting x and a be the distances to the end of the plastic zone and slit, respectively measured from the centre line, letting δ be the plastic displacement at the crack tip, and letting the applied stress σ be measured in units of shear stress for general yield σ_y. Bilby et al showed that in the limit of small stresses ($\sigma < 0.5$)

$$\sigma = \left(\frac{2\mu\sigma_y\delta}{\pi a}\right)^{\frac{1}{2}} \quad \ldots\ldots\ldots\ldots\ldots \quad (14)$$

where μ is the shear modulus. This is significant because $\sigma_y\delta$ is the plastic work done in shearing unit area of the yield zone to produce displacement δ. If δ is identified with the displacement to produce ductile fracture, then referring to equation (1)

$$\sigma_y\delta = 2\gamma$$

the effective surface energy for fracture, or alternatively referring to equation (5)

$$\sigma_y\delta_c = G_c \quad \ldots\ldots\ldots\ldots\ldots \quad (15)$$

Wells[16] has also deduced the relationship in equation (15) by a different route, he considered a sharp slit of length 2a in an infinite plate under a uniform tensile stress σ as in Figure 7. Using the Irwin[17] analysis of stresses and strains near a crack tip the expression for the normal stress on the crack plane is

$$\sigma_{YY} = \frac{\sigma x}{(x^2-a^2)}, \quad x > a \quad \ldots\ldots\ldots \quad (16)$$

Figure 7

Crack Tip and Plastic Zone

(After Wells[16])

for use in linear elastic fracture mechanics this is conveniently approximated to

$$\sigma_{YY} = \sigma\sqrt{\frac{a}{2r}} = \sqrt{\frac{EG}{2\pi r}} \quad , \; r << a \; \ldots\ldots\ldots (17)$$

where r is the distance from the crack tip. Similarly the expression for the normal displacement within the slit

$$\eta = \frac{2\sigma}{E} (a^2 - x^2)^{\frac{1}{2}} , \quad x < a \; \ldots\ldots\ldots\ldots (18)$$

may be approximated to

$$\eta = \frac{2\sigma}{E} (2ar)^{\frac{1}{2}} = 2\sqrt{\frac{2Gr}{\pi E}}, \quad r << a \; \ldots\ldots (19)$$

where r is now measured in the opposite direction.

Using the idea of a notional crack length as described earlier the effective crack can be taken as extending to $a' = a + r_y$ and the real crack experiences an opening $\delta = 2\eta y$ for $r = r_y$ that is at the real crack tip. Substituting the value of r_y, from (17) and (19).

$$\delta = 2\eta y = \frac{4\sigma^2 a'}{E\sigma_y} = \frac{4G_I}{\pi\sigma_y} \; \ldots\ldots\ldots\ldots\ldots (20)$$

where G_I is the corresponding crack extension force allowing for notional crack lengthening. Omitting the subscript, equation (20) may be rewritten as

$$G = \frac{\pi}{4} \sigma_y \delta$$

$$\text{or} \quad G \simeq \sigma_y \delta$$

and this permits new insight into the moving crack situation. The crack faces at the tip of the real crack are visualised as being stretched the distance δ normal to the crack plane, progressively as the crack tip passes a fixed point, while fracture occurs when the extension δ is exceeded. From energy consideration it is possible to specify that $G > \sigma_y \delta$ since it is feasible that more irreversible work might be done within the plastic zone than corresponds with the extension δ alone. More recently Wells[18] has shown that the relationship between δ and G is of the form $G_c = n\sigma_y \delta_c$ where n is a plastic stress intensification factor, which is approximately 1 for plane stress and 2 for plane strain.

Equation (15) with the equality, will be considered exclusively. For the time being, the discussion will be confined to plane stress in which the stress σ_y is not supplemented by a triaxiality factor.

If δ is now specified, it may be noted from equations (15) and (17) that:

$$r_y = \frac{\delta E}{2\pi\sigma_y} = \frac{\delta}{2\pi e_y} \quad \ldots\ldots\ldots\ldots\ldots\ldots (21)$$

where e_y is the overall tensile strain at incipient general yield. Moreover again substituting $a + r_y$ for a, r_y for r and σ_y for σ_{YY} in equation (17)

$$\frac{2\pi e_y a}{\delta} = \frac{a}{r_y} = 2\left(\frac{\sigma}{\sigma_y}\right)^2 - 1, \ \sigma<\sigma_y \quad \ldots\ldots\ldots (22)$$

For an elastic/plastic specimen with no strain hardening, the plastic boundaries are fixed at the moment when general yield intervenes. The elastic zones remain with stresses that are constant in magnitude and distribution and do not further deform with increased overall extension. In the wide tensile plate with a transverse slit, the ends of the latter are joined to the outer boundaries by yield zones and the remaining elastic zones are small in extent. Nevertheless at incipient general yield, the overall tensile strain is still e_y. It is appropriate to assume, that the C.O.D. δ will be directly proportional to overall tensile strain e after general yield has been reached. Retaining the notional plastic zone dimension r_y of equation (21), equation (22) then becomes, after incipient yield.

$$\frac{2\pi e_y}{\delta} a = \frac{a}{r_y} = \frac{e_y}{e}, \quad e > e_y \qquad \ldots\ldots\ldots\ldots\ldots (23)$$

or, more particularly

$$\delta = 2\pi e a \qquad \ldots\ldots\ldots\ldots\ldots\ldots\ldots\ldots (24)$$

Equations (23) and (24) in combination permit δ and r_y to be calculated for a given observed slit length over the whole range of specimen extension from low applied stress to advanced general yield.

Wells has shown empirically that in wide plate tension and bend tests of many 3 inch thick mild steel specimens containing initial notches of widely

varying lengths, the C.O.D.'s are sensibly constant for brittle fracture initiation at low temperatures, whether the fractures occur above or below general yield. The displacements so measured increased with temperature. The notches were machined and finished by cutting with a 0.006 inch jeweller's saw for 0.100 inch to simulate a natural defect.

Burdekin and Stone [19] have extended Wells' [16] load balance approach by incorporating Westergaard [11] type stress functions in their theoretical analysis of C.O.D.

Figure 8 shows the model employed for this analysis, which is based on a real crack of length 2a in an infinite plate. A system of co-ordinates is taken such that the origin lies at the centre of the crack, with the x-axis extending along the line of the crack. Under a uniform stress σ applied in the Y direction at infinity, plastic zones are produced at the tip of the crack extending to $x = \pm a'$. This situation is represented for the purpose of analysis by a crack of length 2a' which is surrounded by an entirely elastic stress field when under load, but which is stressed not only by the externally applied stress σ, but also by a series of internal tensile stresses in the Y direction of magnitude σ_b at $x = b$ in the region $\pm a < \pm b < \pm a'$ The stresses applied within the crack length 2a' represent the stresses in the plastic zone at the tip

Figure 8

Schematic Crack Tip and Plastic Zone (After Burdekin and Stone[19]).

of the real crack and for the purposes of this analysis will be taken as constant and equal to the uniaxial tensile yield stress of the material σ_y. This model is then similar to that originated by Barenblatt[20] and later employed by Dugdale[21] and by Bilby et al[22]. Thus by means of a combination of perfectly elastic solutions for stresses and displacements around a central crack in an infinite plate, the real situation of a crack with local plasticity is replaced by one which can be conveniently analysed. Whilst this analysis may not be a rigorous plastic solution it does appear to give an answer close to that expected for an elastic/plastic material. The assumption that plastic deformation is confined to the plane of the crack would also seem to be justifiable since, for thin sheets of mild steel at least, such deformations are confined to a narrow band along the plane of the crack until the incidence of sliplines and a general yield mechanism[23,24].

The detailed analysis is given by Burdekin and Stone[19] but essentially they show that the C.O.D. δ at the tip of the real crack is, on the model employed, given by the displacement at the point $x = \pm a$ within the elastically stressed crack of length $2a'$ and is shown to be:

$$\delta = \frac{8e_y}{\pi} a \log_e \sec \left(\frac{\pi\sigma}{2\sigma_y} \right) \ldots\ldots\ldots (25)$$

where $e_y = \frac{\sigma_y}{E}$

Equation (25) is in agreement with the expressions developed using different methods by Bilby et al[15] as described earlier, apart from constants which are dependent on the assumptions made with regard to boundary conditions (i.e. plane stress, plane strain, anti-plane strain, etc.)

It is possible to relate the C.O.D. δ, to the crack extension force G, to compare this analysis with the A.S.T.M. treatment for small plastic zones[12].

Expanding equation (25)

$$\delta = \frac{8\sigma_y a}{\pi E}\left\{\frac{1}{2}\left(\frac{\pi\sigma}{2\sigma_y}\right)^2 + \frac{1}{12}\left(\frac{\pi\sigma}{2\sigma_y}\right)^4 + \frac{1}{45}\left(\frac{\pi\sigma}{2\sigma_y}\right)^6 + .\right\}$$

Taking only the first term

$$\delta = \frac{\pi\sigma^2 a}{E\sigma_y} \quad \ldots\ldots\ldots\ldots\ldots\ldots \quad (26)$$

c.f. A.S.T.M.

$$\frac{G}{\sigma_y} = \frac{\pi\sigma^2 a}{E\sigma_y} \quad \ldots\ldots\ldots\ldots\ldots\ldots \quad (27)$$

$$G = \sigma_y \delta$$

The same expression as that developed by Bilby et al[15] and Wells[16].

The results of experiments by Burdekin and Stone confirm the validity of the basic concept of a critical C.O.D. prior to fracture, again a 0.006 inch slot was used as an artificial defect.

The accuracy with which C.O.D. can be measured is very important to the usefulness of the technique. Bilby et al presented only a theoretical paper with no experimental justification, Wells however measured the C.O.D. on wide plate tension tests and bend specimens, the former by means of an optical graticule; reading across the slit, the latter by consideration of the angle of bend of the specimen. The first technique is dependent on the C.O.D. being constant through the thickness and its accuracy depends on the magnification of the optical system, while the second method has a number of inherent inaccuracies.

Burdekin and Stone attempted to refine the measurement of C.O.D. by constructing an instrument capable of continuously monitoring the C.O.D. at the tip of a fine sawcut notch as the test progressed. This instrument which they called a 'codmeter' detects the separation of the notch surfaces at the tip of the crack by the rotation of a small blade which bears on the two faces of the crack.

This instrument advanced the measurement of C.O.D. greatly but still gave some problems because of the blade sticking or not being placed at the root of the notch. It could however measure the C.O.D. at the centre of the specimen, which was found to be the same as that at the surface, within the limits of the instrument. Recently further

attempts have been made to refine the 'codmeter' and remove some of the problems[25].

Fearnehough and Watkins[26] used a photographic technique similar to that of Wells to measure C.O.D.'s during tube burst experiments. The measurements were made by reference to microhardness indentations made on either side of the flaws (0.006 inch slits) close to their tips. An image of these end-of-flaw impressions was projected via a microscope objective lens into a ground glass screen. The magnified image was photographed at various pressure increments and the C.O.D. measured from the displacement of the indentations. In this way the C.O.D. could be measured with a sensitivity of about 2×10^{-4} inch. They also calibrated the C.O.D. during bending of small notched bend specimens against the specimen deflection by means of a similar photographic technique. Thus from a knowledge of the specimen deflection at failure, the critical fracture C.O.D. could be determined. Fearnehough et al constructed calibration curves of C.O.D. versus specimen deflection similar to that shown in Figure 9.

Collaborative tests at many laboratories showed considerable scatter in tests using a 'codmeter'[27] subsequently Elliott and May[28,29] proposed a method to determine C.O.D. using a standard clip-gauge as used in linear elastic fracture mechanics testing[12]. They showed that there is a relationship between the opening of the clip gauge and that at the notch tip,

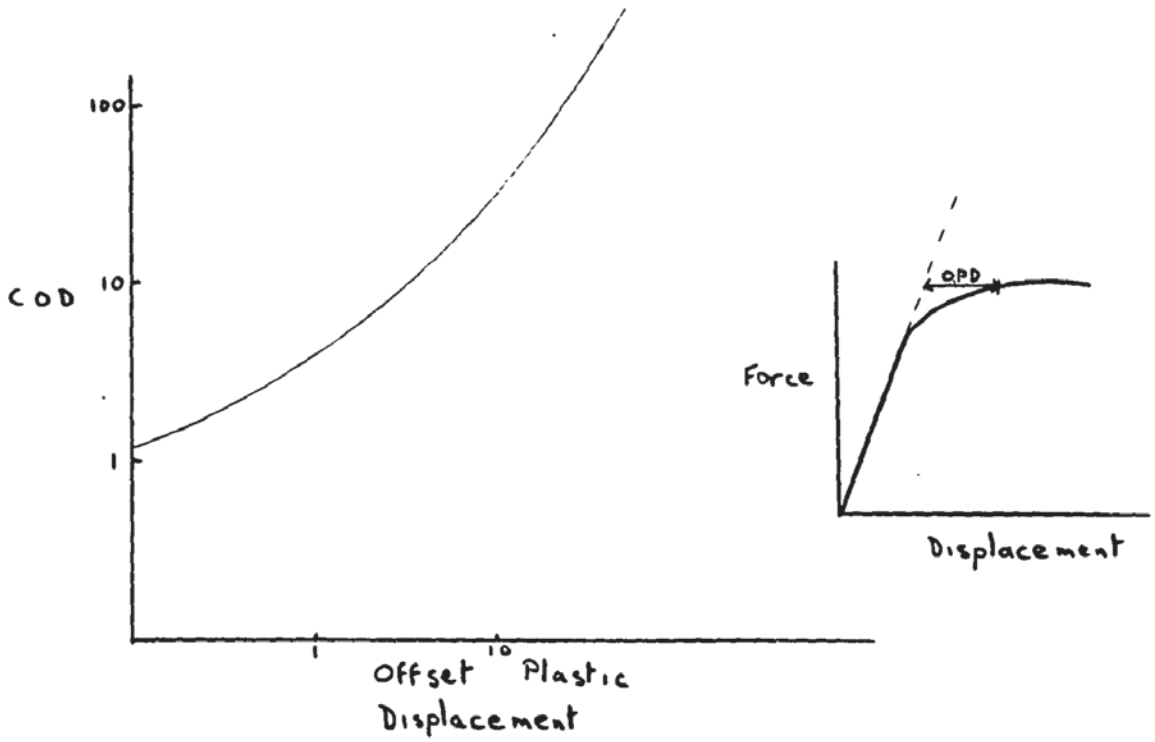

Figure 9

Crack Opening Displacement Calibration Curve

as measured by the photographic method.

Elliott and May find that to obtain the value of the C.O.D. at the tip of a crack it is necessary to consider the notch profile during loading, assuming plastic deformation occurs without crack extension and that the notch faces open as a hinge about a centre of rotation due to three point loading, as shown in Figure 10.

The C.O.D. at the crack tip δ_t can be related to the clip gauge C.O.D. δ_{CG} by a simple geometrical equation such that in the general case:-

$$\frac{\delta_{CG}}{\delta_t} = \frac{n(a+z)}{d} + 1 \quad \ldots\ldots\ldots\ldots\ldots\ldots \quad (28)$$

where n is a rotational constant determined experimentally, a the notch depth, z the position of the clip gauge above the specimen surface and d the uncut ligament depth.

Equation (28) can be rewritten in terms of a/w:

$$\frac{a}{w} = \frac{\frac{\delta_{CG}}{\delta_t} - (1 + \frac{nz}{w})}{\frac{\delta_{CG}}{\delta_t} + (n - 1)} \quad \ldots\ldots\ldots\ldots\ldots \quad (29)$$

Elliott and May have shown experimentally that a value of n approximately equal to 3 best fits the relationship for experimentally determined values of δ_{CG} and δ_t. This method because of the assumptions can only be expected to give at best a reasonable estimate of the crack tip C.O.D. However because

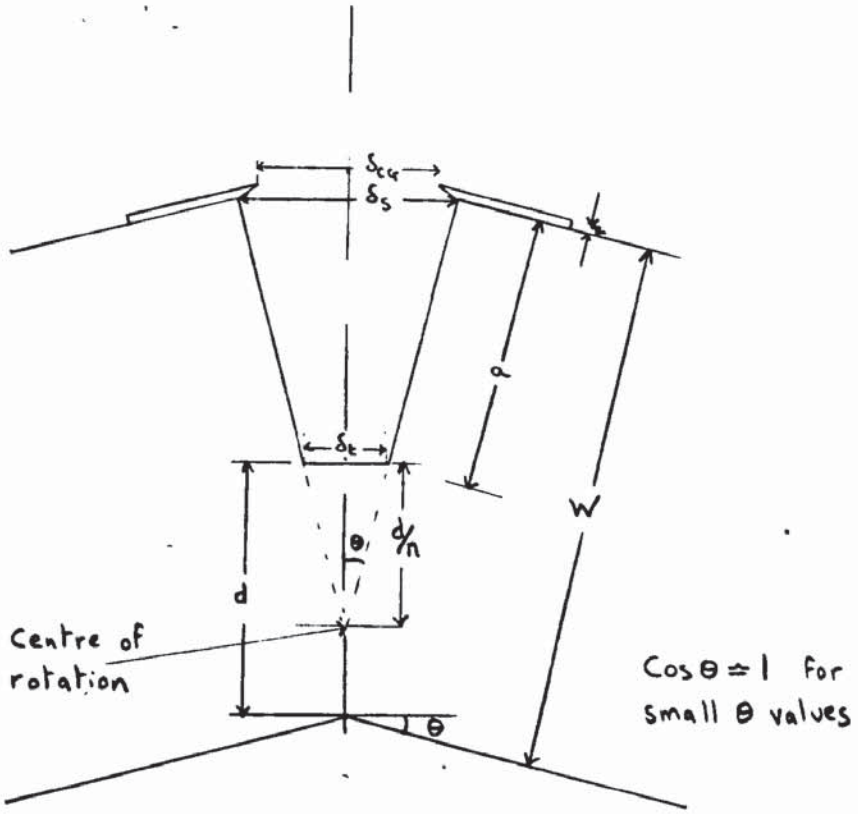

Figure 10

Model used to Relate Clip Gauge C.O.D. to Crack Tip C.O.D.

of its relative simplicity and its compatibility with L.E.F.M. testing, this method is to be put forward in the draft British Standard on C.O.D. testing[30].

It would appear that the Fearnehough and Watkins photographic technique is the best available at the moment since it can be expected to give a consistent and accurate measure of the C.O.D. Furthermore, the technique gives a measure of the C.O.D. at or very close to the elastic/plastic boundary where it is supposed to be measured[16]

Srawley, Swedlow and Roberts[31] have recently attempted to show that this elastic/plastic boundary, used as the point of measurement for C.O.D., is a variable position. Using finite elements these workers appeared to show that the C.O.D. measurement position changes radically during specimen deformation. However, Wells[32] has pointed out that at reasonable loads the C.O.D. position is fixed and that these loads are only just outside the limits for valid L.E.F.M. testing.

A great deal of use has been made of C.O.D. as a technique. Wells and McBride[33] have used it in the study of creep failure, while Burdekin et al[34] have used it to assist in selection of weldments. These and other workers[35-37] have shown it to be a reasonable measure of material toughness beyond general yield.

Thornton[38] has shown that the basic equation linking L.E.F.M. and general yield fracture mechanics namely:-

$$G = \sigma_y \delta$$

is accurate provided that the C.O.D. is measured at the correct position and at the correct point in the fracture process. Thornton used a'codmeter' to determine C.O.D. and took the critical event in the fracture process to be the appearance of a surface crack. When this value of C.O.D. is used in the above equation it gives a reasonable correlation but tends to overestimate G_c. However when a correction based on that of Marcal and King[39] which corrects the C.O.D. measured to that at the crack tip and also corrects σ_y for any stress intensification, was employed, the accuracy of the prediction greatly improved. Thornton used alloy steels which permitted the use of fairly small specimens to obtain valid K_{Ic} and hence G_{Ic} values, according to A.S.T.M. specifications[12]. However an attempt to measure G_{Ic} in the materials to which C.O.D. was designed to be applied, namely structural steels such as X-52, would require excessively large specimens i.e. a thickness of approximately 4 inch for X-52.

Since the X-52 under study is for use at ½ inch thickness it does not seem worthwhile to test such massive sections. Furthermore such a thick specimen

may fail by cleavage whereas a thin section would probably fracture in a ductile manner, thus making comparisons difficult.

A recent paper by Stonesifer and Smith[40] has however presented an opportunity to further check the relationship

$$G_c = \sigma_y \delta_c$$

using values of G_c and δ_c obtained from the same specimen of low strength steel.

A.S.T.M. Committee E-24 has set minimum specimen size limits and recommendations for test validity[12]. One recommendation is that thickness and crack length shall not be less than $2.5 \left(K_{Ic}/\sigma_y\right)^2$. This is based on results from tests on what might be considered materials of medium toughness. The committee has not yet attempted to solve the problem of materials in which the toughness K_{Ic} (Ksi$\sqrt{\text{in}}$) exceeds the uniaxial yield strength σ_y (Ksi). In such cases, as mentioned above, specimen sizes become prohibitive under the recommended practice.

A continuing effort is being made to adjust or correct values obtained from "undersized" specimens to reflect true plane strain conditions. A graphical correction method, based on the Irwin plasticity correction, has been proposed[41], but Stonesifer and Smith's latest method based on equivalent elastic fracture strain which they call the scaling method[40]

appears to work better over a larger range of specimen sizes than their earlier suggestion[41].

This new correction technique assumes that if the specimen had been of sufficient size, general yielding would not have occurred before crack propagation or instability. The total strain at failure would have been completely elastic. Failure would then have occurred at the load represented by the intersection of a line extending through the elastic portion of the load/deflection curve and a constant strain, or deflection, line through the point of crack instability. The load corresponding to this intersection is used in K_{Ic} calculation. Figure 11 illustrates the method used to determine this load. This method appears to work well on the 12% Ni Maraging steel examined by Stonesifer and Smith.

Using this approach it will be possible to calculate a G_c value corresponding to a specific C.O.D. value and hence to compare the G_c value obtained by this method and that determined through the equation:

$$G = \sigma_y \delta$$

The question of what point on the load/C.O.D. curve is to be taken as the critical point now arises. In the recent past the critical event has been taken as the maximum load point and the C.O.D. for this has been measured as the critical C.O.D.[42]. The maximum load C.O.D. probably coincides with the

Figure 11

Method Used to Determine Load Used in Scaling Method.

(Ref. [40])

critical event in the fracture process when the plastic zone size is small but does not when plasticity is extensive. Harrison and Fearnehough[43] have shown that the maximum load C.O.D. varies with specimen geometry even if the thickness is held constant, as did Knott earlier[44], hence this value has no real meaning in the absolute sense. Harrison and Fearnehough have shown that the C.O.D. for the first appearance of a surface crack in their specimens gave a lower and seemingly more constant value of the critical C.O.D. over a range of specimen sizes. Indeed this event was also taken as the critical point by Thornton[38]. It is therefore apparent that a more sophisticated definition of the critical C.O.D. is required, if this quantity is to represent a material property analogous to K_{Ic}. The method of Harrison and Fearnehough can probably be extended to a point where the critical C.O.D. is taken as the C.O.D. for the initiation of a crack at the specimen notch root.

A number of techniques have been used to detect such cracking in fracture toughness specimens, these include potential drop techniques[45], acoustic emission[46] and ultrasonics[47]. Potential drop and acoustic emission techniques require expensive new instrumentation whereas ultrasonic equipment is generally available. An ultrasonic technique in which the growing crack intersects an ultrasonic beam could be used to determine the crack initiation point.

Very recently Knott and Smith have used a different technique to measure the initiation of cracking C.O.D.[48]. These workers tested bend specimens to known C.O.D. values then unloaded the specimens and fractured them in liquid nitrogen. The depth of fibrous thumbnail on each specimen was then measured and plotted against the C.O.D., from this data the initiation C.O.D. could be determined with reasonable accuracy as in Figure 12.

The type of notch used to simulate a real defect in a C.O.D. specimen is important. In the early work 0.006 inch saw cut slots were used but recently fatigue cracks have been recommended as in L.E.F.M. testing, to ensure that the C.O.D. measured is the lowest likely to be experienced[30]. Indeed Knott and Smith[48] showed a variation between initiation C.O.D. values measured on fatigue cracked and slotted specimens. However, Thornton[38] found no difference in initiation values for fatigue cracks or slots up to 0.010 inch wide. These opposing results could be due to material differences or the different techniques used to measure crack initiation.

The conclusive proof of the link between C.O.D. and L.E.F.M. and the determination of a true critical C.O.D. would enable general yield fracture mechanics to become a viable design criterion as is linear elastic fracture mechanics.

Figure 12

Method Used by Knott and Smith[48]

to Determine Initiation C.O.D.'s

2.5 Fracture Toughness as a Design Consideration

Apart from its usefulness in the quantitative determination of the resistance to fracture of a material, the fracture toughness offers an extremely useful design criterion because it is possible to predict critical flaw sizes and also sub-critical flaw growth, structural life and probable fracture mode.

Three types of crack or crack-like defect are normally encountered in service, namely; through thickness cracks, surface flaws and internal flaws. At a given working stress level there is a critical size, for each type of defect, which will give rise to rapid crack propagation. The critical defect size is a function of the fracture toughness of the material. Where the degree of constraint is high, as in the case of surface or internal flaws or through thickness cracks in thick plate, plane strain conditions usually apply, so that the critical flaw size is dictated by the plane strain fracture toughness K_{Ic}. Where the constraint is less, the plane stress or mixed mode conditions apply, and the fracture surfaces will have substantial shear borders.
For structural materials, the plane stress condition is the most desirable, since not only is the fracture toughness higher but the critical crack length is larger and more readily visible giving more prior warning of ensuing failure.

The most likely condition leading to premature catastrophic fractures is the growth of surface or internal flaws to the critical size before the through thickness stage is reached. In this situation it is likely that both the initial flaw growth and the inception of instability will be governed by the plane strain fracture toughness of the material. This type of flaw growth is particularly dangerous since small flaws can cause failure, and moreover, little prior warning is given.

It has been shown by the A.S.T.M. E-24 Committee[49] and by Tiffany and Masters[50] that critical flaw sizes for many types of structures can be calculated with reasonable accuracy using K_c or K_{I_c} fracture toughness values. The half critical crack length for through thickness defects in plate is given by the expression:

$$a_c = \frac{1}{\pi}\left(\frac{K_c}{\sigma_a}\right)^2 - \frac{1}{2\pi}\left(\frac{K_c}{\sigma_y}\right)^2 \quad \ldots\ldots\ldots (30)$$

The critical size for surface flaws can be calculated from:

$$\left(\frac{a}{Q}\right)_c = \frac{1}{1.21\pi}\left(\frac{K_c}{\sigma_a}\right)^2 \quad \ldots\ldots\ldots\ldots\ldots (31)$$

where a_c is the critical crack depth and Q_c the flaw shape parameter which is a function of the elliptical crack dimensions[50].

All materials contain initial flaws, therefore, the critical crack length approach in the design of structures has wide significance, and numerous equations similar to (30) and (31) exist for various geometries.

C.O.D. measurements can be used in the same way as K values by relating δ to K using equations (5) and (6) namely:

$$G_c = \sigma_y \delta_c$$

and $$K^2 = EG$$

More simply the C.O.D. can be used to compare the defect sizes that a component made of different materials can tolerate.

Taking the theoretical equation[19,51] (25)

$$\delta = \frac{8\sigma_y a}{\pi E} \ln \sec \frac{\pi\sigma}{2\sigma_y}$$

which can be approximated to:

$$\delta \simeq \frac{\pi a \sigma_a^2}{2E\sigma_y}$$

then:

$$\delta_1 = \frac{\pi a_1 \sigma_a^2}{2E\sigma_{1y}}$$

and

$$\delta_2 = \frac{\pi a_2 \sigma_a^2}{2E\sigma_{2y}}$$

therefore:

$$\frac{\delta_1}{\delta_2} = \frac{a_1 \sigma_{2y}}{a_2 \sigma_{1y}}$$

or

$$\frac{a_1}{a_2} = \frac{\delta_1 \sigma_{1y}}{\delta_2 \sigma_{2y}} \quad \ldots\ldots\ldots\ldots\ldots\ldots \quad (32)$$

thus comparative sizes of defects can be obtained.

The expressions used to calculate defect sizes have to be considered more fully when attempts are made to apply fracture mechanics to welded joints, especially those not fully heat treated after welding. This is due firstly to the fact that the various weld zones have different yield strengths with correspondingly different toughness values and secondly the stress normal to a flaw in the weld region will be modified by the residual stress system. Since working stresses are usually some proportion of the yield stress it can be seen from equation (31) that the critical defect size which a structure can tolerate is proportional to $\left(K_c/\sigma_y\right)^2$. It is well known that, in general, as the yield strength of a given material is increased its toughness value decreases this implies a reduction in permissible flaw size if the stress remains constant.

In a weld which is not fully heat treated there will be some local residual stress due to welding and this will be added to the applied stress to give a much higher gross stress. This again results in a reduction of permissible defect size. Cottrell[52] has shown that the gross stress across a weld defect can reach the yield stress of the zone in which the defect is located with an applied stress of only 1/3 uniaxial yield magnitude.

Thus if it is not possible to fully heat treat a welded structure, then the safest approach is to base the maximum permissible defect size on an applied stress equal to at least the yield stress of the material.

Further consideration must be given to the use of fracture mechanics as a design tool when applying it to pressurized tubes. The original work on the failure of flawed steel pressure vessels by Irvine et al[53] suggested a relationship between failure stress and crack length of the form

$$\sigma_F^3 \, a^2 = \text{constant}$$

this is vastly removed from the relationship

$$\sigma_F^2 a = \text{constant}$$

which is arrived at by fracture mechanics considerations, equation (5).

The cause of this deviation from theory is due to the fact that the relationship

$$\sigma_F^2 a = \text{constant}$$

is derived for flat plate conditions. In a tube, elastic bulging occurs along the crack because of the internal pressure and sets up bending moments around the crack tip which cause a decrease in failure stress.

Corrections of the form f (a,R,t) have been suggested to account for the difference in stress

distribution between plate and cylinder, where a is half the crack length, R the cylinder radius and t the cylinder wall thickness. The most usual of these corrections is by Folias[54].

$$\sigma_{vessel} = \sigma_{plate} \left(1 + \left(x + y \ln \frac{a}{(Rt)^{\frac{1}{2}}}\right) \frac{a^2}{Rt} \right) \ldots\ (33)$$

where x and y are constants

The term $\left(1 + \left(x + y \ln \frac{a}{(Rt)^{\frac{1}{2}}}\right) \frac{a^2}{Rt}\right)$ is known as the Folias correction factor. Application[55] of this correction factor to the results of fracture of pressurized cylinders shows that the fracture behaviour does in fact correspond to a criterion well represented by a constant value of $\sigma^2 a$.

The Folias correction factor has also been applied to correct for the variation in C.O.D. between plate and cylindrical vessel. Wells[56] has used the relationship:

$$\delta = \frac{8\sigma_y a}{\pi E} \ln \sec \left\{ \left(\frac{\pi \sigma a}{2\sigma_y} \right) \right\} \left\{ \left(1 + 1.6 \frac{a^2}{Rt} \right) \right\} \ldots\ (34)$$

Burst tests on pressurized tubes have shown that for brittle materials, fracture occurs when the C.O.D. at the crack tip reaches a critical value and that this value can be determined on small scale laboratory bend specimens[57]. Fearnehough et al[58] have shown that cracking in pressurized tubes of ductile material can be predicted by small C.O.D.

specimens provided that the critical point is taken as crack initiation and that this is carefully monitored. They found however that failure occurred at a much later stage after considerable slow crack growth and that failure was governed by a plastic collapse or instability criterion[58-60], dependent on geometry and material yield stress only.

Broek[61] has also shown how stable crack growth contributes to final failure. Working on aluminium specimens he showed that there was a relationship between the initial defect size and the defect length at failure, the difference between these two lengths being dependent on specimen dimensions.

Thus, although the fracture toughness value can be used to predict critical defect sizes, these sizes only apply to the first loading and it is important to know how subcritical defects grow and at what rate, to be able to predict structural life under service conditions. The critical C.O.D. results obtained on X-52 can however be used to calculate defect sizes for the initiation of slow tearing. This will provide a conservative estimate of defect sizes for inspection purposes.

It is therefore apparent that fracture mechanics can be used to describe fairly precisely the problem of cracks in the parent plate and the H.A.Z. of the longitudinal seam weld of a pipe, provided that they lie in a longitudinal direction. There is however,

the possibility of cracks existing at an angle to the principal stress, for example in the H.A.Z. of a spirally welded pipe, so that it will be under the influence of both K_I and K_{II} mode stress intensification. Little work has been done on crack propagation in this situation, only that of Erdogan and Sih[62] and Wu[63] seems appropriate.

Erdogan and Sih suggest that in such a situation the failure envelope for an isotropic material, where the direction of initial crack growth obeys a stress criterion, should be an ellipse quadrant whose axes do not necessarily coincide with the K_I and K_{II} axes as shown in Figure 13. Wu obtained results on anistropic materials where the crack propagation direction was on a prolongation of the initial crack. He postulates that the failure envelope is of the general form

$$\left(\frac{K_I}{K_{I_c}}\right)^m + \left(\frac{K_{II}}{K_{II_c}}\right)^n = 1 \quad \ldots\ldots\ldots\ldots \quad (35)$$

describes constraints on the possible values of m and n (namely m = 1 and n = 2) and then obtains similar results by experimentation. Erdogan and Sih's theory suggests that both m and n are equal to 2.

Work on angled cracks in aluminium welds by Pook[64] seems to indicate a relationship more consistent with that of Erdogan and Sih than that of Wu as shown in Figure 13. It is therefore important to assess the effect of angled cracks on X-52 to attempt

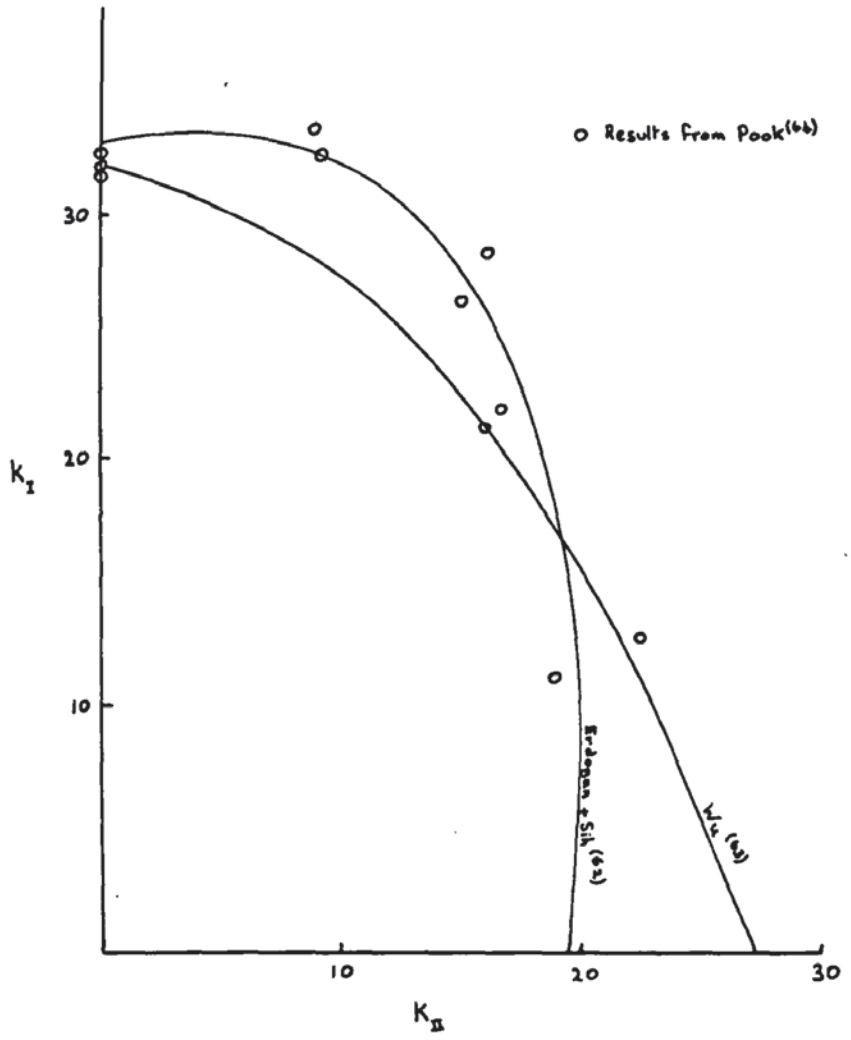

Figure 13

Combined K_I and K_{II} Failure Envelopes

to describe a failure envelope for this material. This is made even more important by the work of Richards[65,66] who has shown that cracks moving perpendicular to an applied stress can turn when they approach a weld to follow the line of the weld. The cause of this deviation is thought by Richards[66] to be the alteration of the shape of the plastic zone ahead of the crack by the higher yield strength material in the weld H.A.Z. The crack running in the material of lower yield stress i.e. larger plastic zone, not in the most brittle material.

2.6 Assessment of the Toughness of Welded Joints and Weld Heat Affected Zones

A great deal of information on testing techniques and toughness can be gained from a study of plate material but if critical operating conditions of stress or defect size are to be assessed it is imperative to determine the worst possible properties of a structure and to design on these. In the case of gas pipelines, as in the case of most welded structures, the worst condition of toughness would be expected to occur in either the weld metal or in the weld H.A.Z. Indeed failures which have occurred during routine pressure testing of pipeline have been predominantly associated with the H.A.Z. of the longitudinal seam weld. Further it has been shown by Archer[67], at least in a qualitative manner, that in steels similar to those used in pipeline construction the H.A.Z. is the region of lowest toughness.

There is some difficulty in determining the fracture toughness of weldments particularly of given parts of the H.A.Z., mainly because of geometry. This arises because in for example a double-vee type weld, the notch of a fracture toughness test piece will be in a large number of structures across the weld and H.A.Z. The problem can be overcome to a certain extent by the use of simulated H.A.Z.'s[68,69] producing by thermally cycling a specimen a wide H.A.Z. structure corresponding to one part of the real weld H.A.Z. This approach seems to work well[70] but some doubts have been raised about the correlation of grain size between simulated and real H.A.Z.'s [71] although this seems to have been overcome[72]. The main disadvantages of simulation however are that firstly present simulators are somewhat limited in the size of specimen that they can accommodate, one quarter of a square inch being about the maximum cross sectional area that can be heated and cooled over the temperature cycles normally encountered in real welds. Secondly a test carried out on a simulated H.A.Z. may bear no relationship to what would happen in a real weld since different constraints and plastic zone shapes can exist in the two situations.

Since it is essential to test C.O.D. specimens at service thickness the only reliable approach is to test real welds. This also removes any doubt about temperature cycles or thermal strains produced

during welding, the latter can only be approximately reproduced on simulators. The geometrical problem of the notch can be overcome to a large extent because of the well known crack growth phenomena by which cracks grow in a parabolic (thumbnail) shape[73-75]. Crack initiation can thus be expected to occur in the centre of the ligament, and since crack initiation is to be taken as the critical point in the fracture process for the measurement of toughness; the toughness of the material at the notch tip in the centre of the specimen thickness will be measured. The variation of the toughness in the different parts of a weldment can thus be assessed.

The use of specimens cut from the welds of actual pipes presents some difficulty for a research project because of handling large sections and possible material variation. It would be far easier to use welds made on small test pieces. Roberts and Wells[76] have shown that a test plate of half-width of ten, or more, melted bead widths is a satisfactory size for a test weld plate. If a marginal length of ten melted widths is then neglected at both ends of the plate the remaining points can be regarded as having temperature cycles as in a plate of infinite length. Thus it is possible to reproduce the heat flow conditions of a real pipeline weld on a test plate. It can also be shown[77] that it is possible to reproduce the same width of heat affected zone on a

test plate as in an actual pipe weld even if the welding parameters are vastly different. From Wells' formula[77]

$$H = 8\kappa T \left(\frac{1}{5} + \frac{vd}{4\alpha} \right) \quad \ldots\ldots\ldots\ldots \quad (36)$$

where H is the rate of heat input to the plate (cal/sec/cm), κ the thermal conductivity, α the thermal diffusivity, T the temperature rise above ambient, v the welding velocity and d the width heated to temperature T. It can be seen that alterations to H and v the only two independent variables in the equation can be made without altering T or d.

It is therefore possible to produce under laboratory conditions small test welds truly representative of those which could be obtained from an actual pipeline.

2.7 Crack Initiation and Propagation in Ductile Material

Unlike the fatigue, creep and low temperature brittle types of fracture, the process by which a ductile material finally separates, to produce a fracture, e.g. the typical cup and cone failure in a tensile test, has not been investigated until relatively recently. This type of failure is technically important because it is frequently the first step in what becomes brittle fracture in structural steel and because rapidly propagating ductile fractures sometimes occur.

One of the earliest investigations of ductile fracture was that of Parker et al[78] who showed by etch pit techniques, that there was a qualitative difference between the fibrous and cleavage portions of the low temperature tensile fractures of structural steel. In particular, they demonstrated that the flat fracture portion of a cup and cone failure was not, on a micro scale, parallel to the cleavage planes of the individual crystals but more nearly at 45^{o} to the cleavage planes and therefore some form of shear failure.

Another important observation concerning ductile fracture was made by Plateau et al[79] who showed by microfractography, that the rupture surface in ductile fracture had a characteristic appearance which they deduced resulted from failure by void formation in the heavily deformed region at the tip of an advancing ductile crack.

The most detailed study of the ductile fracture process has been made by Rogers[80] using O.F.H.C. copper deformed in tension until a neck and an internal flaw developed. The specimens were then sectioned to reveal the void structure at various points in the specimen neck. The voids were found to form either along grain boundaries or in bands of heavily deformed material. With continuing deformation the voids grow and link up to form larger voids which tend to localise the deformation

into narrow bands originating at the larger voids and extending outwards at about 30^{o}-40^{o} to the tension axis. Void formation is then enhanced in these bands and the voids grow along these bands. In the most severely deformed region in the centre of the neck a macroscopic crack develops which then propagates outwards by strain concentration in two bands at approximately 30^{o}-40^{o} to the tension axis, void formation along these bands, and extension of the original crack along one of the two deformation bands. The crack then propagates along a zig-zag path by repetition of this process until the surface is approached.

The final separation near the surface leading to the cone is of a somewhat different character and a number of suggestions concerning this final stage have been put forward[81]. In any event the most important steps in the process leading to the formation of a large internal crack are void formation and the linking up of voids to form a continuous crack.

Puttick[82] in a similar study on tough-pitch copper and Armco iron also found void formation to be the initial step in ductile fracture and further showed evidence that in his material many of the voids were caused by non-metallic inclusions. Plateau et al[79] were also of the opinion that the cavities formed in their material were nucleated at

inclusions or precipitate particles since they found evidence that oxide or other particles were present in each cavity. These observations have led Puttick[82] and Cottrell[83] to the conclusion that the cavities in ductile fracture are always nucleated at inclusions and Cottrell cites several examples of the effect of purification increasing the reduction in area. The evidence is quite convincing that foreign particles are a common nucleating site for cavities in ductile fracture, however, there is some evidence from Rogers' observations that cavities may be nucleated in regions of very severe plastic flow without any indication of the presence of inclusions. However, by far the most common case is that associated with inclusions, final failure then occurring by void coalescense in the manner described by Gurland and Plateau[84] and revealing a dimple type fracture surface as first observed by Crussard et al[85] and described fully by Beachem and Pelloux[86].

In hot rolled steels of the types used for pipeline there is often gross mechanical segregation of ferrite and pearlite[87] forming effectively a fibre reinforced structure and these steels are often unexpectedly resistant to fracture when the crack travels normal to the plane of segregation. This type of behaviour has been observed in impact tests on hot rolled plate[88-90] where decohesion

occurs at ferrite - inclusion interfaces; these regions link up and thus divert the crack. If the delamination of the interface requires extensive plastic strain, then the interfaces will not affect crack propagation at lower temperatures[91] where much smaller plastic zones accompany crack propagation. This appears to be the case in structural steels where there is relatively little delamination below the impact transition temperature, but above this temperature, where fracture occurs after general yield, there is a substantial difference in the shelf energy of rolled steel specimens of different orientations.

Almond et al[92] refer to two basic geometries of laminate which can be expected to increase the resistance to crack propagation, they term these crack arrester and crack divider laminates and they are illustrated in Figure 14. Indeed there exists in the literature a considerable body of experimental evidence to indicate that both of these geometries may usefully enhance the fracture resistance of materials such as mild steel[93]. Almond et al[94] in a later paper have demonstrated that a laminated cylinder of the crack divider geometry (analogous to the case of a longitudinal defect in a pipe made of heavily banded steel) has substantially better fracture properties than a solid wall cylinder.

The cause of the increase in fracture properties is that the weak interface delaminates and the stress system approaches plane stress in all the thin ligaments. It is possible that this type of metallurgical structure could suppress the propagation of a fracture originating in a local region of high stress or poor toughness such as a weld H.A.Z.

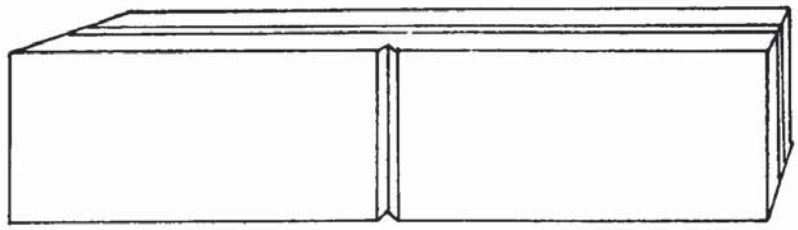

a) Crack Arrester.

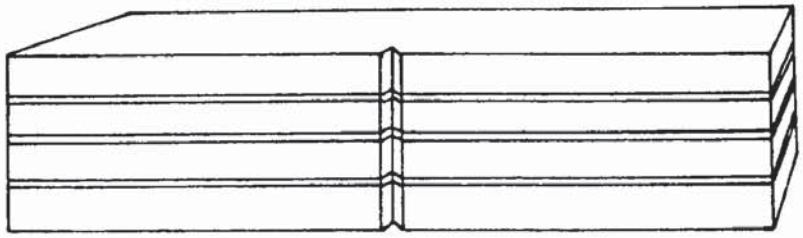

b) Crack Divider.

Figure 14

Lamellae/Notch Orientations

3. SCOPE OF RESEARCH

The major aims of this research programme were to make a study of the C.O.D. concept of fracture mechanics on unwelded X-52 plate. The findings of this study are used where applicable to assess the fracture toughness of the weld and weld H.A.Z. in X-52, welded under conditions equivalent to those in a pipeline.

The effect of cracks running at angles to a weld H.A.Z. were studied in an attempt to arrive at a failure criterion for this type of situation.

4. EXPERIMENTAL TECHNIQUES AND MATERIALS

This section covers only the material and techniques used in this work, the results obtained have all been gathered together in the next section.

The major part of the experimental work to be described was carried out using material supplied to the A.P.I. 5 LX - 52 specification [1]. A.P.I. 5 LX - 60 was also used in part of one experiment. The X-52 material was received from the steelmaker as a single plate thus removing the possible error of plate to plate variations, although the plate was large enough to reveal any in plate variation of properties. The X-60 was received as large specimen blanks from the Gas Council.

The two batches of steel were analysed by wet chemical methods and by spectroscopy to establish that they were within the specified limits.

The X-52 was supplied as a semi-killed steel, hot rolled into a single pipe length, that is, ½ inch thick x 6 foot wide x 40 foot long, which had been cut into four 10 foot lengths for transportation. The X-60 received from the Gas Council had a similar history except that the steel is grain refined by the addition of one or more of the elements, niobium titanium or vanadium, to give it its increased yield strength.

Metallographic examination was carried out on the X-52 plate to determine microstructure and grain size. Metallographic examination was performed using

a Vickers Projection microscope and the grain size was determined with the aid of a Quantimet Image Analysing microscope.

The more usual mechanical properties of strength and hardness were determined on the two plates. Tensile data was obtained by testing standard Number 11 Hounsfield specimens cut from the longitudinal and transverse directions of the plate, these were tested on a 5000Kg capacity Instron Testing Machine at a cross-head speed of 0.02cm/min. Vickers hardness and microhardness measurements were made on specimens prepared for metallography using loads of 30Kg and 100gm respectively.

The fracture toughness of the material was determined by measuring its crack opening displacement. As shown in the literature review, a number of methods exist for measuring C.O.D. values. The most direct method, that of the "paddle-codmeter" has, as was discussed, certain limitations, its major failing being that it cannot be used in the case of fatigue cracked specimens. The method in common use at the present time, that of the clip gauge was tried but finally it was decided to use a photographic calibration technique.

Bend specimens were cut from the X-52 plate, 1 inch deep x $\frac{1}{2}$ inch thick x 4 inch span. These were machine notched on the centre line using a 1/16 inch milling cutter and this machined notch was extended

by 0.100 inch using a 0.008 inch thick jeweller's saw to simulate a natural defect. A typical specimen is shown in Figure 15. The finished specimens had various total notch depth to specimen depth ratios, a/w, but were more usually in the region of 0.5

The side surface at the notch tip of these C.O.D. bend specimens was metallographically polished. Microhardness indentation were made on either side of the 0.008 inch slot, approximately 0.005 inch from the sides of the slot and 0.010 inch apart starting from the tip of the slot. These indentations were used as gauge marks for the photographic calibration. A typical specimen prepared in this manner is shown in Figure 16.

The specimens were tested in three point loading using the Inston Testing Machine again at a crosshead speed of 0.02 cm/min. The testing arrangement is shown in Figure 17. A force/time curve was plotted on the machine chart, operating at 1 cm/min, as the test proceeded. Photographs were taken of the slot tip using the microscope and camera attachment shown in Figure 18 and an electronic flash gun to illustrate the specimen. The Instron chart was marked to show the time at which the photographs were taken.

The C.O.D. at the crack tip was measured from the photographs obtained, a typical series of which is shown in Figure 19. From Figure 19 it can be seen that the gauge marks at the notch tip tend to be obscured as the test proceeds due to plastic

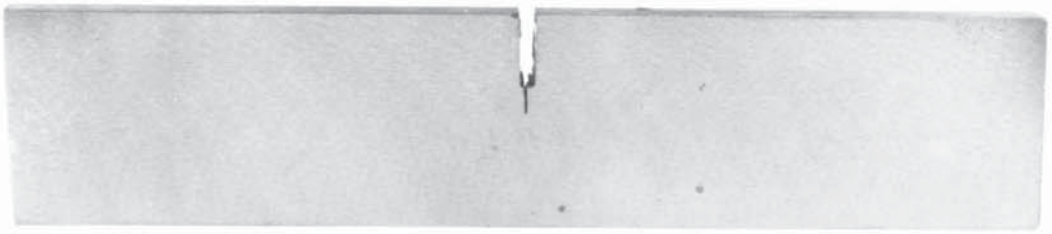

Figure 15 x1

Bend Specimen

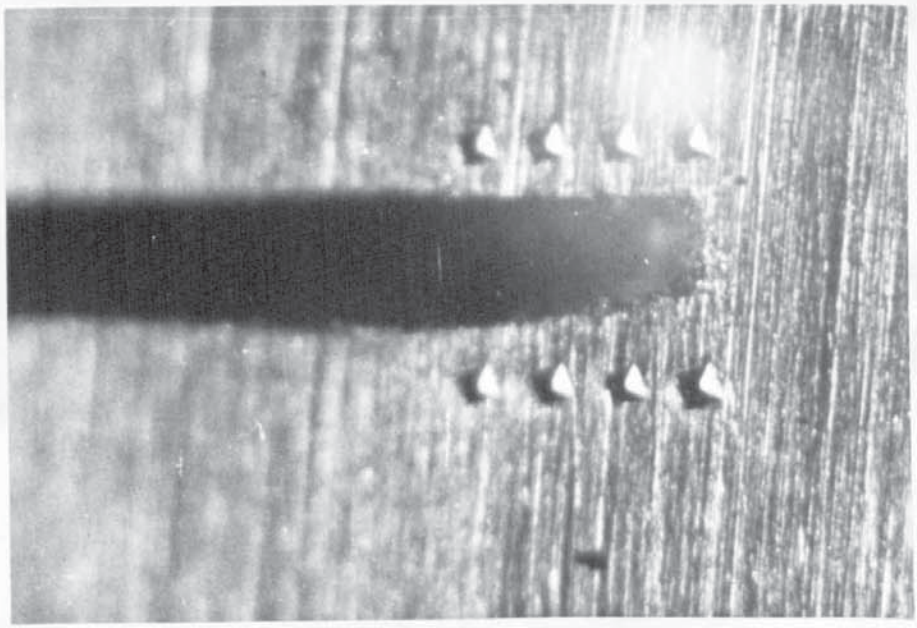

Figure 16 x50

Notch Tip of a Specimen Prepared for Photographic Calibration

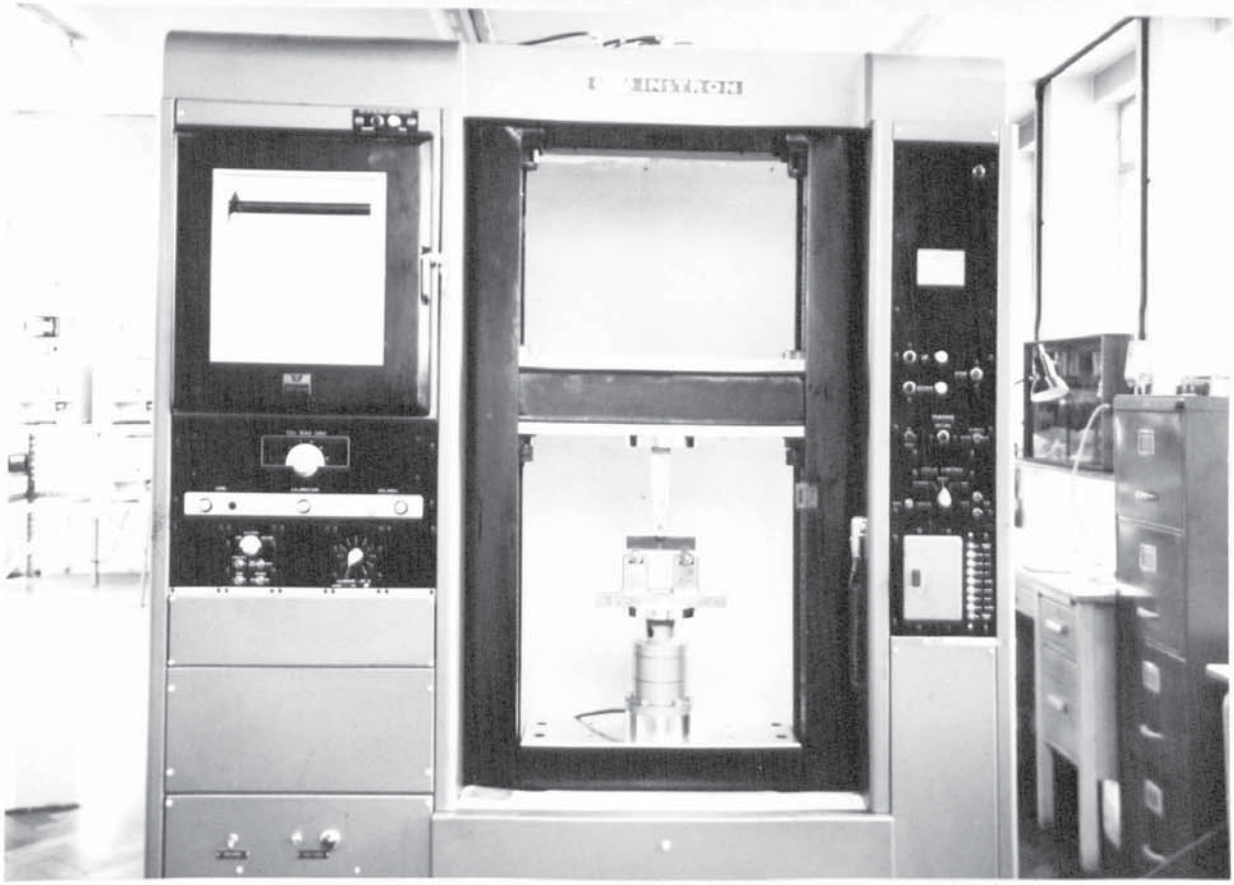

Figure 17 Testing Machine and Bend Rig.

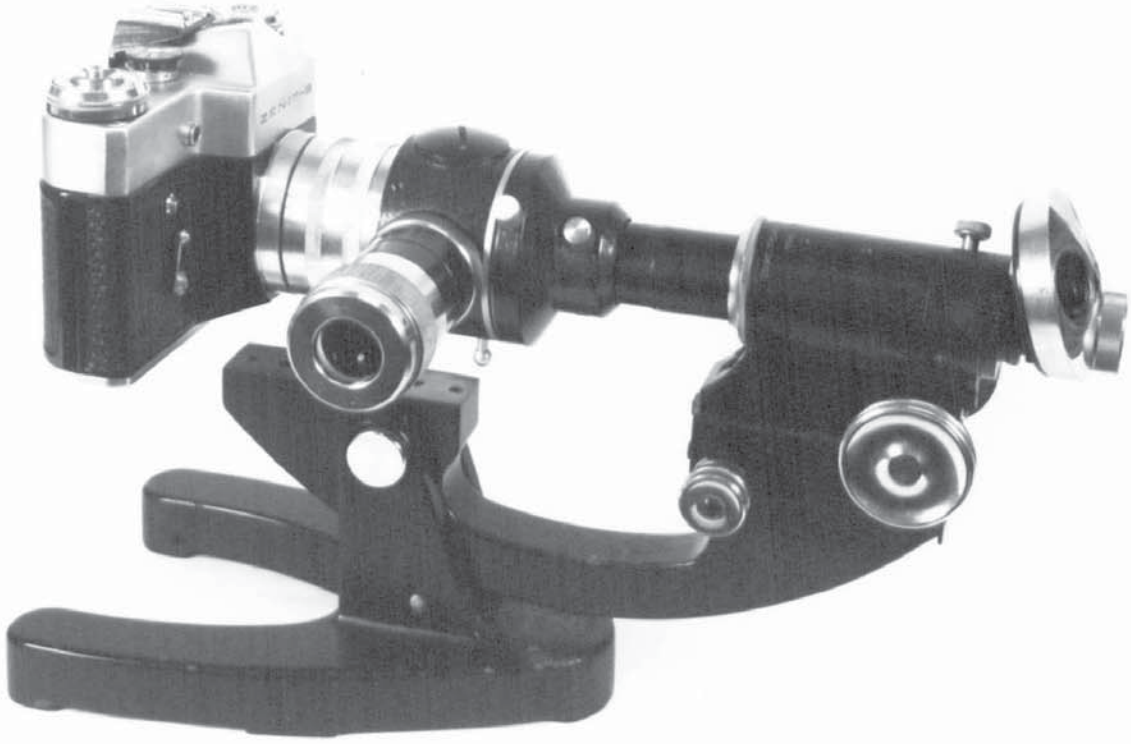

Figure 18 Microscope and Camera Attachment

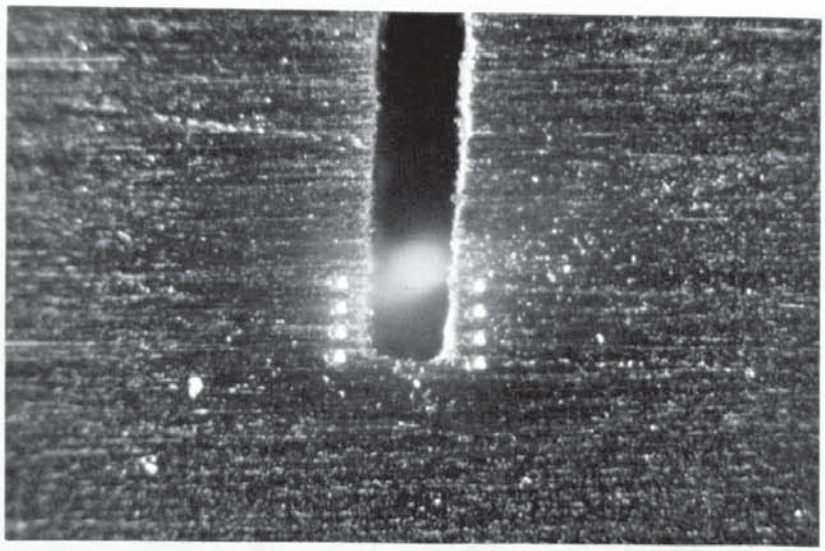

(a)

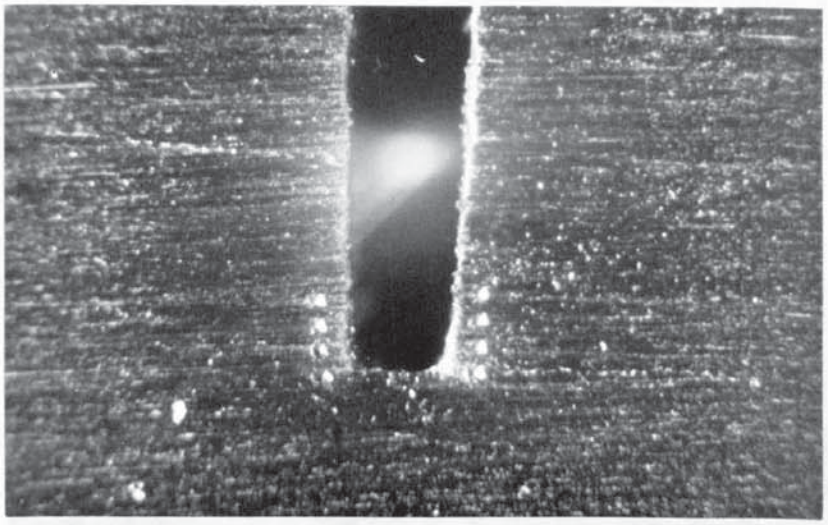

(b)

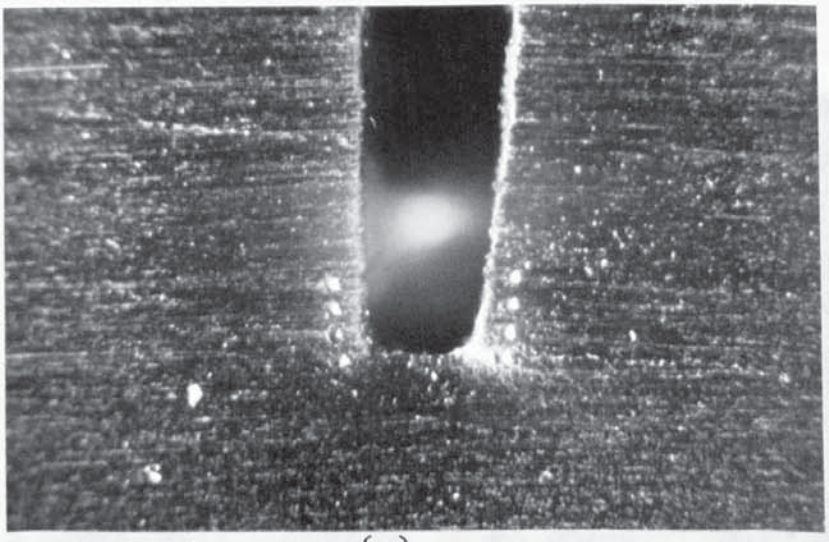

(c)

Figure 19 C.O.D. Calibration Series

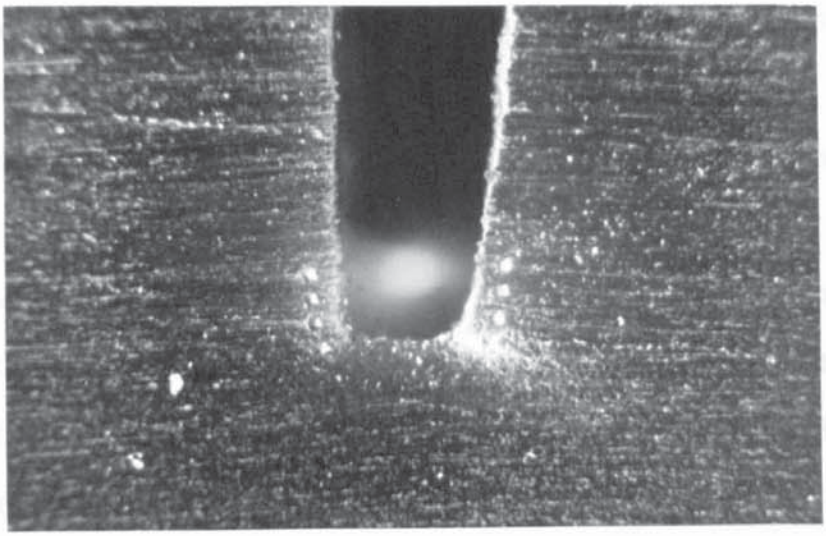

(d)

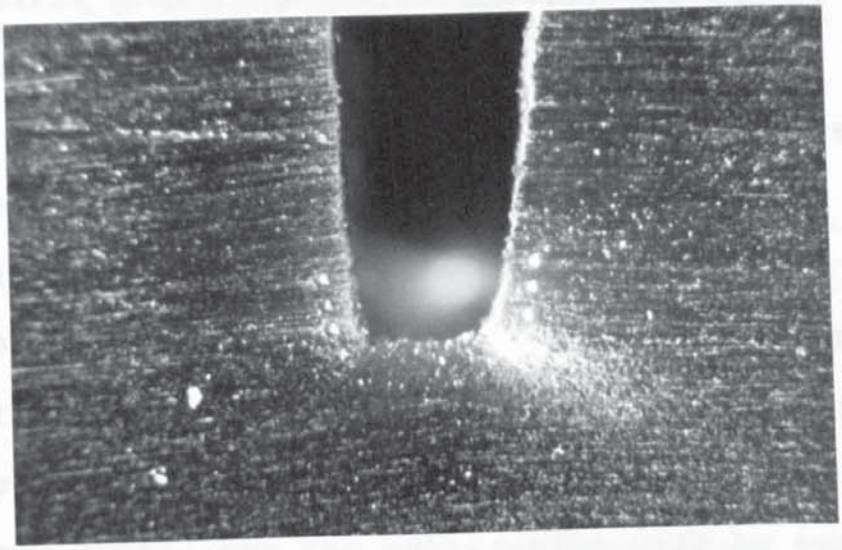

(e)

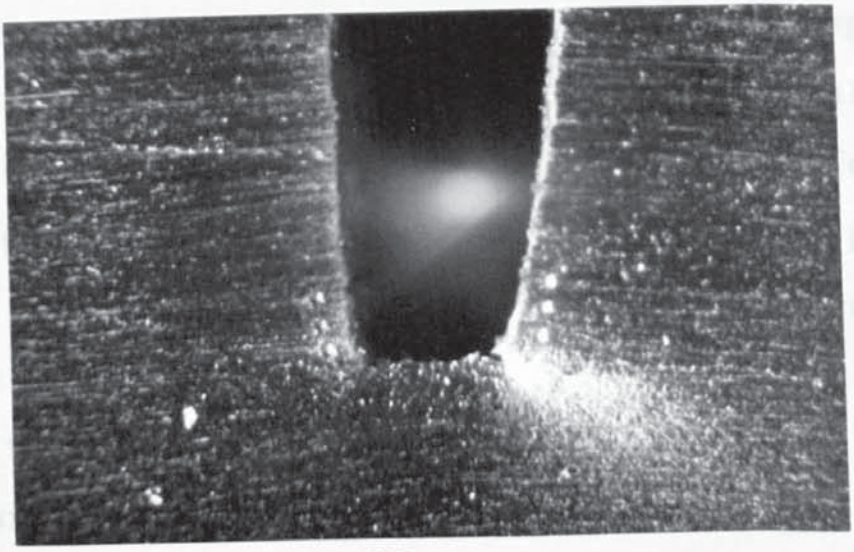

(f)

Figure 19 (cont.) C.O.D. Calibration Series

flow at the crack tip: it is for this reason that four, or on occasions more, pairs of hardness marks were put along the slit. If the notch tip marks became obscured the others could be measured and a value of the notch tip C.O.D. found by extrapolating the other values. This extrapolation is not linear however and only an approximate value of the notch tip C.O.D. can be obtained. This is not expected however to produce any error in actual test measurements because the obscuring of the slot tip marks usually occurred towards the end of the calibration.

The notch tip C.O.D. values obtained were correlated with the offset plastic deflection of the specimen as shown in Figure 9 (Page 33) and a calibration curve of C.O.D. versus displacement was plotted as also shown in Figure 9. The offset plastic deflection was in fact measured as a distance on the Instron chart, but the calibration will be valid on all specimens of the particular geometry tested, provided that the cross-head speed and chart speed used in the calibration are used for the actual tests. Calibration curves were obtained in this way for all the specimen sizes and geometries used in the present work, the calibration being performed on at least three specimens of each geometry. On an actual test the critical C.O.D. can be determined by measuring the offset deflection at the critical point for example maximum load and looking up the

C.O.D. value for this point from the calibration curve for that particular geometry.

The question arises as to whether the C.O.D. measured at the surface using gauge marks is the same as that which occurs at the centre of the specimen. In order to examine this a number of specimens were unloaded during various stages of test. The surface C.O.D. was measured using a microscope and then the specimen was ground down and the C.O.D. measured every 0.050 inch until the centre line was reached. The slight inaccuracy introduced by making these measurements on unloaded specimens was considered to be acceptable.

Before the photographic calibration technique was finally chosen an attempt was made to use the method generally recommended at the moment namely the clip gauge method which was described in the literature survey. This technique proved unsuccessful because the quoted relationship[29] between clip gauge opening δ_{CG} and crack tip opening δ_t namely;

$$\frac{\delta_{CG}}{\delta_t} = \frac{n(a+z)}{d} + 1$$

was tested and found to be too inaccurate for the present purposes. Using the photographic method described, the notch tip C.O.D. was measured at the same time as the clip gauge C.O.D, no simple relationship between δ_{CG} and δ_t was found.

Once the photographic calibrations had been determined the next problem was the choice of the point on the load/C.O.D. trace at which to measure the critical C.O.D. As shown earlier this critical C.O.D. point is in question and it was decided to take the initiation of cracking as the point at which to measure the critical C.O.D.

The initiation of cracking was detected by an ultrasonic method. A 6 megacycle split beam probe, shown in Figure 20, was used, the probe is approximately 1 cm square and may be used in two ways. Firstly, it may be attached to the end of a bend specimen and used as an ordinary transceiving probe as shown schematically in Figure 21. The probe was set before the test began so that the beam just missed the tip of the slot, crack growth was then detected by the rise of a signal from the base-line of the oscilloscope, midway between the impulse signal and the back wall echo, as the crack grew into the beam. Alternatively, the probe can be attached to the side of the specimen as shown in Figure 22. Using the probe in this manner, a signal from the back of the specimen was observed when the probe was set up before the test, the onset of cracking was detected as a fall in the back wall echo signal because the reflection of the beam to the receiving side of the probe was progressively cut off by the growing crack. This latter technique was especially useful compared to the end probe

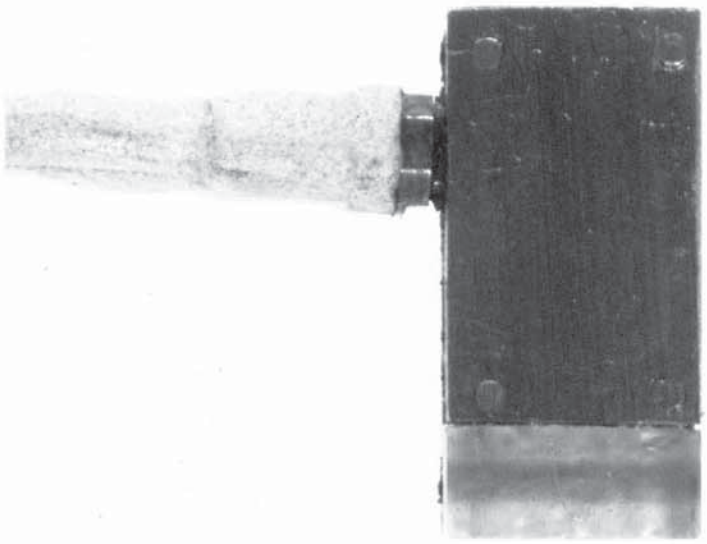

(a)

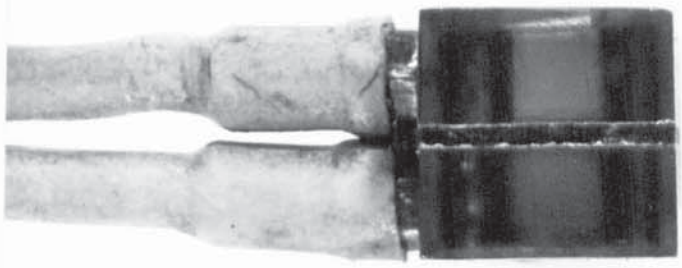

(b)

Figure 20

Probe Used to Detect Crack Initiation

x 3.5

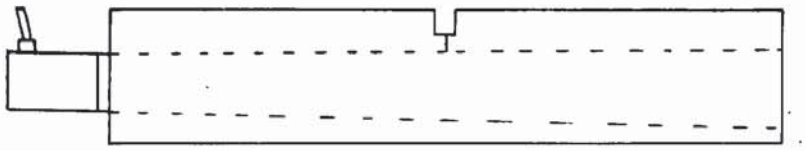

Figure 21 Probe on End of Specimen

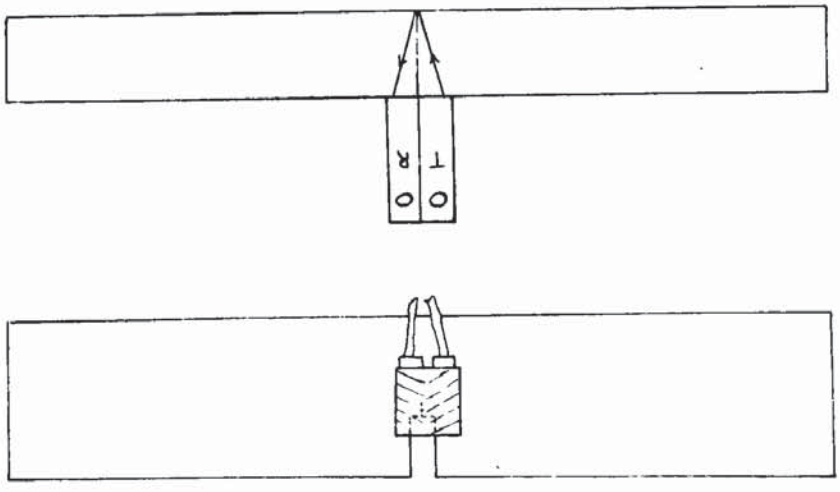

Figure 22 Probe on Side of Specimen

method when testing specimens containing long notches. The end probe method always produced a reflection from a deeply notched specimen because of the dispersion of the ultrasonic beam. It was therefore more difficult to determine the onset of cracking.

An experiment was performed to determine the sensitivity of the ultrasonic technique. Bend specimens were tested with the probe attached in both the ways described. The specimens were loaded until specific changes were noted in the signal strength between 1 and 5 decibels, the test was then stopped and the specimen unloaded and sectioned to determine the amount of crack growth. This permitted a level of signal change to be selected which corresponded to the smallest amount of crack growth which could be detected consistently.

The ultrasonic crack initiation detection technique was also used on compact tension specimens, Figure 23, in which the crack length a, specimen height 2H and thickness B were held constant at $2\frac{1}{2}$ inch, 4 inch and $\frac{1}{2}$ inch respectively. The methods used were the same as those for bend specimens except that a slight refinement was added to facilitate exact positioning of the probe, this was accomplished by attaching a micrometer to the probe as shown in Figure 24.

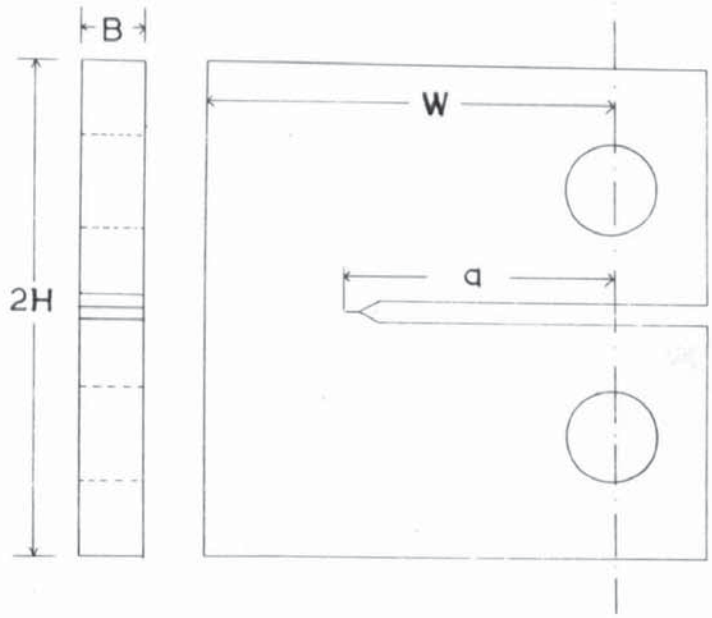

Figure 23 Compact Tension Specimen

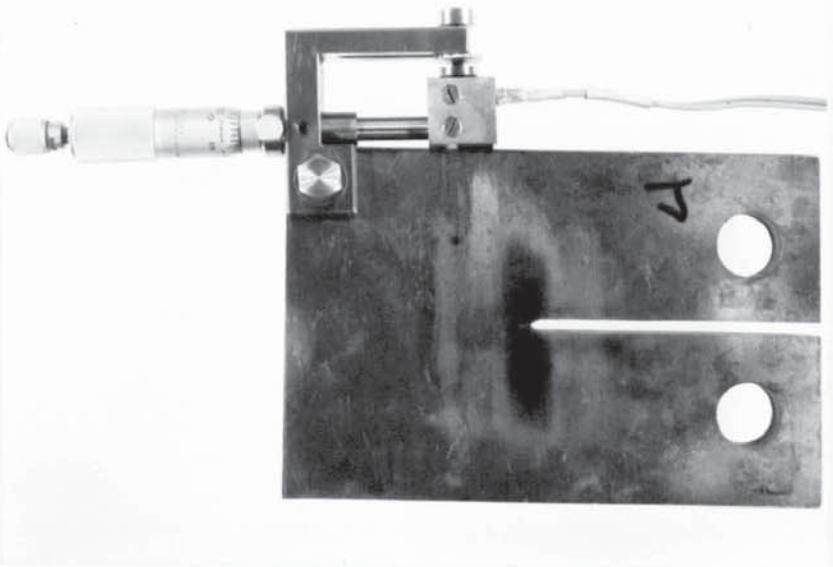

Figure 24 Probe and Micrometer Attachment

In order to confirm that the C.O.D. measured at the onset of cracking δ_i gave a constant value of the critical C.O.D., the δ_i value was measured on a range of X-52 bend specimens in which the ratio of crack length to gross width a/W, was varied between 0.100 and 0.700 by keeping W constant and varying a. Similarly a series of X-60 compact tension specimens was tested in which a was held constantandW varied to give a range of a/W values between 0.550 and 0.910. The δ_i values and the values of C.O.D. corresponding to maximum load δ_m were measured on these two series of specimens.

It was not possible to use the C.T.S. type of specimen below an a/W of approximately 0.5 because below this value the crack path became unstable as shown in Figure 25. This pheonomenon has been observed by other workers[95,96] and it is covered more fully in the appendix.

The ultrasonic technique was compared with a destructive method of measuring the initiation C.O.D.[48] Bend specimens of a given a/W were loaded until the C.O.D. reached a known value, the specimens were then unloaded. The test pieces were then broken in liquid nitrogen to make possible an optical examination of the fracture surfaces with no danger of extending any fibrous fracture. The area of "fibrous thumbnail" was measured on each test piece.

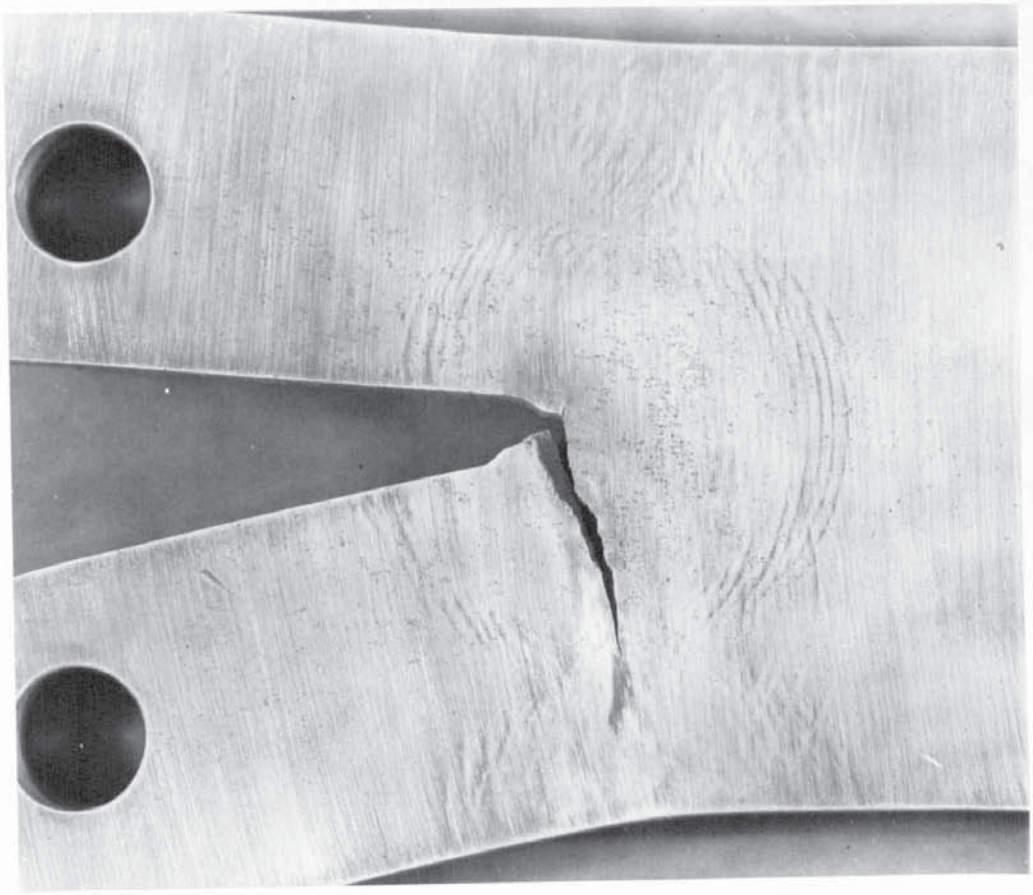

Figure 25 x1

Crack Path Instability in C.T.S. Specimen

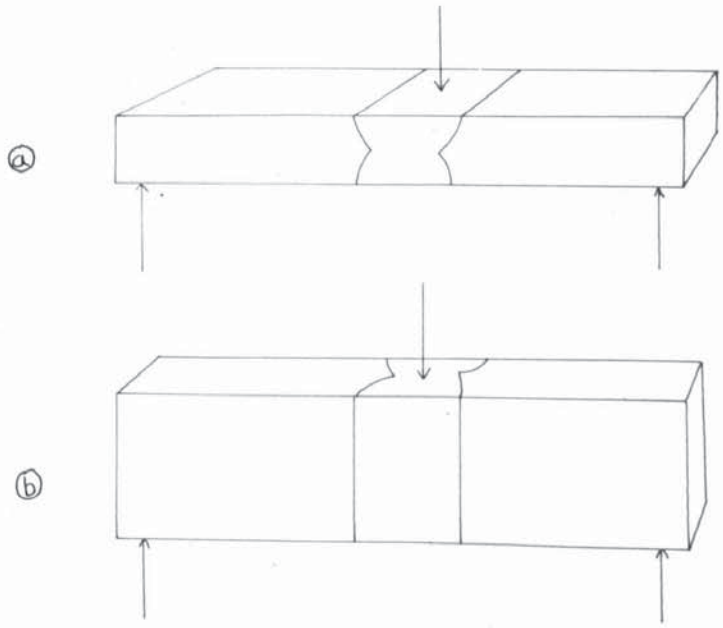

Figure 26 Bend Test Directions

The values of C.O.D. to which the specimens had been loaded were then plotted against the corresponding area of fibrous thumbnail, the curve obtained being extrapolated to zero growth to give the value of δ_i. This technique is extremely time consuming but it does give an accurate value of δ_i for reference purposes.

The ultrasonic technique was then used almost exclusively in the measurement of δ_i, the destructive technique being used occasionally to confirm some experimental results.

A number of exploratory experiments were undertaken to determine the effect on δ_i of various testing conditions, to examine the sensitivity of δ_i as a measure of toughness and also to examine the latitude permissible in such things as notch acuity and size of test pieces.

Firstly the effect of notch acuity was studied by measuring δ_i, using the ultrasonic technique, on a series of bend specimens cut from the as received X-52 plate such that the cracks ran in the longitudinal i.e. rolling direction. These specimens were of the standard size with a/W values of approximately 0.5. The notch tips of this series of specimens had the last 0.100 inch extended by fatigue cracking, slitting with an 0.008 inch thick saw and slitting with an 0.012 inch thick saw. It was considered that any

effect of notch tip geometry on δ_i would be revealed within the range tested. This experiment was repeated using fatigue cracked and 0.008 inch slotted specimens but using the destructive visual examination technique to determine δ_i.

The effect of specimen size was next examined, specimens were cut in the same direction as in the previous experiment but were made smaller such that they were $\frac{1}{2}$ inch thick x $\frac{1}{2}$ inch deep x 2 inch span. This series of specimens was tested to measure δ_i, in order to see if it remained constant, because specimens of a similar geometry would have to be used to assess the toughness in the case where the crack ran through the thickness of the plate.

The effectof thickness was next examined to determine the sensitivity of δ_i to this change in specimen geometry. X-52 bend specimens were tested 1 inch deep x 4 inch span but with thicknesses of 0.4, 0.3, 0.2 and 0.1 inch.

The techniques developed were then used to measure the initiation C.O.D. in the three directions of the as received plate namely longitudinal, transverse and through-thickness. Longitudinal specimens were also tested down to - 50^{o}C in order to determine whether or not there was any likelihood of the plate becoming seriously embrittled at low service temperatures. These low temperature tests

were carried out on the Instron Machine by placing the bending jig in a small box into which the coolant mixture of solid CO_2 and acetone could be added.

The techniques of measuring the toughness of this ductile material having been refined and tested the second major part of the work was begun, this was to assess the effect on toughness of welding the X-52 material. It was decided to perform the toughness tests on weldments made up using the X-52 plate supplied by the steelmakers, which had been used in the earlier experiments. This meant however that the weldments would have to be made up on the equipment available at the University although it is much smaller than that used in the actual manufacture of pipe. As was shown in the review of the literature, the work of Roberts and Wells[76] has shown that it is possible to obtain quasistatic heat flow conditions in small test weldments, provided that the components welded together are at least 10 x the melted bead width wide and that a similar length of material is discarded at each end. The melted bead width in a pipeline weld is of the order of $\frac{1}{2}$ inch so that if a similar width was obtained on a test weld the size requirements for a butt weld would be two plates at least 5 inches wide and something in excess of 10 inches long.

Welding trials were therefore begun on plates 9 inches wide x 18 inches long, the longest direction being in the rolling direction of the plate. These plates were square-butt welded together with two passes

using the submerged arc process, as is used for an actual pipe seam weld. Conditions of voltage, current, traverse speed and wire feed speed were determined which gave full penetration welds and also weld beads of the same shape and size as those on actual pipes. Using Roberts and Wells equation:-

$$H = 8\kappa T \left(\frac{1}{5} + \frac{vd}{4\alpha} \right)$$

where H = rate of heat input to plate (cal/sec/cm thickness)

κ = thermal conductivity (cal/cm/sec^{o}C)

α = thermal diffusivity (cm^2/sec)

v = welding speed (cm/sec)

T = Temperature rise (^{o}C)

d = heated width (cm)

the welding conditions to be used for test specimens were selected which gave heat affected zone widths the same as those on actual pipeline welds. It will be shown that the calculated values of H.A.Z. width in test plates and actual pipe are extremely close. Therefore the centre 8 inches of the test welds ought to truly represent the properties of the welded X-52 material.

These first test plates were however somewhat unwieldy being on the size limits of available shaping machines which were used to prepare the faces for butt welding, and also the welding table. Because of this smaller plates 6 inch x 12 inch were welded together

to see if it would be possible to use this smaller size. No difference was found between the properties and microstructure of the centre 6 inches of these smaller weldments and the centre 8 inches of the large test welds. Furthermore on the smaller plates the weld bead width remained constant across the whole of the specimen whereas if the plates had been too small for quasi static heat flow conditions to be established the weld bead width would have increased from the starting point to the finishing point because of stored thermal energy in the plate. Consequently for ease of production it was decided to use the 6 inch x 12 inch plates for the test pieces and their preparation and joining will be described fully.

Plates approximately 12 inch x 6 inch were flame-cut from the as received ½ inch plate, these were shaped square along the 12 inch side, this direction being the rolling direction of the plate. Two shaped plates were then butted together and tack-welded at the ends, small run-on plates were then manually welded onto the ends of the plate to provide time to strike the arc and stabilise the welding conditions prior to the arc reaching the square butt preparation. The test plates were then welded together using a British Oxygen Company Quasi Arc Universal Welding Machine. Two passes were made using the submerged arc welding head. The wire and flux for the welding process were 1/8 inch diameter Dorman Long AB and ESAB 104S

respectively, both supplied by the pipe manufacturing company as typical of material used in seam welding of actual pipes. The wire, flux and weld deposit were analysed in order to compare them with the parent plate material.

Metallographic examination of the weldments produced was carried out in order to study the structure of the H.A.Z. produced by the welding process. Macro and micro hardness measurements were made on the weld and H.A.Z. in order to try to detect any zones of possible embrittlement. Attempts were also made to obtain tensile data on the joints. Tensile properties of the weld deposit itself were obtained using standard No. 11 Hounsfield specimens but even with tensile specimens with very short gauge sections no reliable information was obtained on the tensile properties of the H.A.Z. However it is possible to make reasonable estimates of the H.A.Z. strengths from the hardness values.

In order to test the integrity of the welds produced, bend tests in accordance with BS709 were performed. Specimens 1 inch x 6 inch x $\frac{1}{2}$ inch with the weld down the centre were bent round a 2 inch diameter former in the two directions shown in Figure 26.

C.O.D. fracture toughness tests were then carried out on specimens cut from the centre sections of the test weld plates. These specimens were the same size as the majority used in the studies of the parent plate material i.e. 1 inch deep x $\frac{1}{2}$ inch thick x 4 inch span.

In this series of specimens the notch tip was positioned so that it scanned the structure from weld metal through H.A.Z. to parent plate as shown schematically in Figure 27. Figure 28 shows that as the notch tip position is moved across from the weld metal to the parent plate, in all but the two extreme cases the notch tip spans a number of metallurgical structures. Cracking usually begins however at the mid-thickness point so that it ought to be possible using this technique to assess the toughness of all the components of the joint by taking the C.O.D. measured as indicative of the toughness of the material at the tip of the slot in the mid-thickness of the specimen. In order to confirm that cracking did occur in the centre of the specimen a series of weld specimens were loaded until crack initiation was detected then unloaded, cooled in liquid nitrogen and broken to reveal the position of crack initiation.

The initiation C.O.D.'s δ_i were then measured across the weldment with the crack growing down the weld as it would if travelling down the seam weld of a pipe.

The toughness in the through thickness direction across the joint was then measured by testing specimens ½ inch deep x ½ inch thick x 2 inch span, these being notched so that the crack would grow through the plate as in the case of a partial wall defect in a pipe, as shown in Figures 29 and 30. Apart from giving information about the toughness in this direction these specimens served as a check on the results from the longitudinal

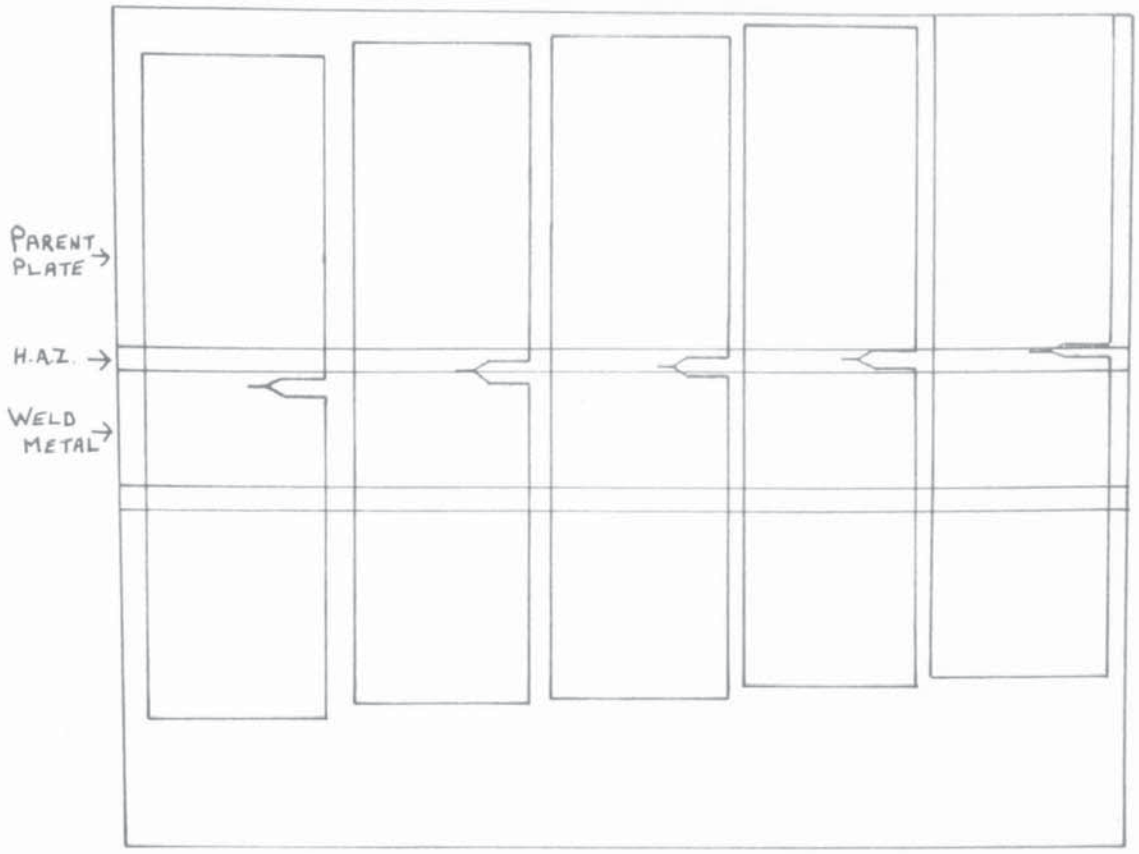

Figure 27 Positioning of Specimens Across the H.A.Z. in Longitudinal Specimens.

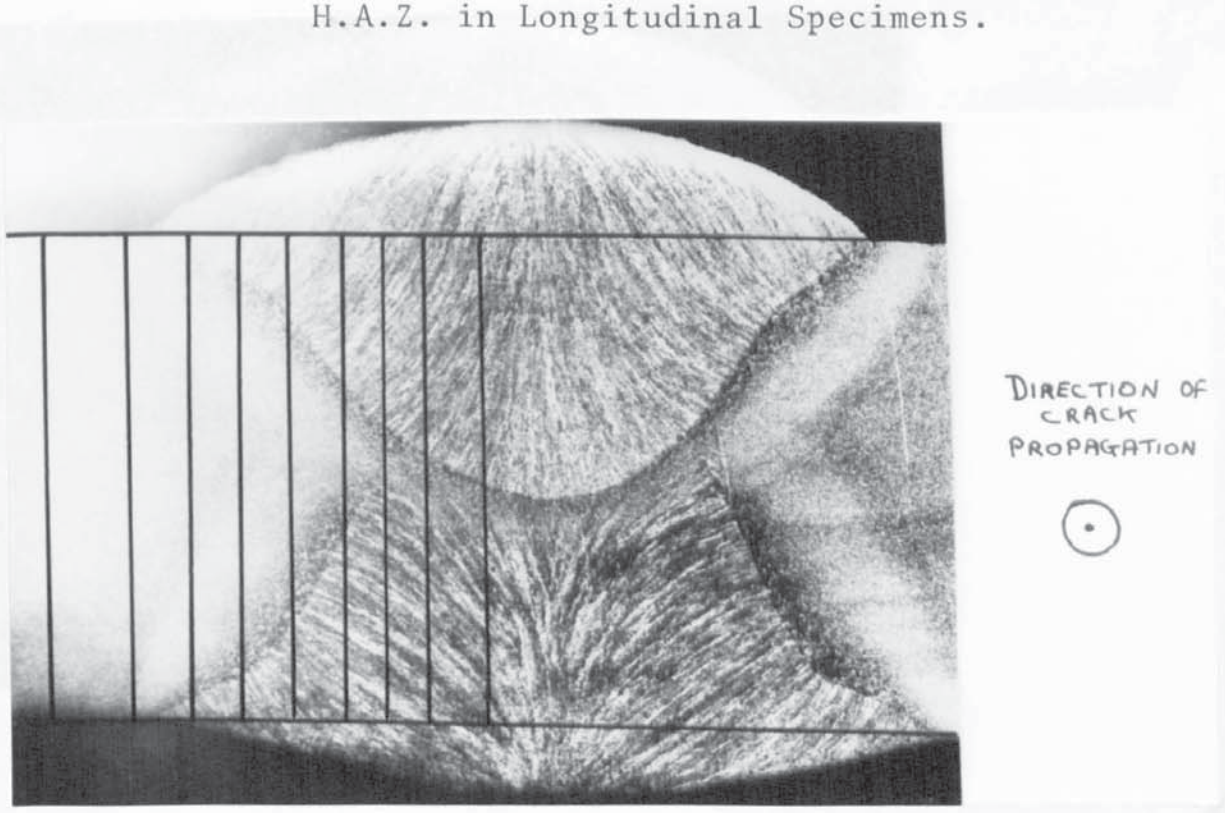

Figure 28 Positions of Notch Tip in Longitudinal Specimens

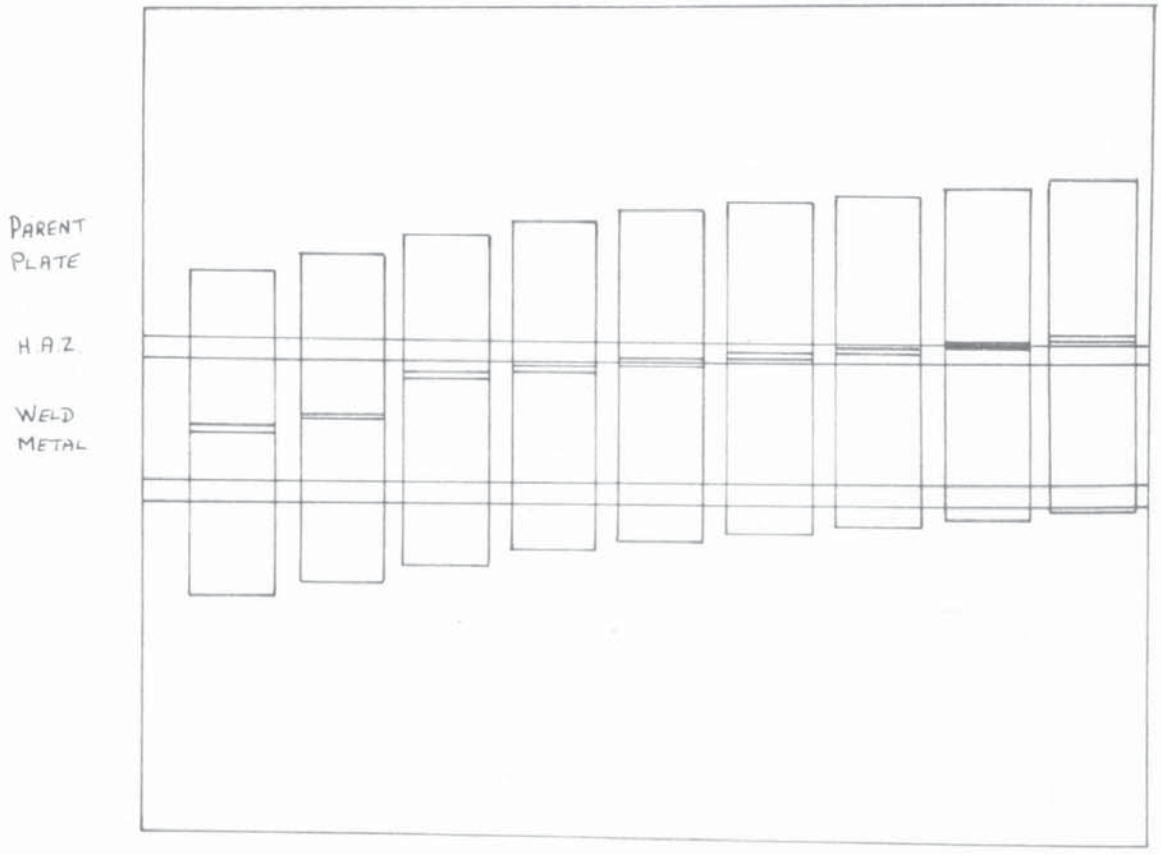

Figure 29 Positioning of Specimens Across the H.A.Z. in Through-Thickness Specimens

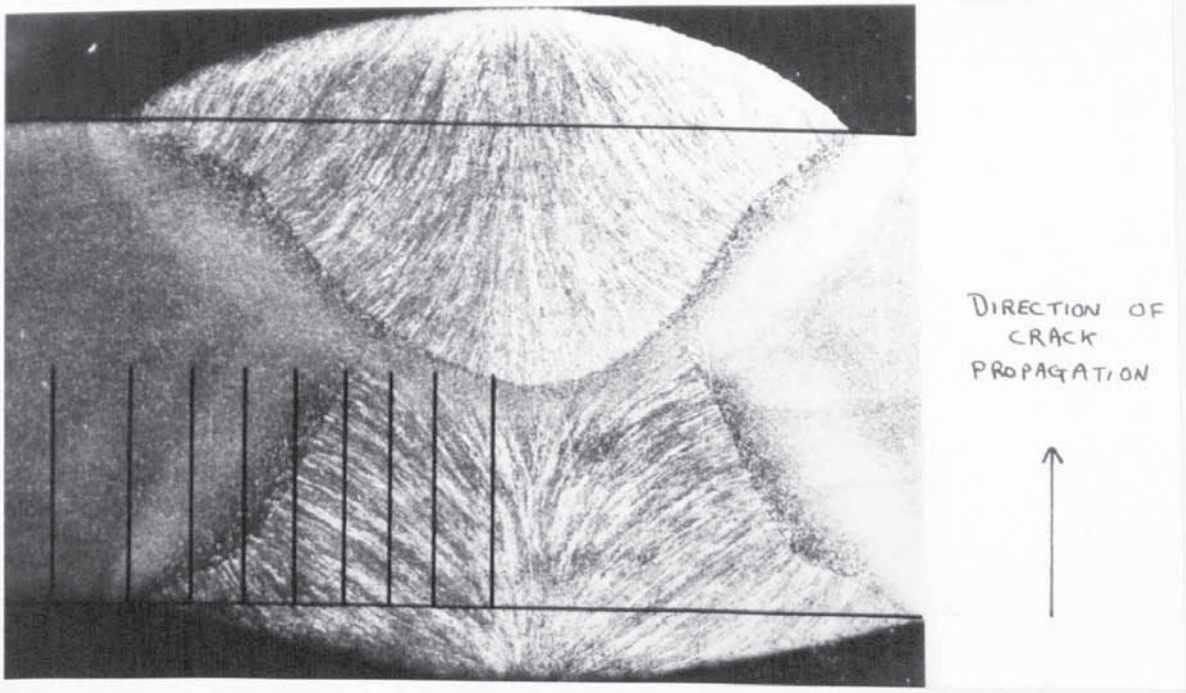

Figure 30 Positions of Notch Tip in Through-Thickness Specimens

specimens since in the case of the through-thickness specimens the notch tips could be located in one particular structure at a time.

The toughness in the longitudinal direction was later also measured on a series of bend specimens supplied by the Gas Council. These specimens had been machined from the seam weld of an X-52 pipe.

The effect of cracks approaching welds at angles rather than growing along the weld was then examined. Compact tension and bend specimens were cut from welded plates so that the angles between the specimen slot and the weld bead varied from 0^{o} to 90^{o} as shown schematically in Figures 31 and 32. These specimens were tested using an Instron testing machine in order to determine initially the crack paths in this situation. Up to an angle of about 75^{o} the crack was observed to turn from the normal to follow the line of the weld. This occurred on both bend and C.T.S. specimens, therefore eliminating any doubt that the effect could be connected with the peculiarities of the crack path in C.T.S. specimens, discussed earlier. This enabled the C.T.S. type of specimen to be used for the next part of the experiment thus providing a larger test area on which to study the effect.

Two more series of C.T.S. specimens were prepared with welds at various angles across the specimen, one series to examine the effect observed in the first series and to attempt to deduce its cause and the other series to make measurements of the C.O.D. in this situation.

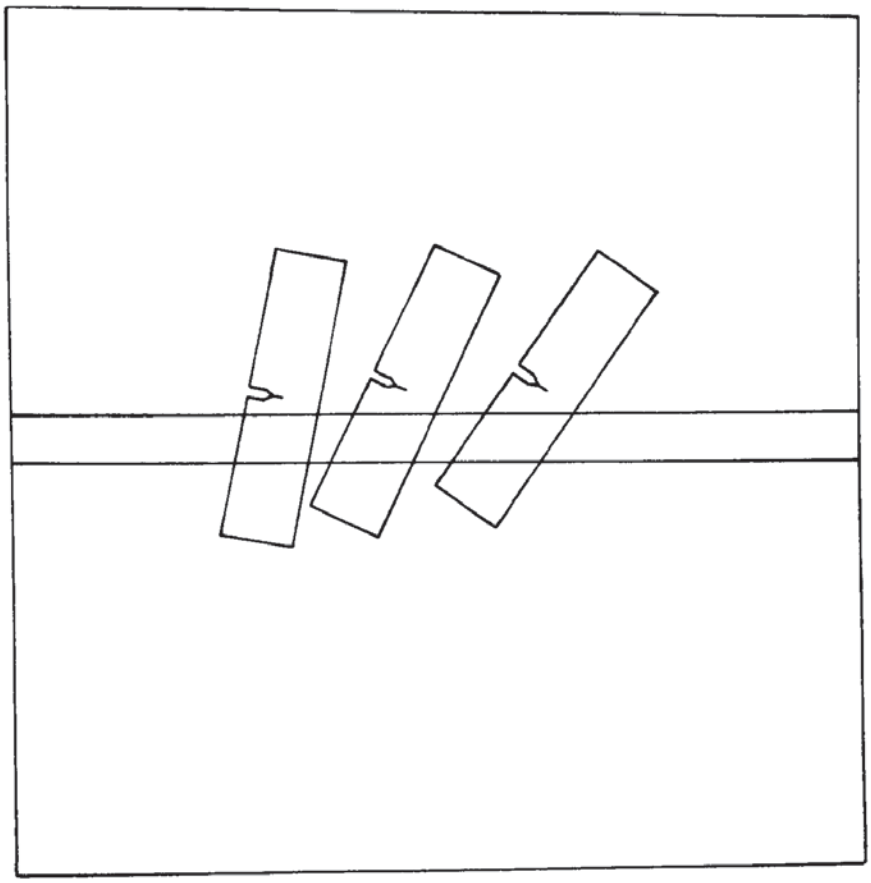

Figure 31 Preparation of Angled Bend Specimens

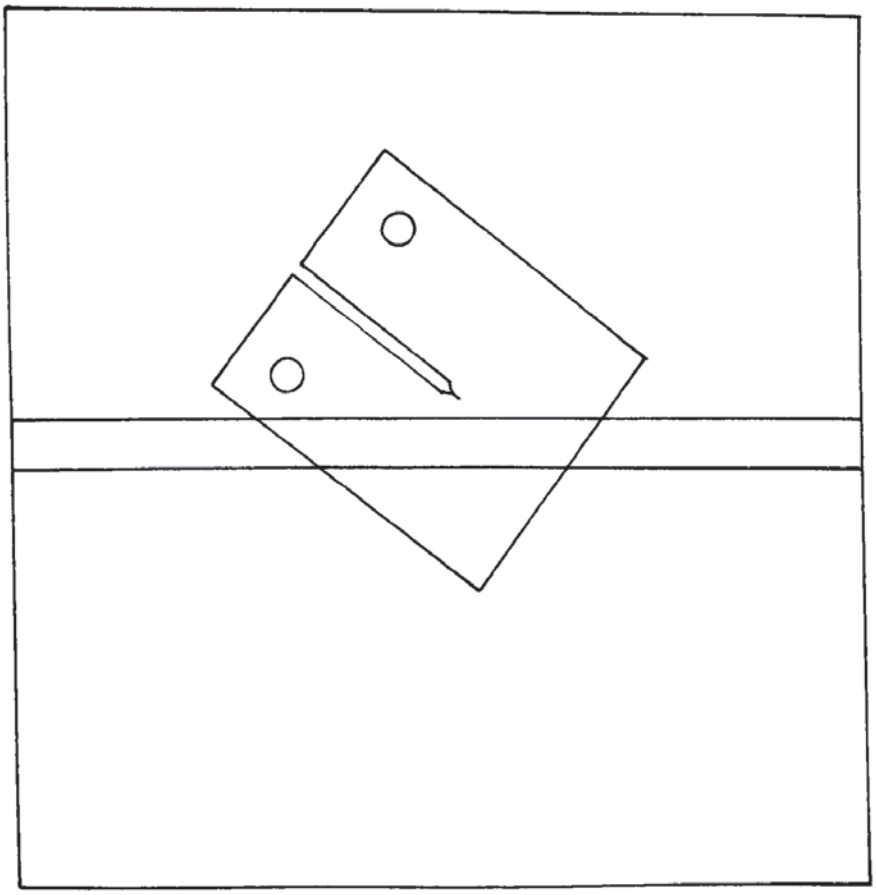

Figure 32 Preparation of Angled C.T.S. Specimens

Recent theoretical work at the University of Cambridge[97] has shown that the plastic zone at the tip of a crack can be highly distorted by the presence of a bimetal interface where one side of the interface has a lower yield stress than the other side. This is precisely the case in the present work where there exists such an interface between the parent plate and the hard heat affected zone. The specimens were therefore prepared with this in mind, they were surface ground and then coated with a brittle-laquer, Stresscoat ST-70, so that on testing the extent of plasticity could be observed.

The second series of specimens was used to measure the C.O.D. at the tip of the crack when it was moving parallel to the weld, at an angle to the normal and the maximum stress. In this situation the crack tip is subjected to both opening and shearing and 0.010 inch square grids were scribed onto the specimens in an attempt to measure the displacements occuring in both these directions. After testing the specimens and allowing the cracks to propagate they were unloaded and the grids remeasured to determine the opening mode C.O.D. δ_I, and the shearing mode C.O.D. δ_{II}, at the crack tip after crack arrest. This technique cannot be expected to be as accurate as that used in the earlier work to determine critical C.O.D.'s because of difficulty in locating the actual crack tip and also relaxation once the specimen is unloaded. It was felt however that the values measured

were very close to those which would have been measured on load and would in any case show the general form of the relationship between δ_I and δ_{II}. This simple method of measuring the two displacements was chosen because it was felt that the most direct measurement in this complex situation would provide the most reliable answers.

A few simple experiments were carried out in an attempt to add to the experimental evidence showing that C.O.D. is a valid measurement of post general yield fracture toughness. Even though the theoretical justification for C.O.D. cannot at present be extended beyond general yield where the technique finds its application, it was decided to try to examine the theoretical relationship between linear elastic and general yield fracture mechanics parameters namely:

$$G_c = \sigma_y \delta_c$$

In order to accomplish this it was necessary to measure G_c or K_c directly on a specimen on which the C.O.D. could also be measured. It was not possible to measure the C.O.D. on specimens which produce valid L.E.F.M. toughness values because the C.O.D.'s occurring on such specimens were too small. It was therefore necessary to make an estimate of the G or K value of a material which failed in a ductile manner and the method advanced by Stonesifer and Smith[40] which was described in the literature review gives such a means of estimating K_c from undersized specimens.

Bend specimens were tested and δ_i values determined on them. Using Stonesifer and Smiths technique the value of K, corresponding to the point at which δ_i was measured, was also calculated. These tests were performed on as received plate, weld metal and plate which had been given a variety of heat treatments simply to vary its toughness.

The value of K_c for the as received material was also estimated from the size of the plastic zone on C.T.S. specimens which had been coated with the brittle-laquer to indicate the extent of plasticity using the equation (11).

$$r_y = \frac{K_I^2}{2\pi\sigma_y^2}$$

The values of δ occurring at the crack tip corresponding to the calculated K value were also determined using the derivation of the above equation (21)

$$r_y = \frac{\delta E}{2\pi\sigma_y}$$

The metallography of the crack growth mechanisms in the X-52 material, the weld H.A.Z. region and the weld metal were studied using ordinary light microscopy and also scanning electron microscopy. This was carried out in order to determine the crack paths in the different structures which might explain any differences in toughness, and might enable some recommendations to be made for the improvement of the toughness of the material or the weld.

5. RESULTS

The results of the chemical analyses on the X-52 and X-60 plates are shown in Table I along with the A.P.I.5L.X specification of chemical composition for these materials. It can be seen that in both cases the manganese content is slightly higher than the maximum specified.

The metallographic examination of the X-52 plate revealed gross mechanical fibering in the rolling direction as is usual in hot worked products. Sections were examined as shown in Figure 33 and the metallographic structures obtaining in these sections are shown in Figures 34-36. The ferrite grain size in this material was determined to be 18 microns.

Tensile data obtained on the two plates by testing Number 11 Hounsfield test pieces isshown in Table II. In the condition tested the X-52 material has a yield stress significantly lower than the specified value of 52,000p.s.i.

The hardness of the two plates was 170 H_{V30} for the X-60 and 150 H_{V30} for the X-52. The X-52 plate was also examined for residual stresses by making a microhardness traverse across the thickness of the plate; no marked difference in hardness was observed from the surface to the centre line, as can be seen from Figure 37.

Table I

ANALYSES

	C_{max}	Mn_{max}	P_{max}	S_{max}	Nb_{min}	V_{min}	Ti_{min}
X-52 Plate							
Analysis	0.21	1.34	0.007	0.026	-	-	-
Specification	0.28	1.25	0.04	0.05	-	-	-
X-60 Plate							
Analysis	0.21	1.45	0.022	0.025	0.05	0.06	<0.001
Specification	0.26	1.35	0.04	0.05	0.005	0.02	0.03

Table II

TENSILE PROPERTIES

	Y.S. p.s.i.	U.T.S. p.s.i.	R of A %	ELONG $\frac{N}{}$ %
X-52 Plate				
Longitudinal	49,350	72,650	70	37
Transverse	49,200	72,500	55	34
X-60 Plate				
Longitudinal	65,100	90,250	50	28
Transverse	64,550	87,300	62	34

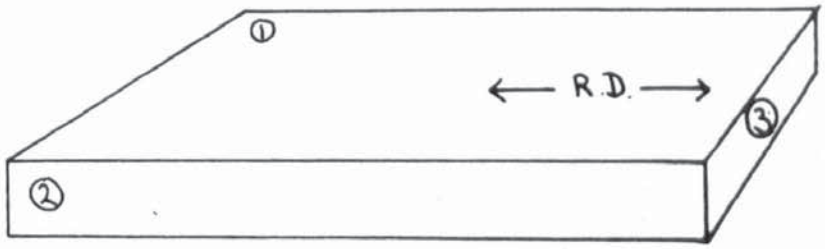

Figure 33 Positions of Microsections Shown in Figures 34-36

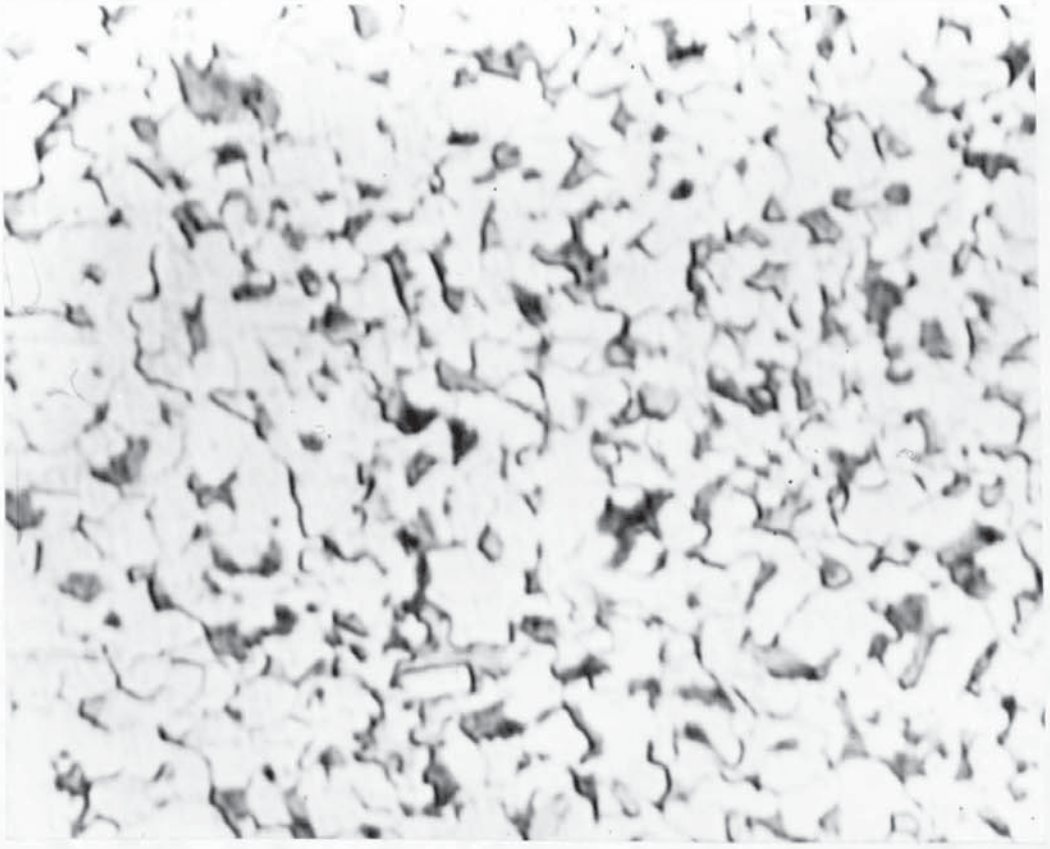

Figure 34 Microsection (1) x 400

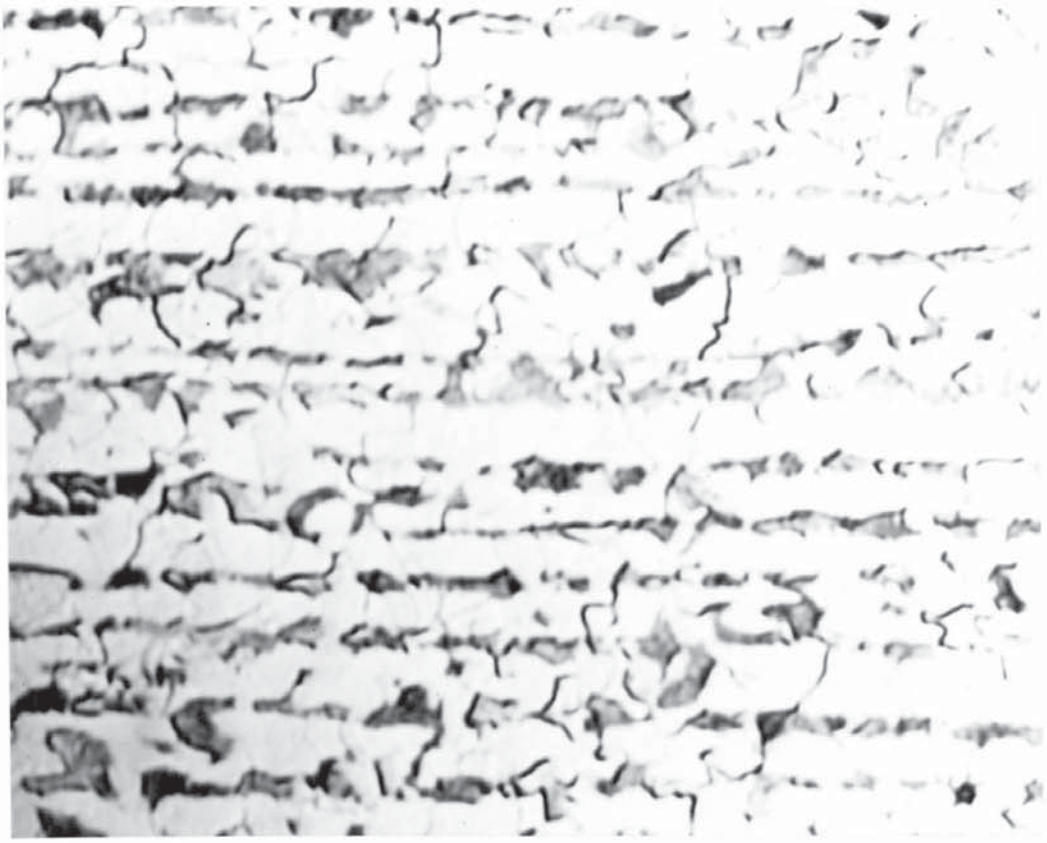

Figure 35 Microsection (2) x 400

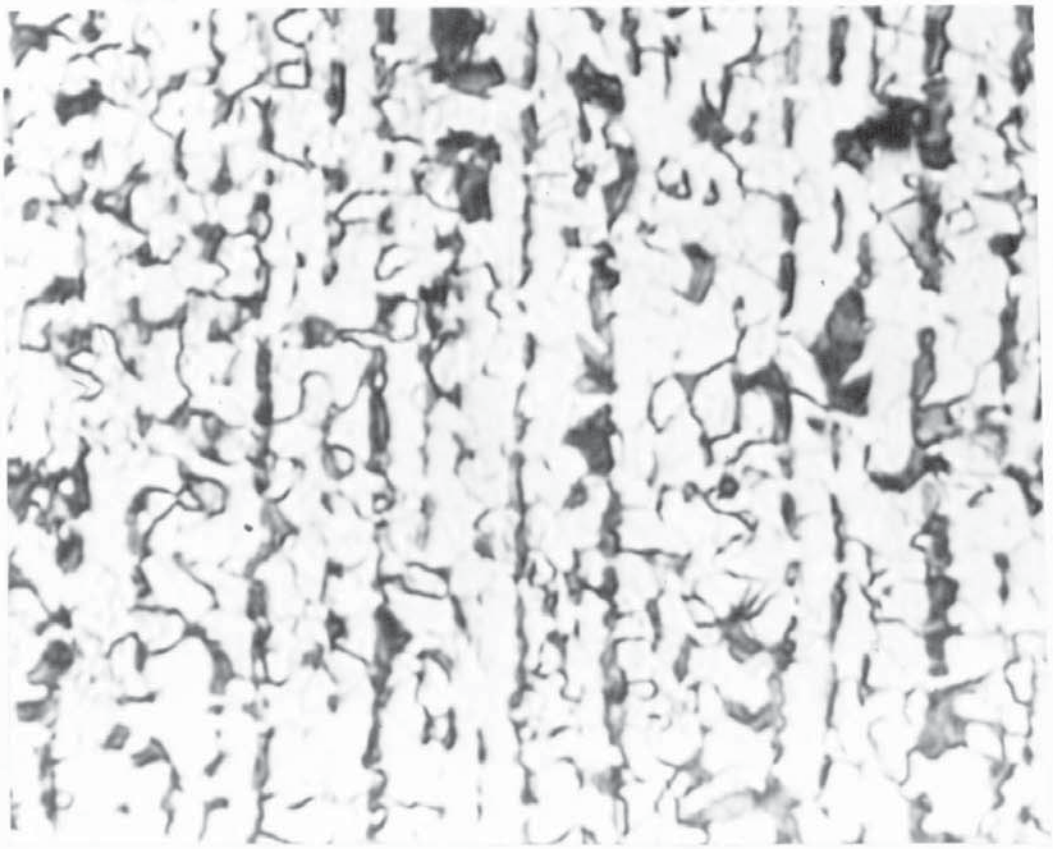

Figure 36 Microsection (3) x 400

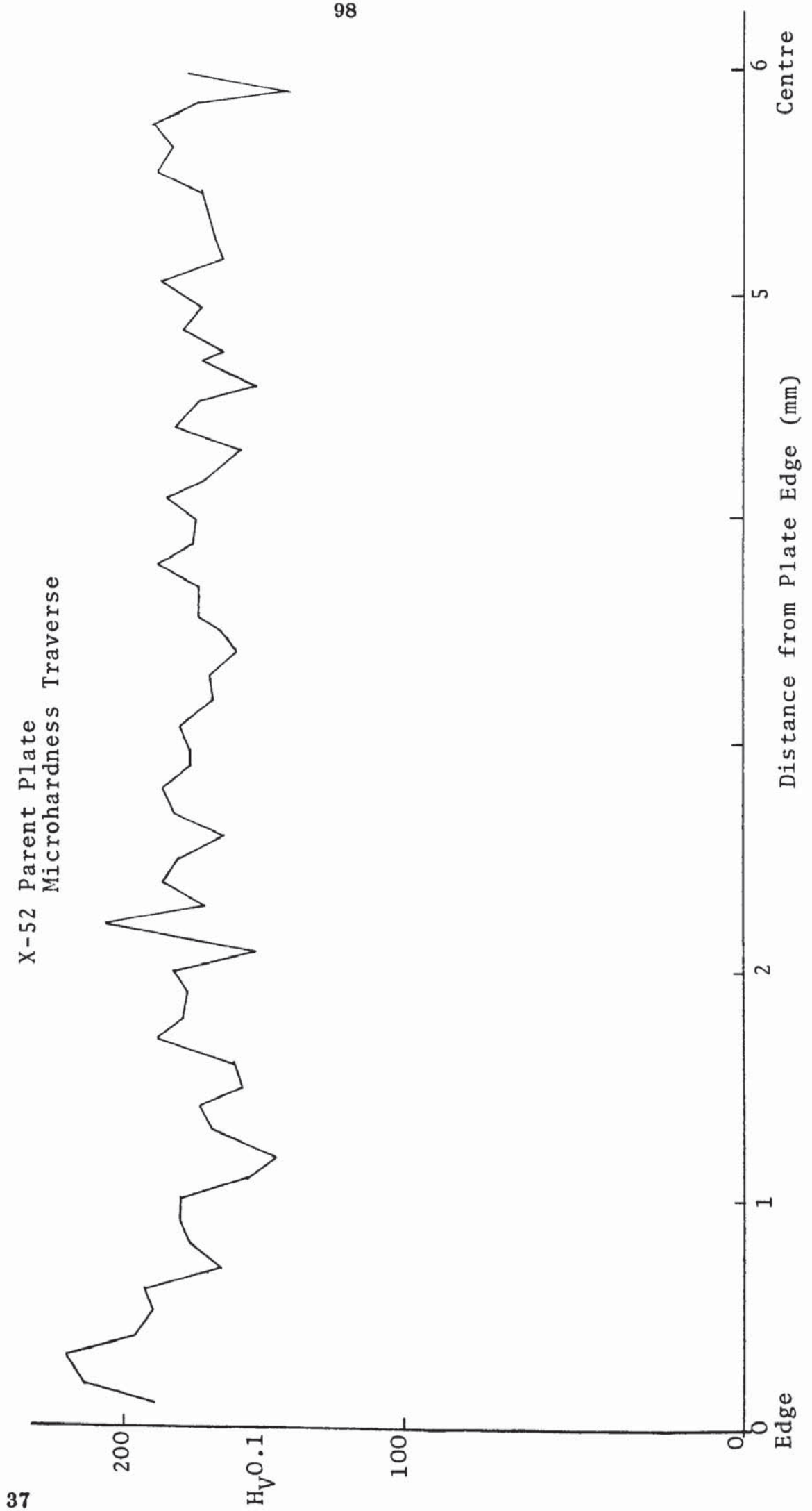
X-52 Parent Plate
Microhardness Traverse
200
100
0
H_V0.1
0
Edge
1
2
5
6
Centre
Distance from Plate Edge (mm)

Figure 37

Photographic calibration curves of C.O.D. versus offset plastic deflection were determined for all the types and geometries of specimens used in the investigation and are shown in Figures 38-41 During the calibration of the crack tip C.O.D. versus deflection, the variation of the C.O.D. with distance from the crack tip was also examined. Calibration curves were determined of C.O.D. against displacement for various positions relative to the notch tip, Figure 42. The curves obtained from a number of specimens were analysed by measuring the C.O.D.'s at distances from the crack tip for given increments of cross-head movement (0.02cm intervals). The results obtained revealed the general distribution of C.O.D. along a crack during various stages of a test. All the tests analysed showed that the C.O.D. variation along a crack is not linear as can be seen from the two sets of data presented in Figures 43 and 44.

The photographic calibration method was chosen in preference to the more usual clip gauge technique because when calibration of the accepted equation linking clip gauge to crack tip C.O.D., namely

$$\frac{\delta_{CG}}{\delta_t} = \frac{n(a + z)}{d} + 1$$

was attempted, to determine a value of n the equation was found to be unacceptably inaccurate.

C.O.D. Calibration Curves

Bend Specimens

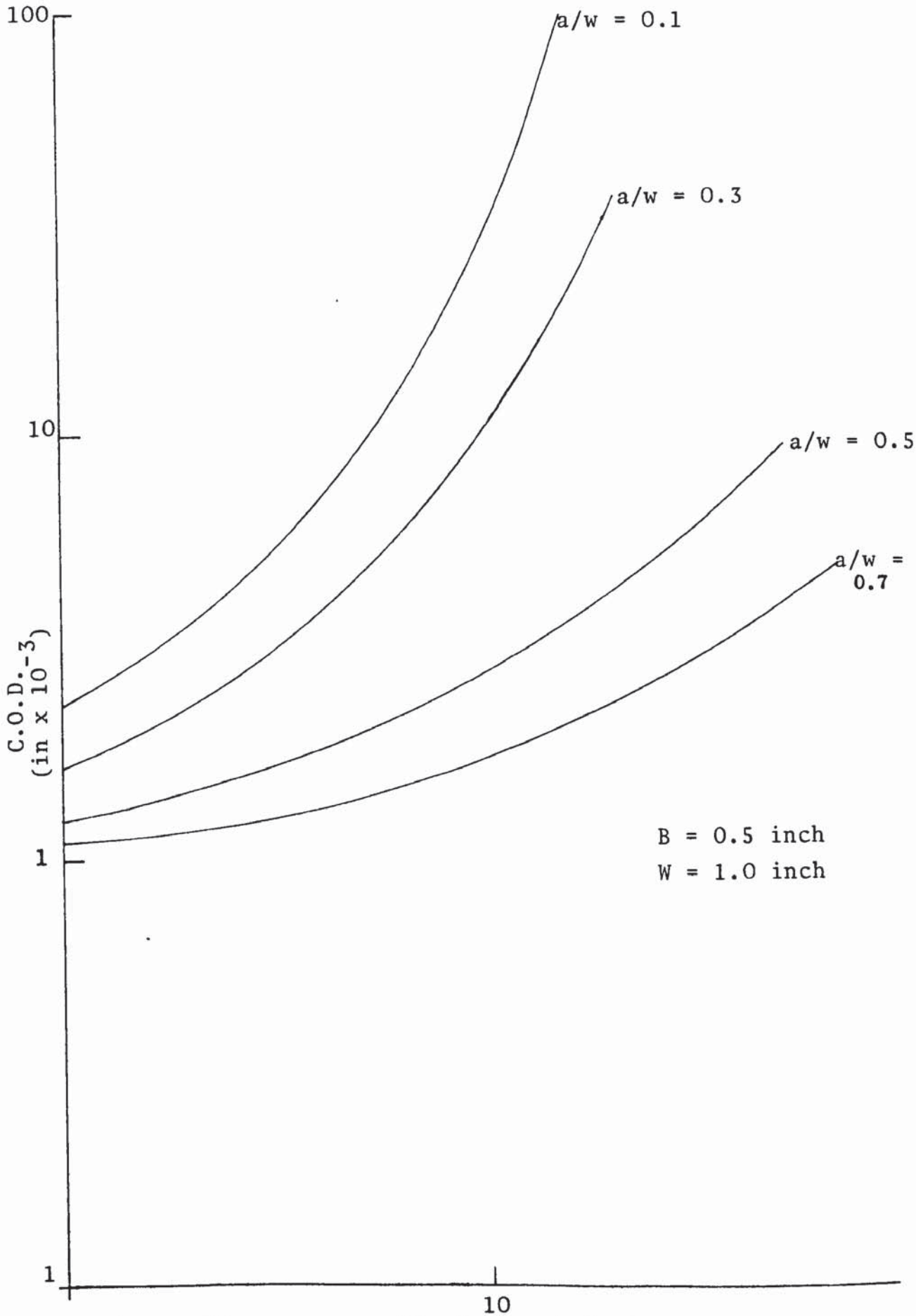

Figure 38

C.O.D. Calibration Curves

Reduced Thickness Bend Specimens

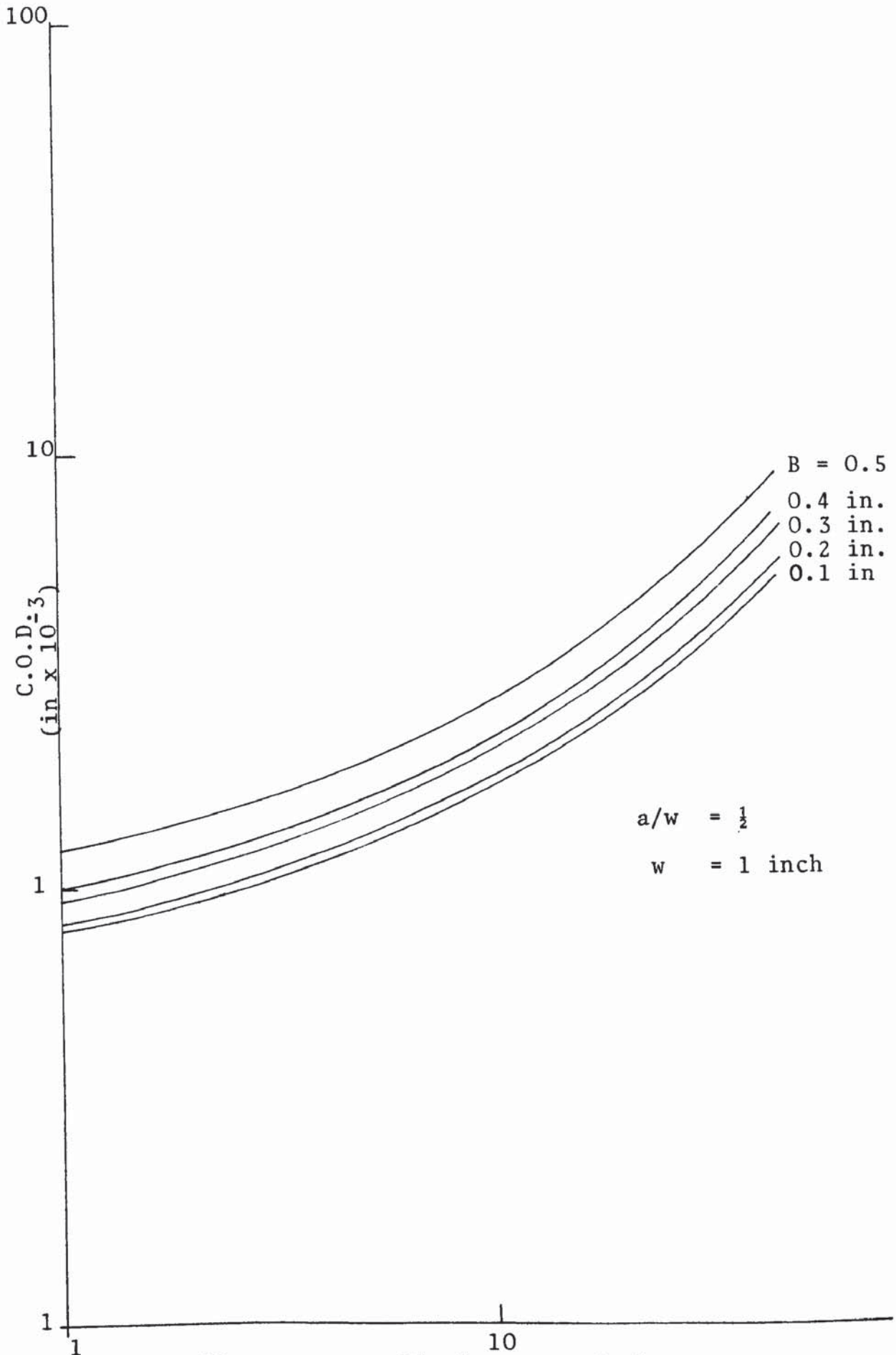

Figure 39

C.O.D. Calibration Curves

Sub-Size Bend Specimens

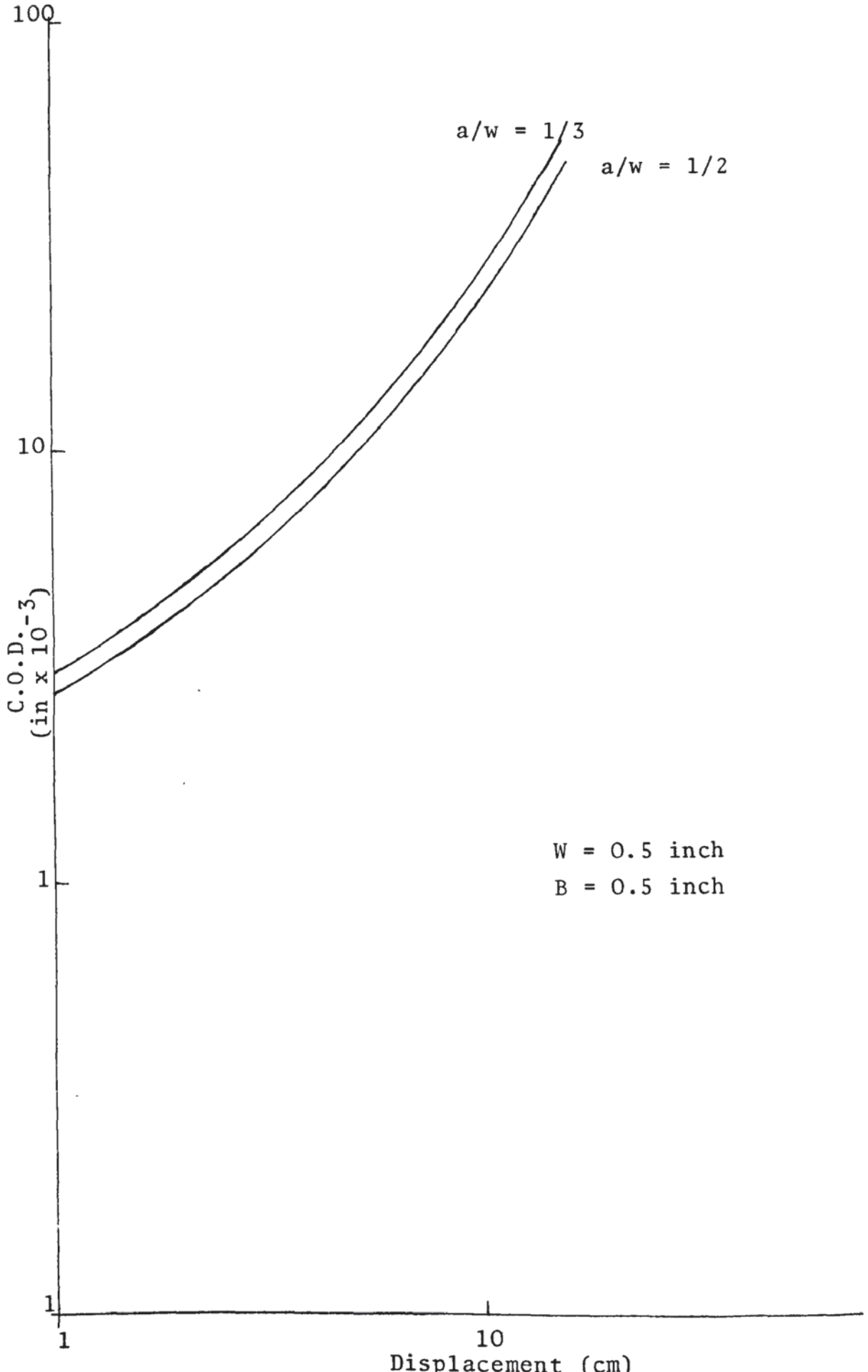

Figure 40

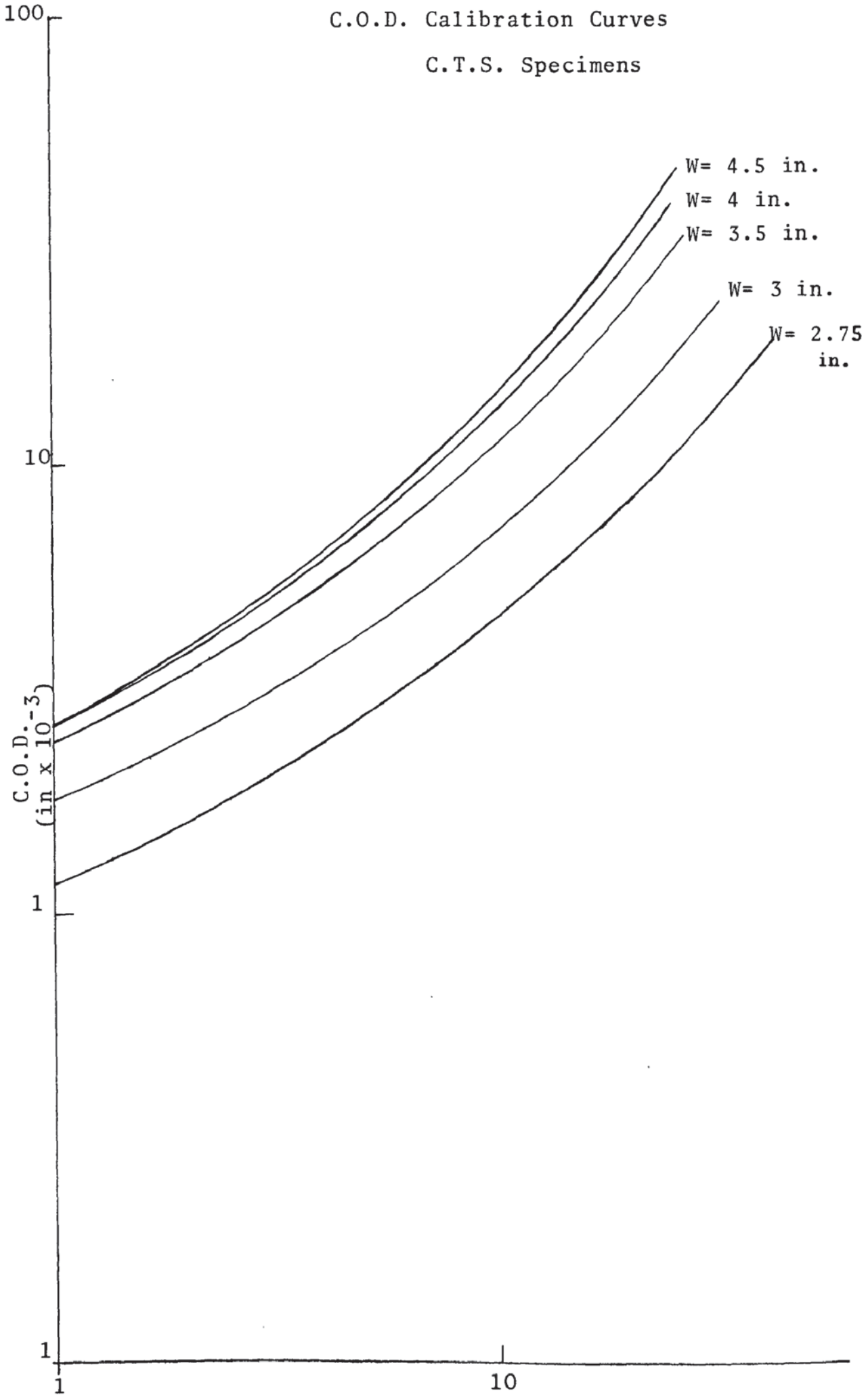
C.O.D. Calibration Curves
C.T.S. Specimens
W= 4.5 in.
W= 4 in.
W= 3.5 in.
W= 3 in.
W= 2.75 in.
100
10
1
1
1
10
C.O.D.-3 (in x 10)
Displacement (cm)

Figure 41

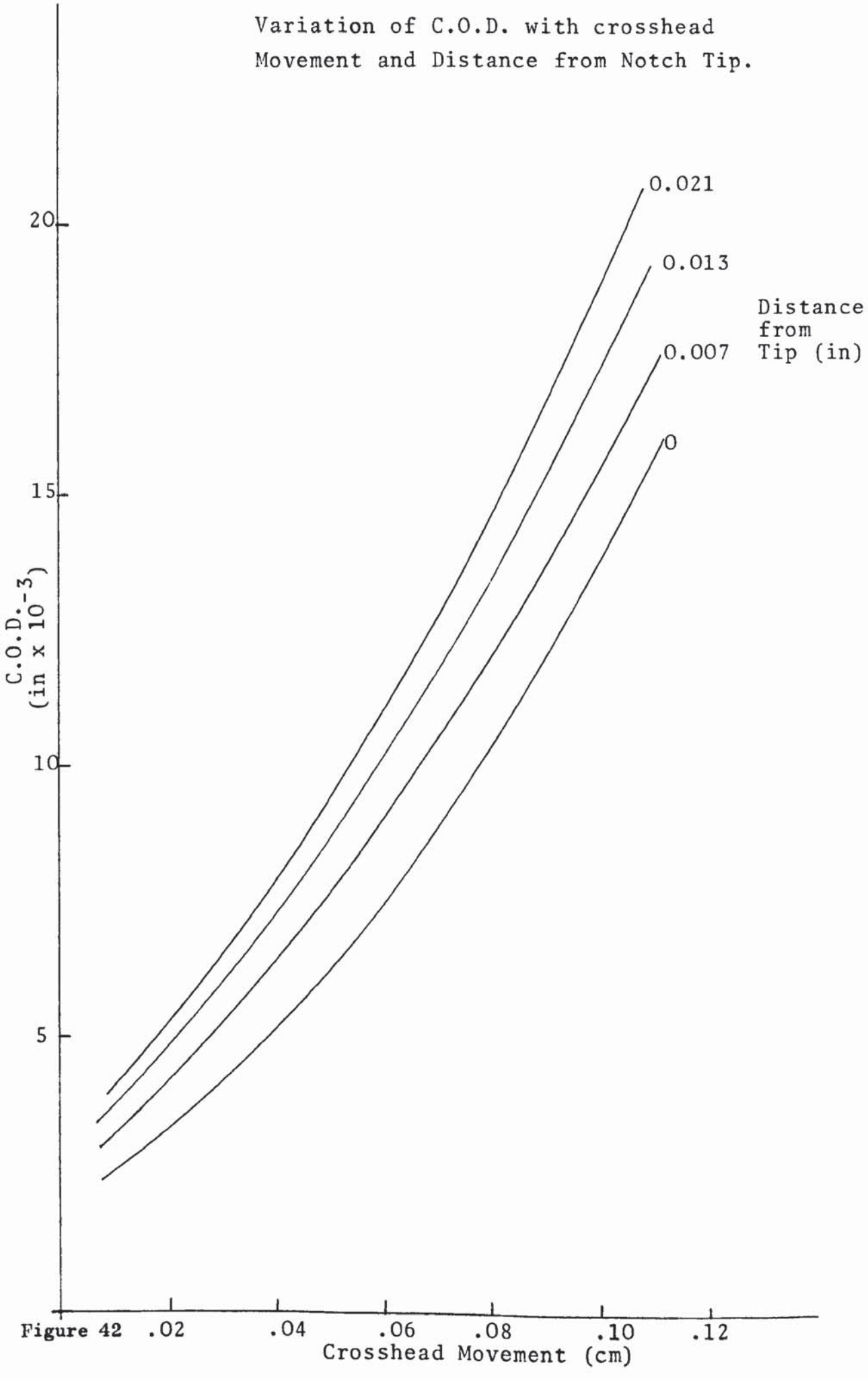
Variation of C.O.D. with crosshead
Movement and Distance from Notch Tip.
0.021
0.013
0.007
0
Distance
from
Tip (in)
20
15
10
5
C.O.D. (in x 10^-3)
.02
.04
.06
.08
.10
.12
Crosshead Movement (cm)

Figure 42

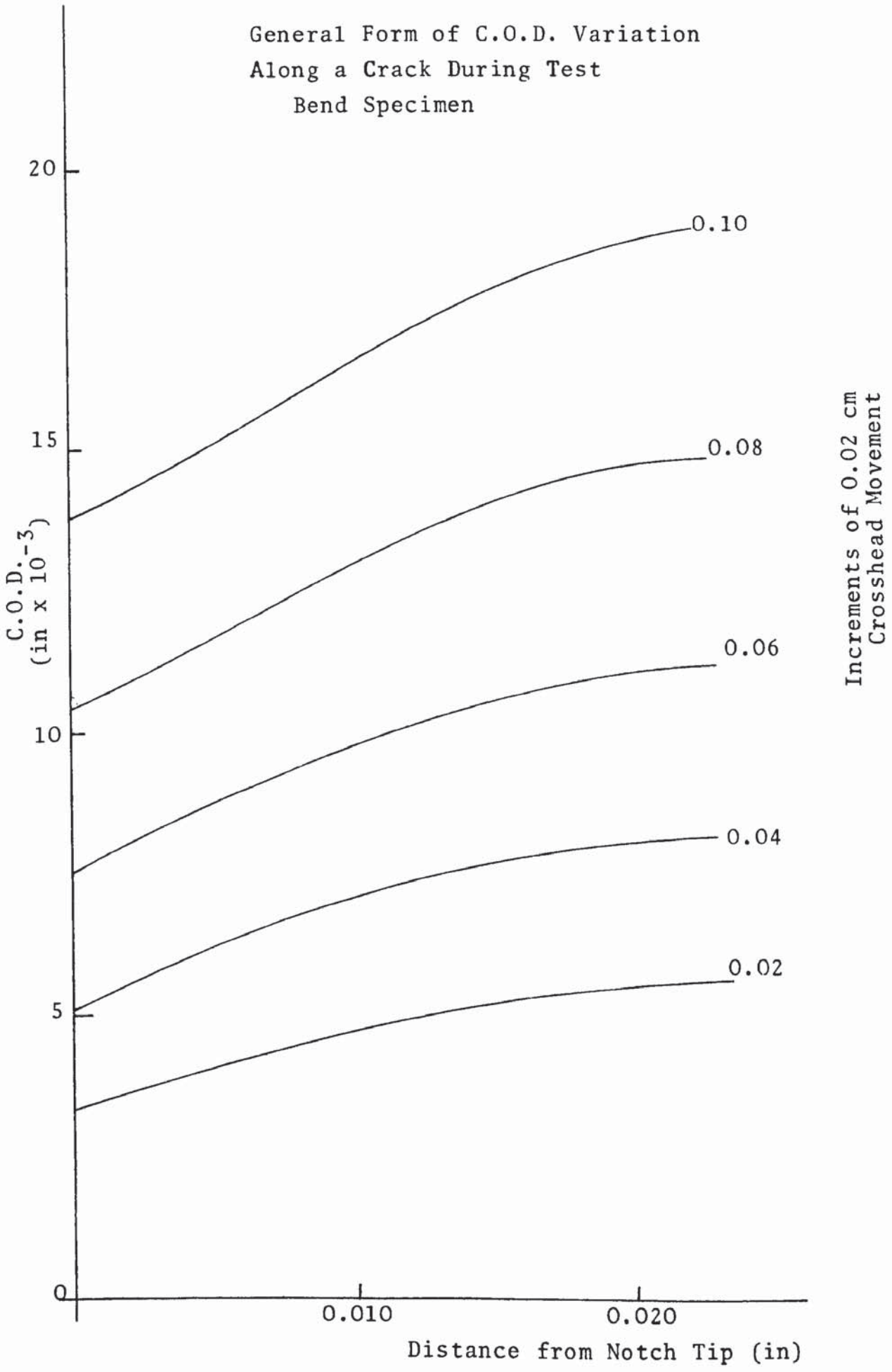
General Form of C.O.D. Variation
Along a Crack During Test
Bend Specimen
20
15
10
5
0
C.O.D. (in x 10^{-3})
0.10
0.08
0.06
0.04
0.02
Increments of 0.02 cm
Crosshead Movement
0.010
0.020
Distance from Notch Tip (in)

Figure 43

General Form of C.O.D. Variation
Along a Crack During Test
C.T.S. Specimen

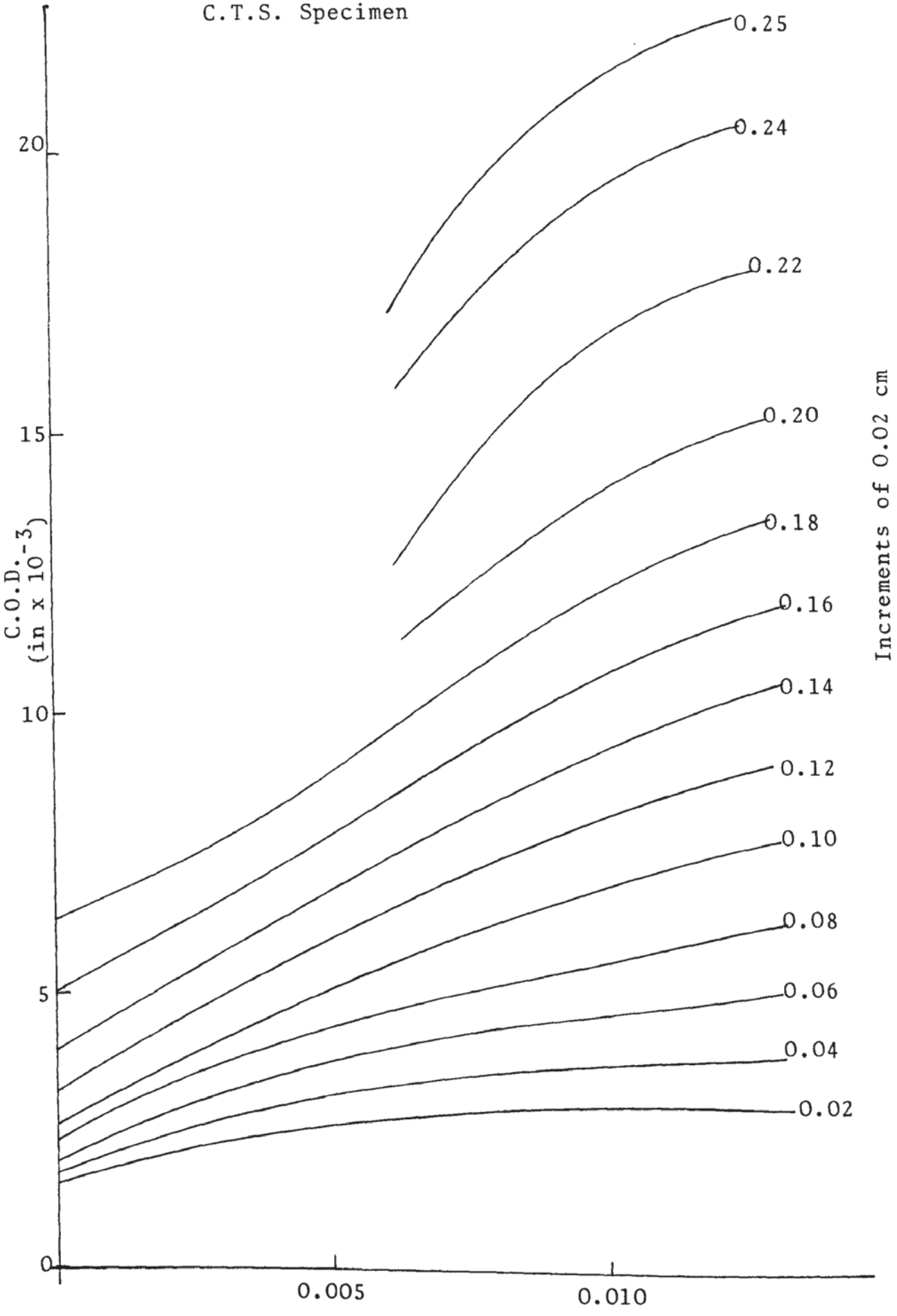

Figure 44

Figures 45 and 46 show the results of attempts to obtain such a calibration, by photographing the crack tip at the same time as obtaining the clip gauge opening. Straight lines corresponding to the published equation for various values of n between 2 and 6 are shown along with the actual calibration which can be seen to be a parabola. In order to use to clip gauge technique therefore, photographic calibrations would have to be produced for every type of specimen just as in the technique actually used. It was therefore decided to eliminate the clip gauge and its associated electronic equipment which might have produced errors and use only the displacement on the machine chart as the measure of C.O.D.

The C.O.D. variation from surface to centre was checked by stopping several tests, unloading the specimen and measuring the surface C.O.D. optically, then grinding the specimen down and measuring the C.O.D. every 0.050 inch. All the specimens examined showed no variation of C.O.D. between surface and centre other than that which could be associated with measurement errors that is within $\pm$ 0.0005 inch.

The ultrasonics system used to determine the initiation of cracking was calibrated by measuring the crack growth on specimens unloaded and sectioned after various signal level changes.

Relationship between Clip Gauge and Notch Tip C.O.D.

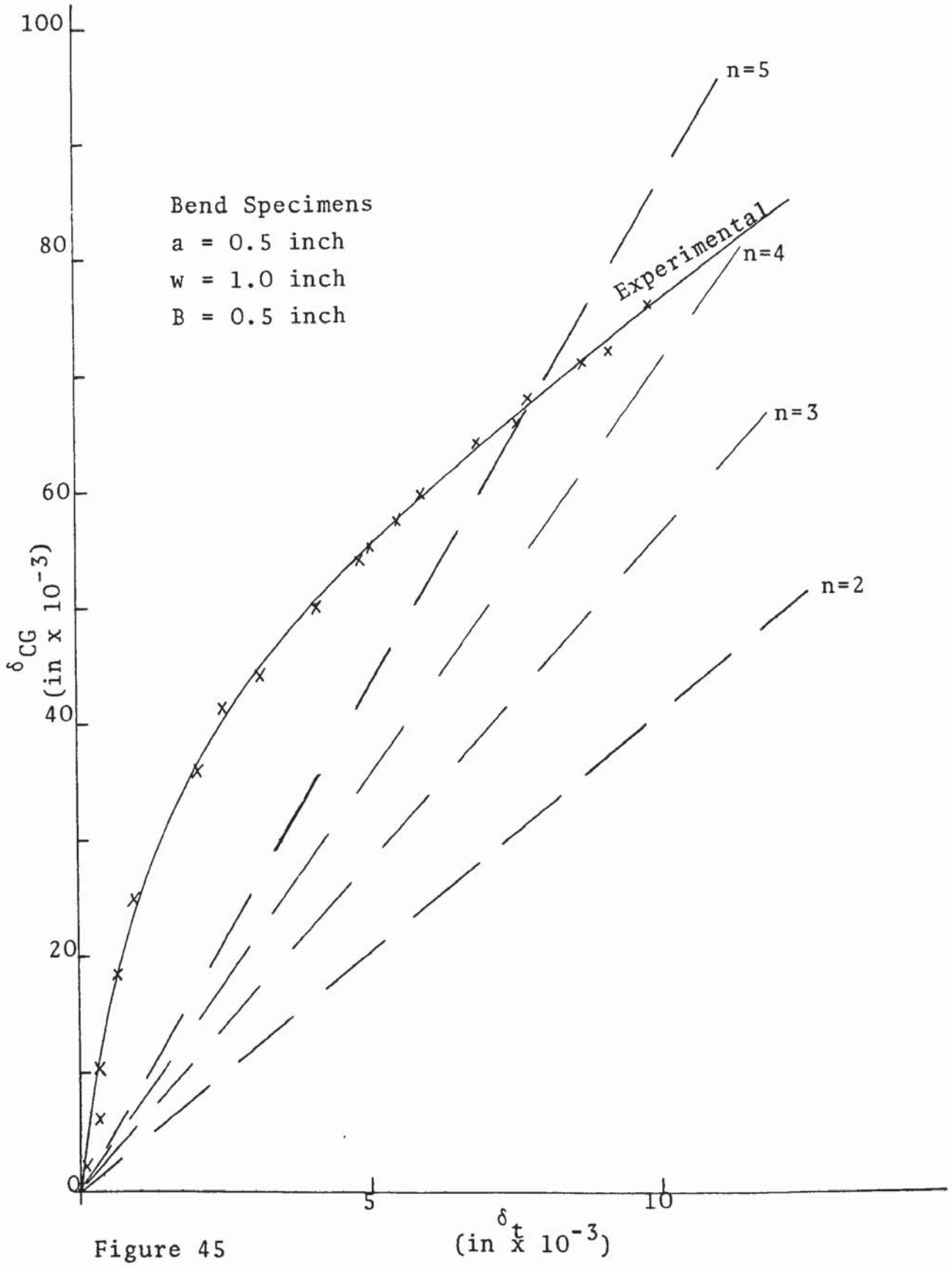

Figure 45

Relationship between Clip Gauge
and Notch Tip C.O.D.

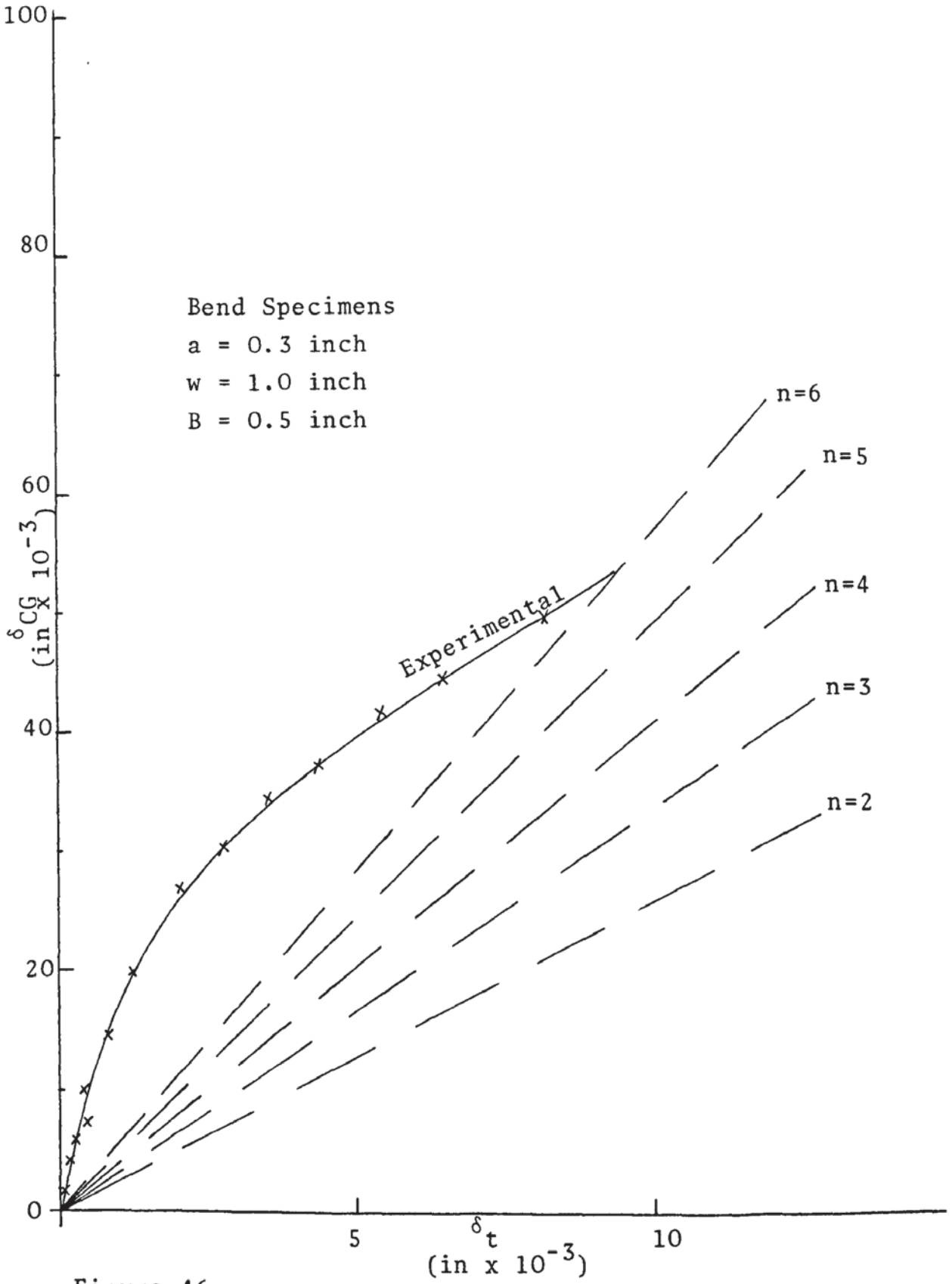

Figure 46

From these measurements it was decided to use a signal level change of 2 decibels as being that which gave a meaningful measure of crack growth which was of the order of 0.025 inch deep.

The use of the initiation of cracking C.O.D. δ_i, as a measure of the critical C.O.D. was checked by measuring δ_i and the maximum load C.O.D. δ_m, on bend and C.T.S. test pieces. The results are tabulated in Table III and shown graphically in Figures 47 and 48. These tests showed that the δ_i value was ostensibly constant over the whole range of specimens tested as opposed to the maximum load C.O.D. which varied widely.

The initiation C.O.D. as measured using the ultrasonic technique was checked using the destructive technique and the results for bend specimens containing both 0.008 inch slots and fatigue cracks are shown in Table IV and Figure 49. These results give very nearly the same δ_i as the ultrasonic technique namely 0.004 inch for fatigue cracked specimens and 0.0039 inch for specimens containing a 0.008 inch slot; that is the same value on both fatigue cracked and slotted specimens. This effect was also noted in the next experiment where δ_i was measured using the ultrasonic technique on bend specimens containing fatigue cracks, 0.008 inch slots and 0.012 inch slots. Both fatigue cracks and 0.008 inch slots gave δ_i values of approximately 0.004 inch while the 0.012 inch slotted specimen gave a value around 0.005 inch. These results are shown in Table V and Figure 50.

Table III

BEND SPECIMENS W CONSTANT AT 1 inch

a/w	δ_i in x 10^{-3}	δ_m in x 10^{-3}
0.100	3.2	11.0
0.100	3.8	10.0
0.125	3.9	9.5
0.125	-	7.5
0.125	4.0	9.0
0.130	3.0	9.0
0.200	5.0	-
0.220	-	12.0
0.240	-	6.8
0.250	3.6	6.5
0.260	-	11.0
0.270	3.4	6.5
0.270	6.0	-
0.290	4.8	6.0
0.480	-	4.8
0.480	3.4	6.0
0.480	3.7	4.5
0.490	3.6	6.5
0.490	4.0	5.2
0.500	3.1	4.8
0.500	3.6	6.0
0.700	-	4.7
0.700	4.7	5.1
0.700	3.4	5.9
0.700	4.8	-
0.710	4.2	5.4
0.710	4.5	4.5
0.720	4.0	-
0.750	3.8	5.5
	Mean 3.97 S.D. 0.51	

C.T.S. SPECIMENS a CONSTANT AT 2.5 inch

a/w	δ_i in x 10^{-3}	δ_m in x 10^{-3}
0.556	3.5	23.0
0.556	4.1	28.0
0.625	3.1	20.0
0.625	4.5	24.0
0.715	4.0	23.0
0.715	4.0	27.0
0.835	3.1	12.0
0.835	4.0	22.0
0.910	3.0	14.0
0.910	4.0	10.0
	Mean 3.73 S.D. 0.52	

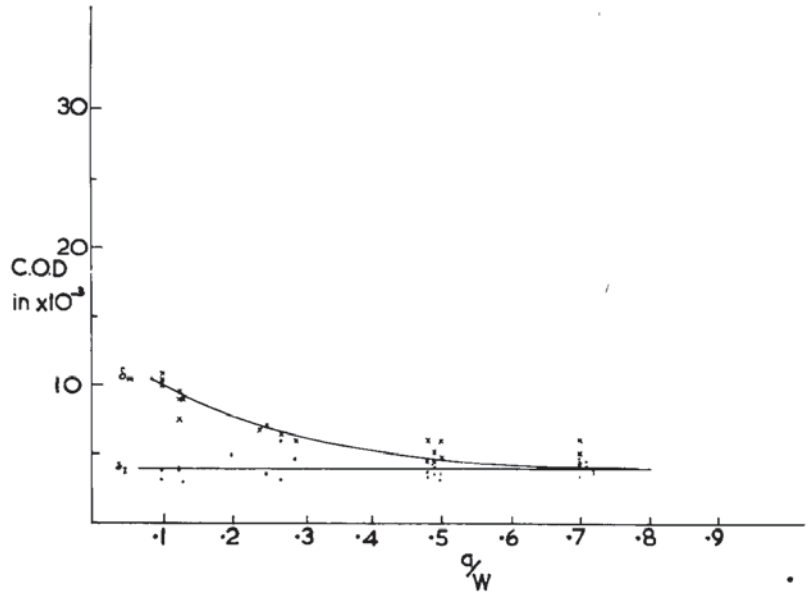

Figure 47 Effect of a/w on δ_i and δ_m
Bend Specimens

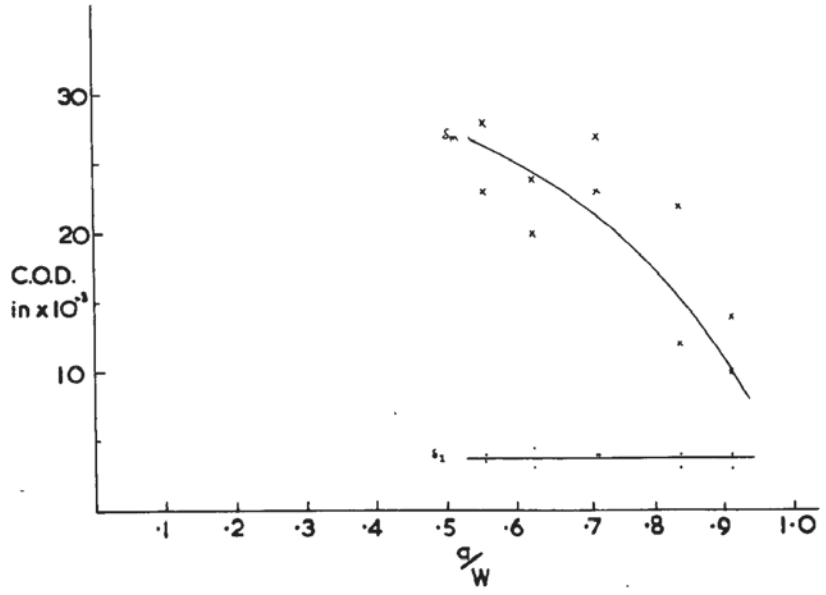

Figure 48 Effect of a/w on δ_i and δ_m
C.T.S. Specimens

Table IV

AREA OF SLOW CRACK GROWTH VERSUS C.O.D.

FATIGUE CRACKED		0.008 inch Slot	
δ(in x 10^{-3})	Area (Relative)	δ(in x 10^{-3})	Area (Relative)
4.2	0.115	4.3	0.075
4.5	0.200	4.6	0.100
5.0	0.550	4.8	0.140
5.2	0.370	5.1	0.200
5.4	0.315	5.1	0.255
5.5	0.230	5.5	0.395
5.7	0.435	5.6	0.310
6.1	0.605	6.0	0.490
6.4	0.720	6.5	0.430
6.5	0.525	6.8	0.360
7.0	0.640	6.9	0.515
		7.2	0.570
		7.2	0.625
		7.7	0.645
		7.7	0.690

Table V

EFFECT OF NOTCH ACUITY ON δ_i

FATIGUE CRACKED δ_i(in x 10^{-3})	0.008 inch Slot δ_i(in x 10^{-3})	0.012 inch Slot δ_i(in x 10^{-3})
4.0	3.0	4.5
3.8	3.9	5.5
3.6	4.0	4.7
4.2	4.2	3.8
3.7	3.8	5.8
Mean 3.86	Mean 3.78	Mean 4.86
S.D. 0.24	S.D. 0.46	S.D. 0.80

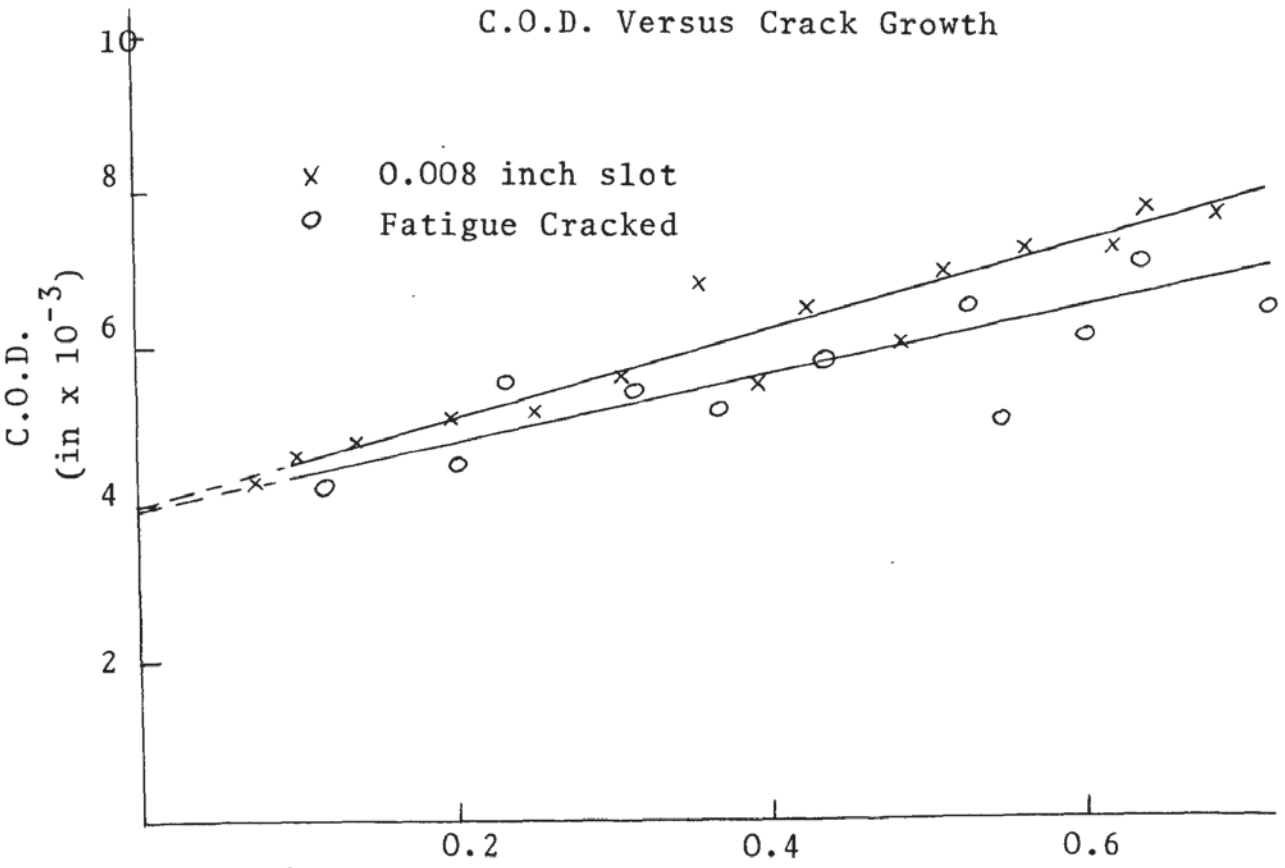

Figure 49

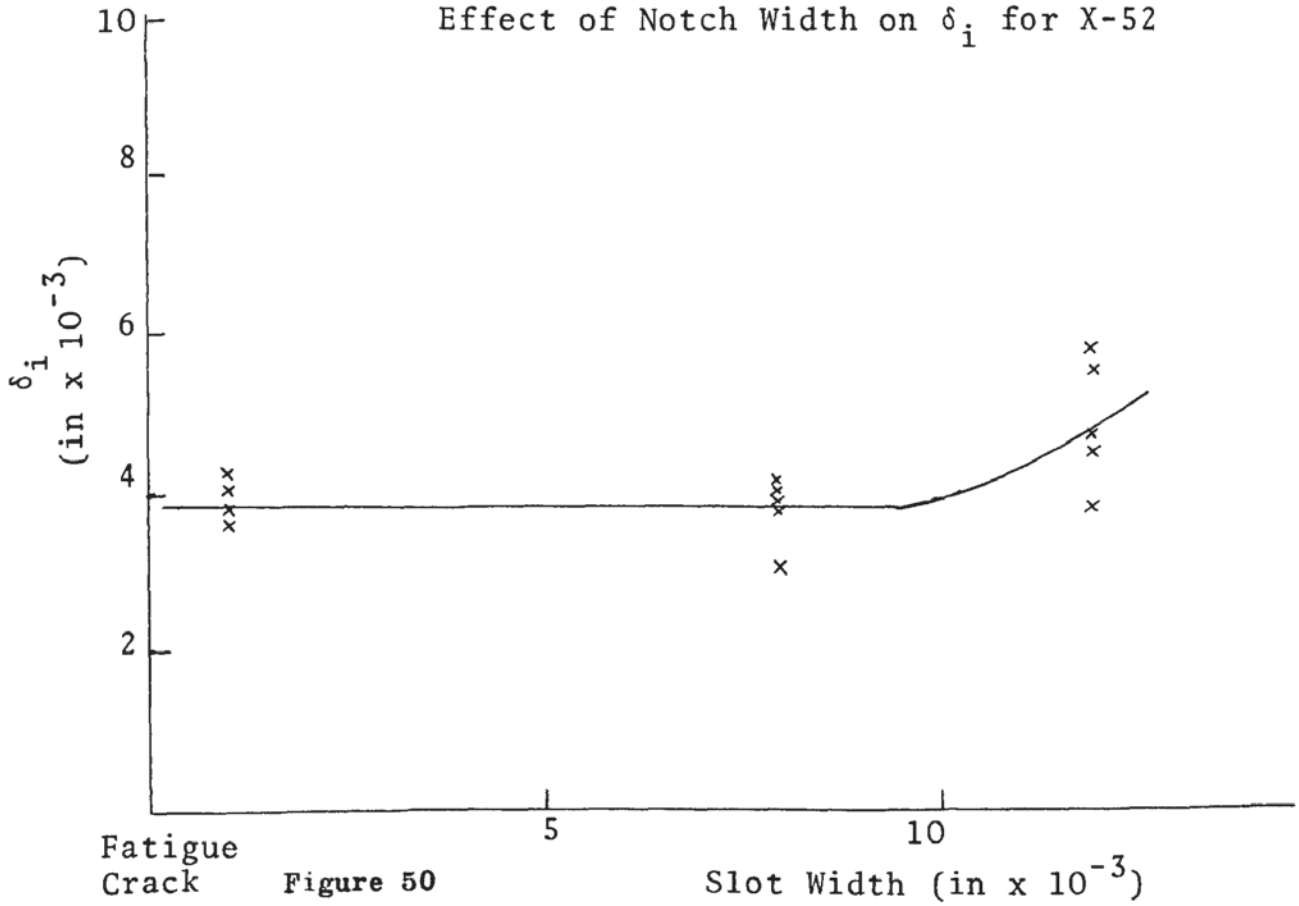

Figure 50

The tests on sub-sized specimens also showed no effect on δ_i as can be seen in Table VI, but the effect of reducing the thickness of the test pieces produced a small increase in δ_i from 0.004 inch at 0.5 inch thick to 0.005 inch at 0.1 inch thick as shown in Table VII and Figure 51.

The measurements of δ_i in the different orientations of the as received X-52 plate showed marked directionality, the initiation C.O.D.'s being 0.004 inch in the longitudinal direction, 0.011 inch in the transverse direction and 0.008 inch in the through thickness direction as shown in Table VIII. The longitudinal toughness however appeared to be unaffected by temperature down to -50°C as shown in Table IX.

The welding conditions chosen to produce the welds used in the second part of the research programme are shown in Table X along with the conditions used on actual pipe seam welds.

Using Roberts and Wells equation the width of the H.A.Z.'s can be calculated for both situations.

$$H = 8\kappa T \left(\frac{1}{5} + \frac{vd}{4\alpha} \right)$$

H = rate of heat input to plate (cal/sec/cm)

κ = thermal conductivity (0.17 cals/cm sec°C)

α = thermal diffusivity (0.2 cm^2/sec)

v = welding speed (cm/sec)

T = Temperature rise (°C)

d = heated width (cm)

Table VI

SUB-SIZE BEND SPECIMENS

INITIATION C.O.D.'s

	δ_i (in x 10^{-3})
	3.8 3.2 3.4 4.2 4.1
Mean	3.74
S.D.	0.43

Table VII

EFFECT OF THICKNESS ON δ_i

Thickness	0.4 inch	0.3 inch	0.2 inch	0.1 inch
	δ_i (inx10^{-3})	δ_i (inx10^{-3})	δ_i (inx10^{-3})	δ_i (inx10^{-3})
	3.5 5.0 4.0 3.7	4.5 5.0 4.7 5.2	4.6 5.0 4.9 4.2	4.5 5.0 5.8 4.5
Mean	4.05	4.85	4.68	4.95
S.D.	0.67	0.31	0.36	0.61

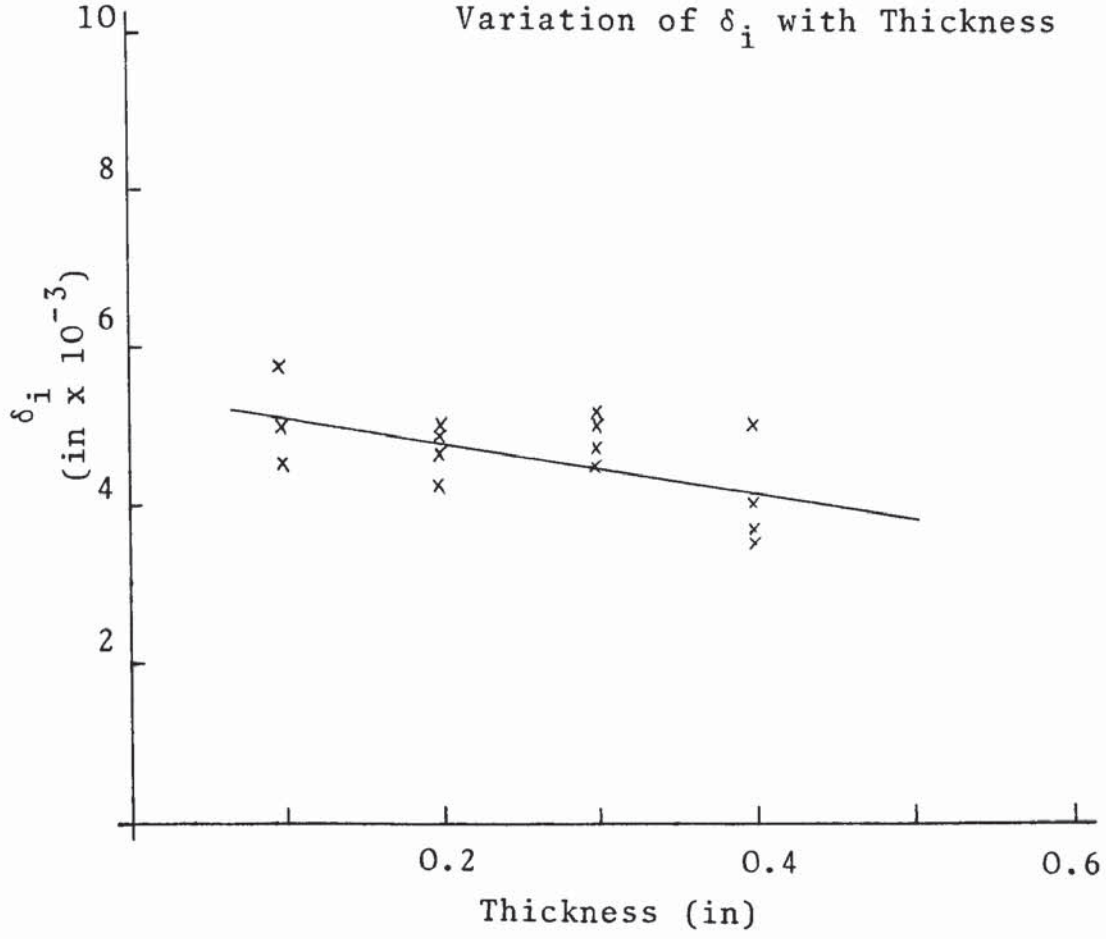
Variation of δ_i with Thickness
10
8
6
4
2
δ_i (in x 10^{-3})
0.2
0.4
0.6
Thickness (in)

Figure 51

Table VIII

EFFECT OF PLATE ORIENTATION ON δ_i

LONGITUDINAL	THROUGH-THICKNESS	TRANSVERSE
δ_i (in x 10^{-3})	δ_i (in x 10^{-3})	δ_i (in x 10^{-3})
3.0 3.9 4.0 4.2	12.0 11.0 10.0 10.5	8.0 8.4 9.5 7.7
Mean 3.78 S.D. 0.53	Mean 10.88 S.D. 0.85	Mean 8.40 S.D. 0.79

Table IX

EFFECT OF TEMPERATURE δ_i

TEST TEMPERATURE ^{o}C				
+20	0	-20	-40	-60
δ_i (inx10^{-3})	δ_i (inx10^{-3})	δ_i (inx10^{-3})	δ_i (inx10^{-3})	δ_i (inx10^{-3})
3.0 3.9 4.0 4.2	3.8 4.2 4.7 3.7	4.0 4.8 3.6 3.6	4.5 3.4 3.1 4.0	4.0 3.7 3.0 4.8
Mean 3.78 S.D. 0.53	4.10 0.45	4.00 0.57	3.75 0.62	3.88 0.75

Table X

WELDING CONDITIONS

TEST WELDS

	CURRENT (amps)	VOLTAGE (volts)	SPEED (in/min)
1st Pass	600	32	19
2nd Pass	700	32	19

PIPE WELDS

	LEADING ARC (D.C.)		TRAILING ARC (A.C.)		SPEED (in/min)
	CURRENT (amps)	VOLTAGE (volts)	CURRENT (amps)	VOLTAGE (volts)	
1st Pass (Inside)	720	34	700	40	65
2nd Pass (Outside)	950	35	730	39	52

Table XI

CALCULATED H.A.Z. WIDTHS

PASS	TEST WELD H.A.Z. WIDTH (cm)	PIPE WELD H.A.Z. WIDTH (cm)
1	0.765	0.755
2	0.970	0.890

If the H.A.Z. is taken as being bounded by the temperatures of 1500°C at the fusion boundary and 700°C at the parent plate boundary, the first pass of a test weld will produce a width d heated to 1500°C given by

$$\frac{32 \times 600}{4.2 \times 1.25} = 8 \times 0.17 \times 1500 \ (0.2 + d)$$

$$d = 1.6 \text{ cm}$$

Similarly a width of 3.1 cm will be heated to 700°C giving an H.A.Z. width of 0.765 cm. The H.A.Z. width produced by the second pass and those produced on the actual pipe can be calculated similarly and the values so obtained are shown in Table XI. From this table it can be seen that the calculated values for both situations are extremely close. The closeness of the calculated values of H.A.Z. widths was confirmed by the actual macro sections of the welds which are shown in Figures 52 and 53, Figure 52 being an actual weld and 53 being a weld made at the University. The shape of the weld beads are a little different in this particular case but the H.A.Z. widths are extremely close indicating that the heat flow conditions in both cases and the heat inputs are comparable.

The analyses of the welding materials namely, plate, wire and flux and the final weld deposit are shown in Table XII.

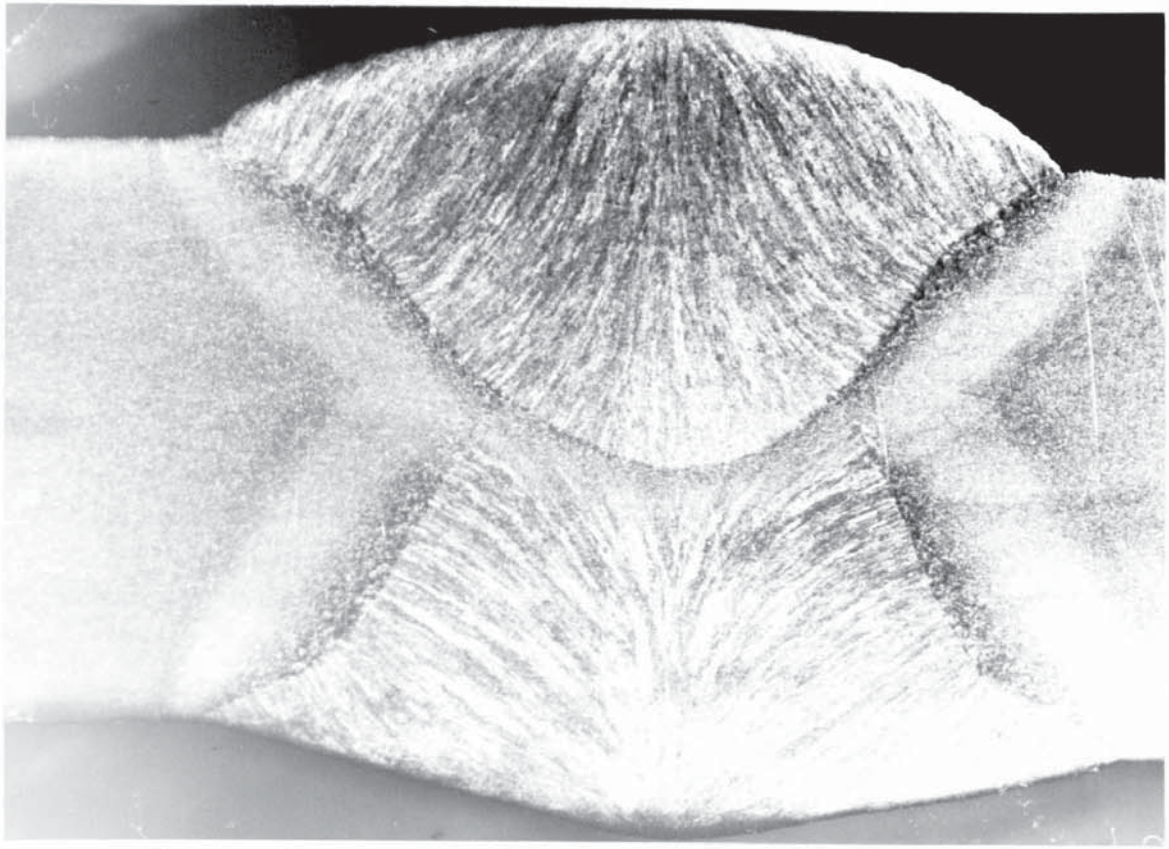

Figure 52 Actual Pipe Weld x 5

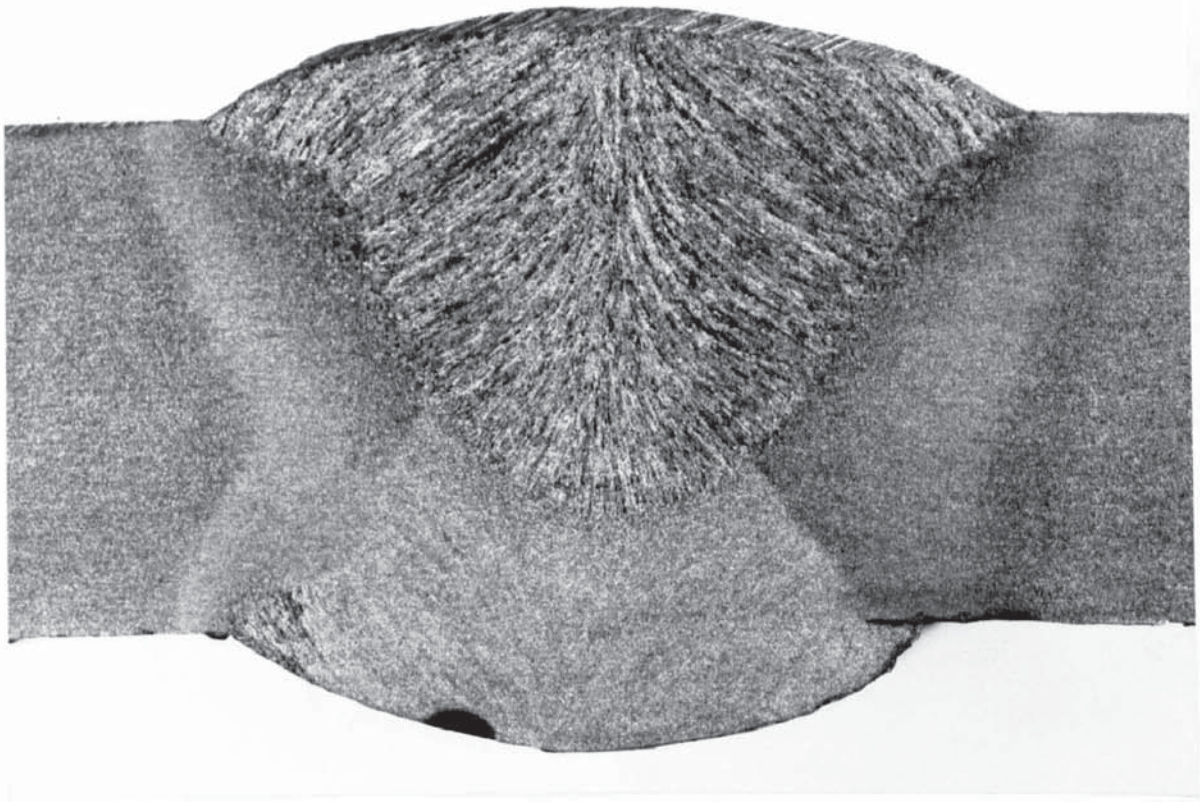

Figure 53 Laboratory Test Weld x 5

Table XII

ANALYSES OF WELDING MATERIALS

ELEMENT	PLATE	WIRE	FLUX	WELD METAL
C	0.21	0.078	0.028	0.12
Mn	1.34	0.34	29.26	1.24
S	0.027	0.20	<0.001	0.027
P	0.007	0.027	<0.001	0.018
Si	0.22	<0.001	18.50	0.073
Al	0.04	<0.001	-	0.008

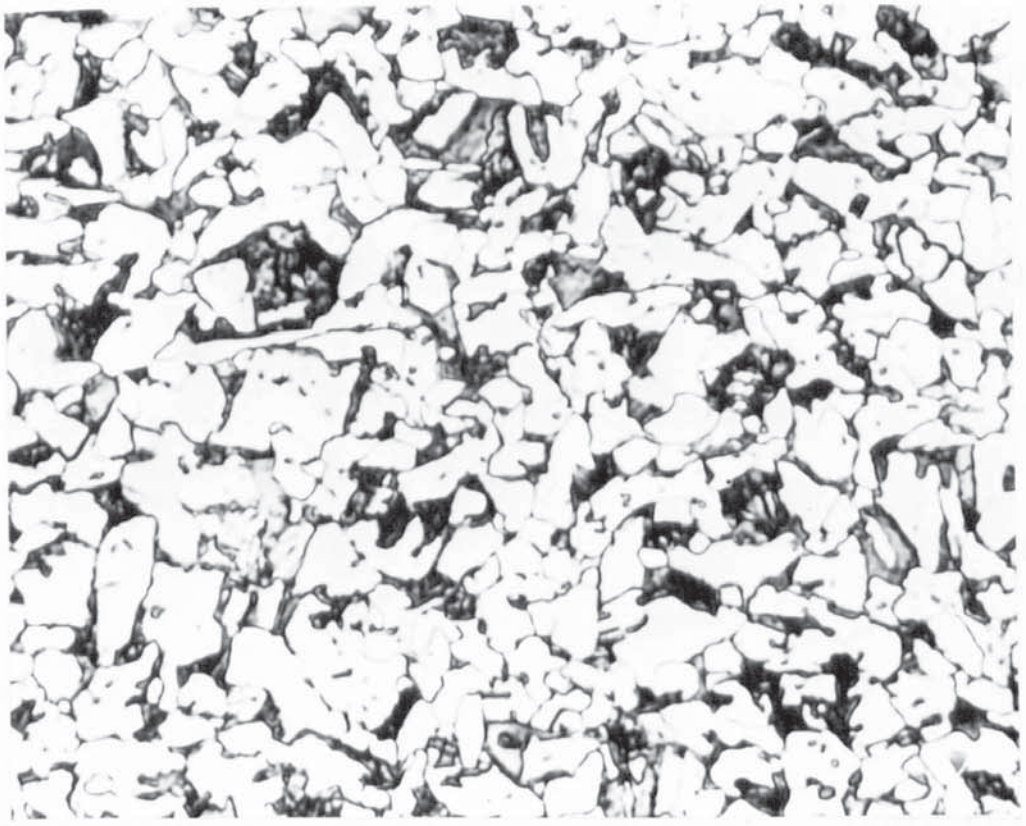

Figure 54 Laboratory Weld
Grain Refined Region x 400

The metallography of the welds produced is shown in Figures 54-56 which show the grain refined H.A.Z., Widmanstätten H.A.Z. and weld metal respectively. The hardness of these three regions is H_V30 155, 183 and 155. The tensile properties of the weld metal were determined to be 48 Ksi yield, 75 Ksi U.T.S. an elongation of 30% and reduction in area of 65%.

Micro hardness determinations across the weld regions showed that although the first pass is substantially stress relieved and heat treated by the second pass to a fairly even level of hardness Figure 57, the second pass H.A.Z. is particularly hard especially in the Widmanstätten structure occurring at the fusion boundary, Figure 58.

The integrity of the welds was found to be good. When specimens 1 inch x 6 inch x ½ inch were bent round a 2 inch diameter mandrell in the two directions shown in Figure 59 they bent completely without failure provided that the weld reinforcement was completely removed as shown in Figure 60. If the weld reinforcement remained, as indeed it does in service, the stress concentration existing at the toe of the weld caused small cracks to occur in the Widmanstätten H.A.Z.; these cracks did not propagate unstably however.

The results of the toughness scans across the weld region are presented in two forms. Figure 61 shows the trend of toughness with distance from the weld centre line in longitudinal specimens. This

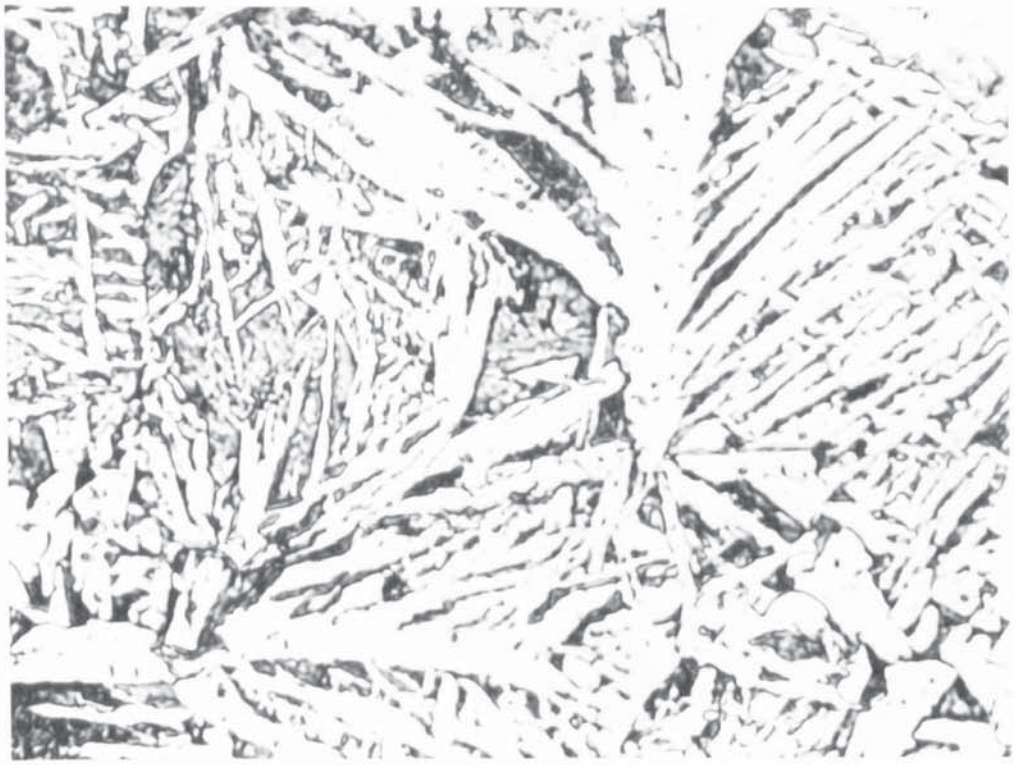

Figure 55 Laboratory Weld
Widmanstätten Region x 400

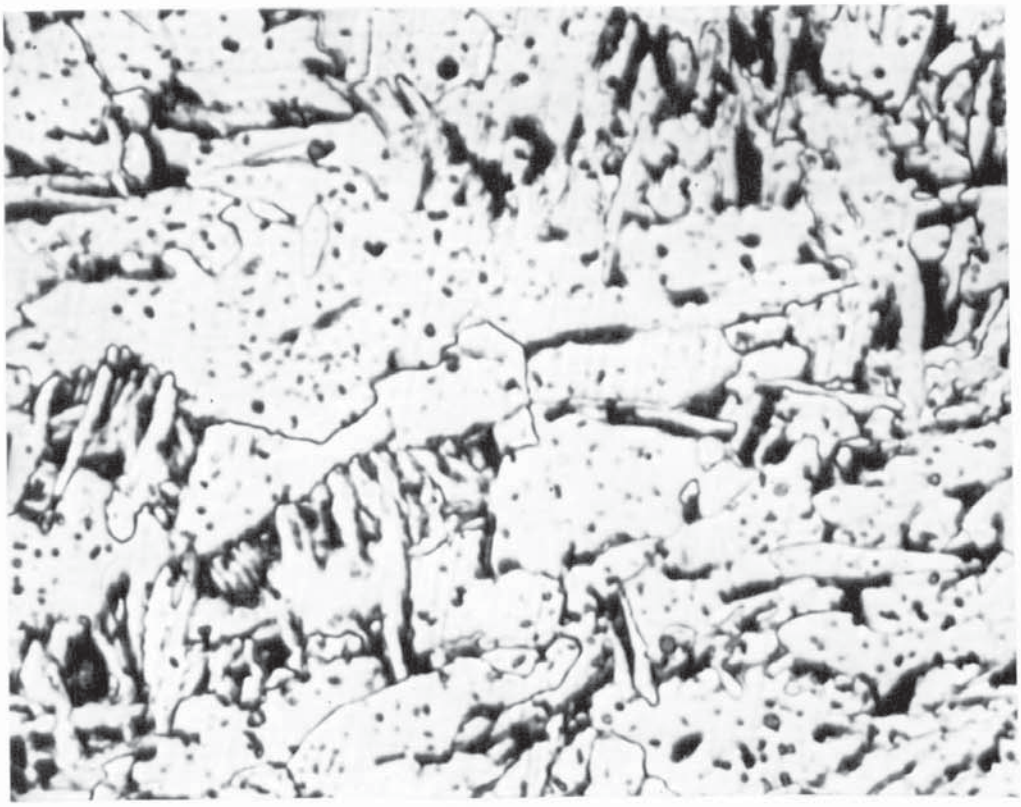

Figure 56 Laboratory Weld
Weld Metal Region x 400

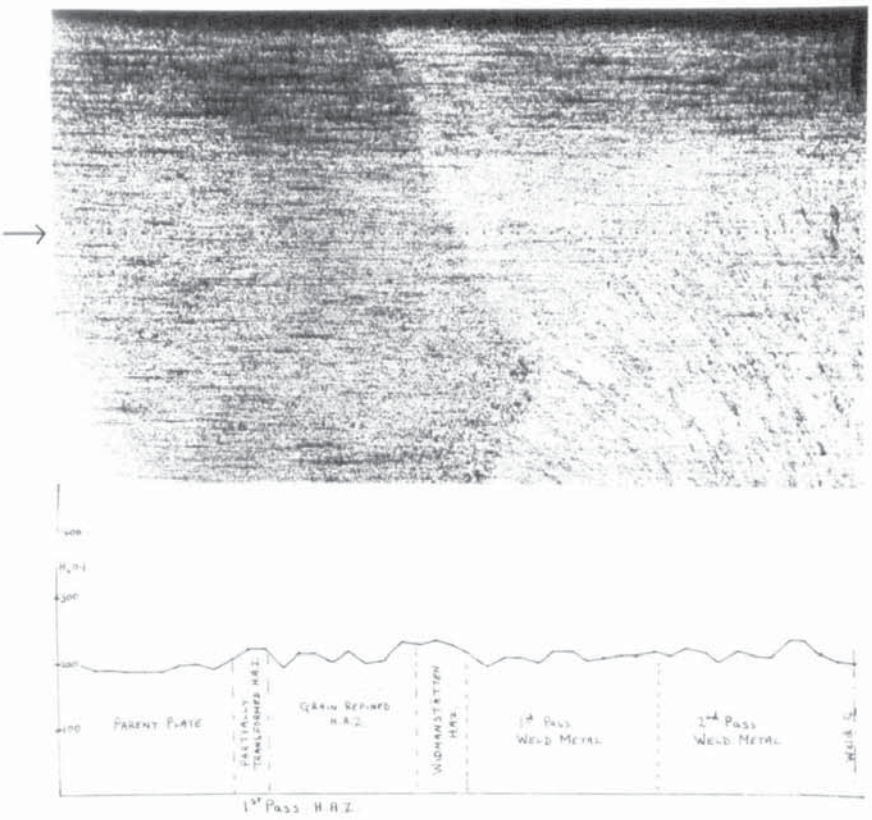

Figure 57 Microhardness Traverse Across 1st Pass H.A.Z.

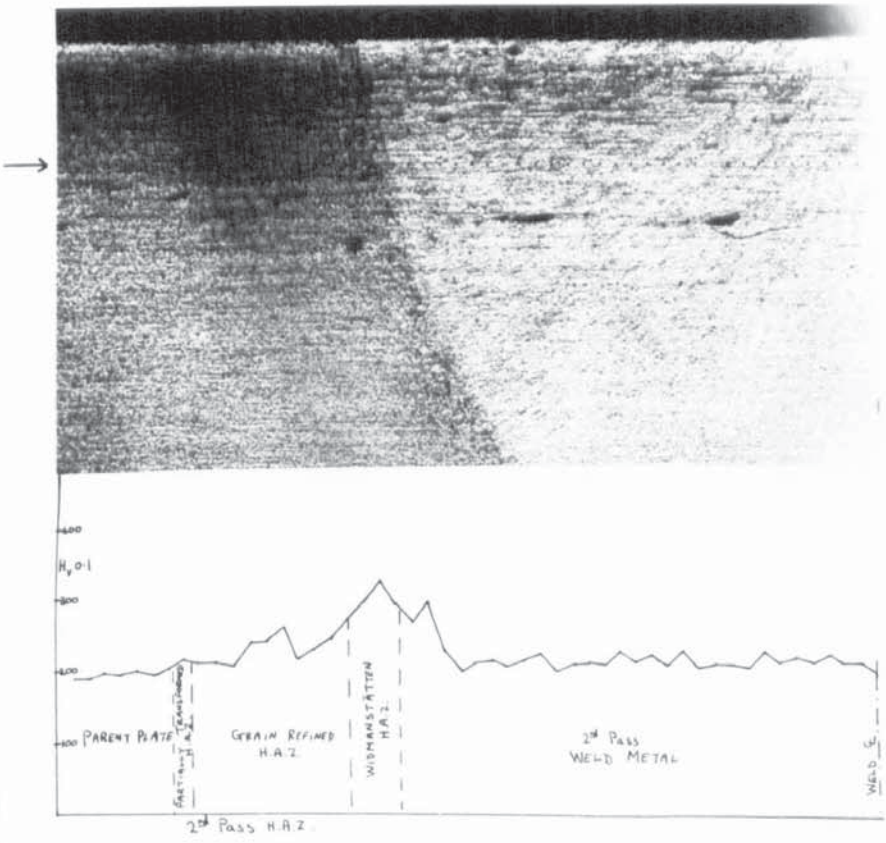

Figure 58 Microhardness Traverse Across 2nd Pass H.A.Z.

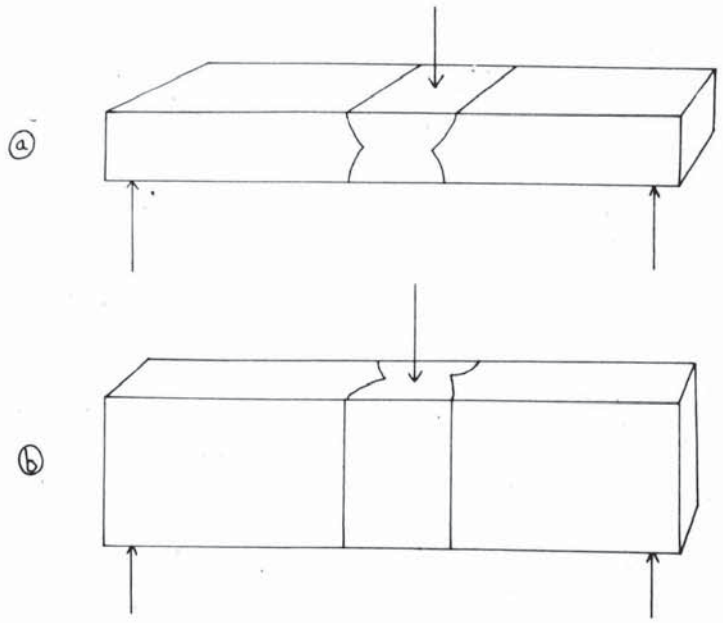

Figure 59 Bend Test Directions

Figure 60 Typical Bend Specimen x 1

shows a marked decrease in δ_i in the region approximately 0.175 inch from the weld centre-line. On Figure 62 this data is presented pictorially and it can be seen that this area of low toughness is associated with the Widmanstätten H.A.Z. on the weld fusion boundary. The value of toughness for this material being about 0.0018 inch as opposed to the plate which has a δ_i of 0.004 inch and the weld metal 0.0065 inch.

The position of crack initiation in these longitudinal specimens was examined by loading specimens up to the detection of crack initiation then unloading, cooling in liquid nitrogen and breaking open the specimen. Figures 63 and 64 show the results from one such experiment; Figure 63 shows a small tear (arrowed) in the centre of a specimen intended to measure δ_i in the Widmanstätten H.A.Z. Figure 64 shows a polished cross section at the point of crack initiation which can be seen to be the Widmanstätten H.A.Z. Similar results were obtained on other specimens, the point of crack initiation always being in the centre of the section. Thus the δ_i's measured are those for the structures at the centre of the specimen.

The results from the through thickness specimens generally confirmed those from the longitudinal specimens, a decrease in toughness being noted at the fusion boundary, the results are shown graphically in Figure 65 and pictorially in Figure 66.

Figure 61 Variation of δ_i with notch tip position
Longitudinal Specimens

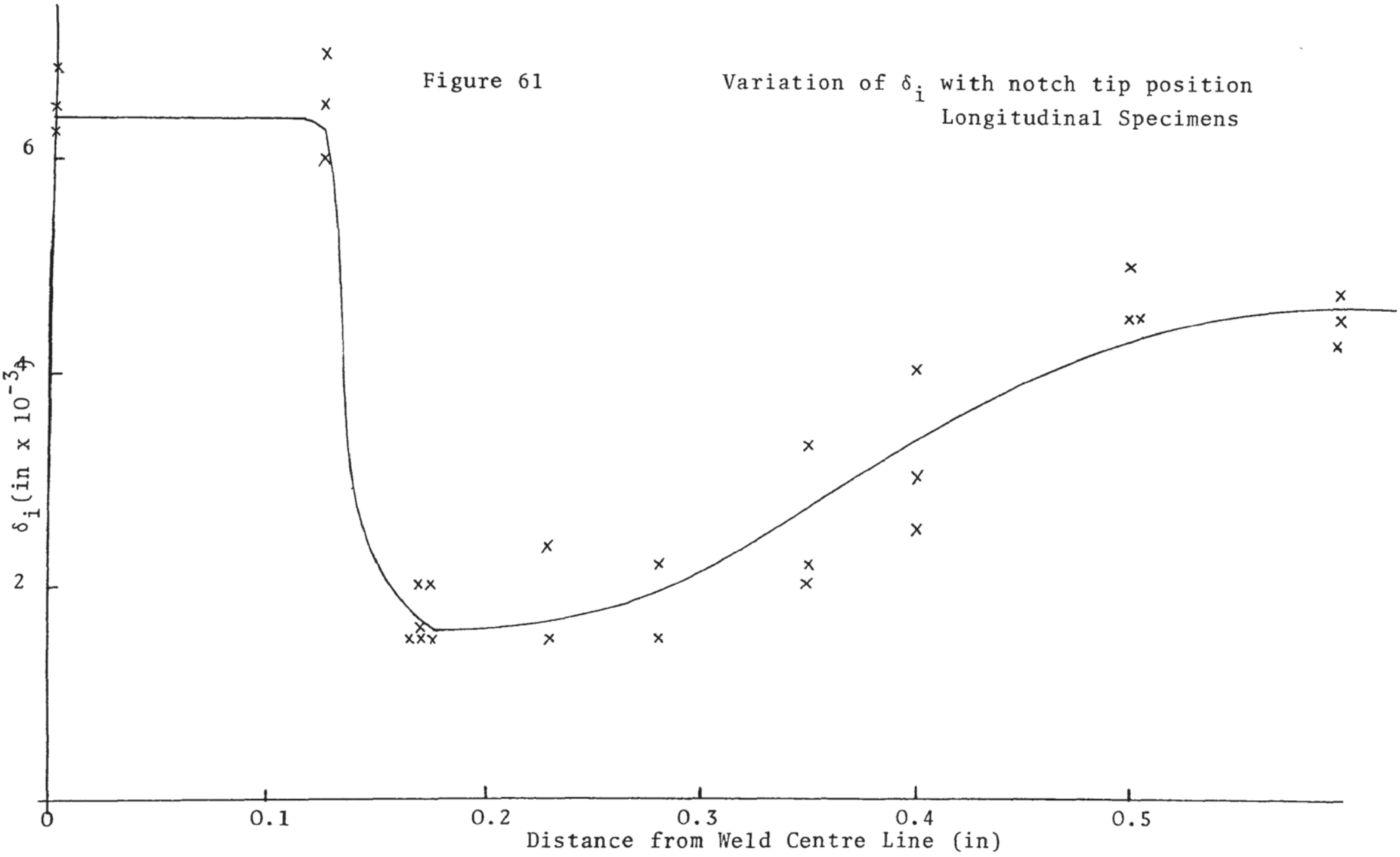

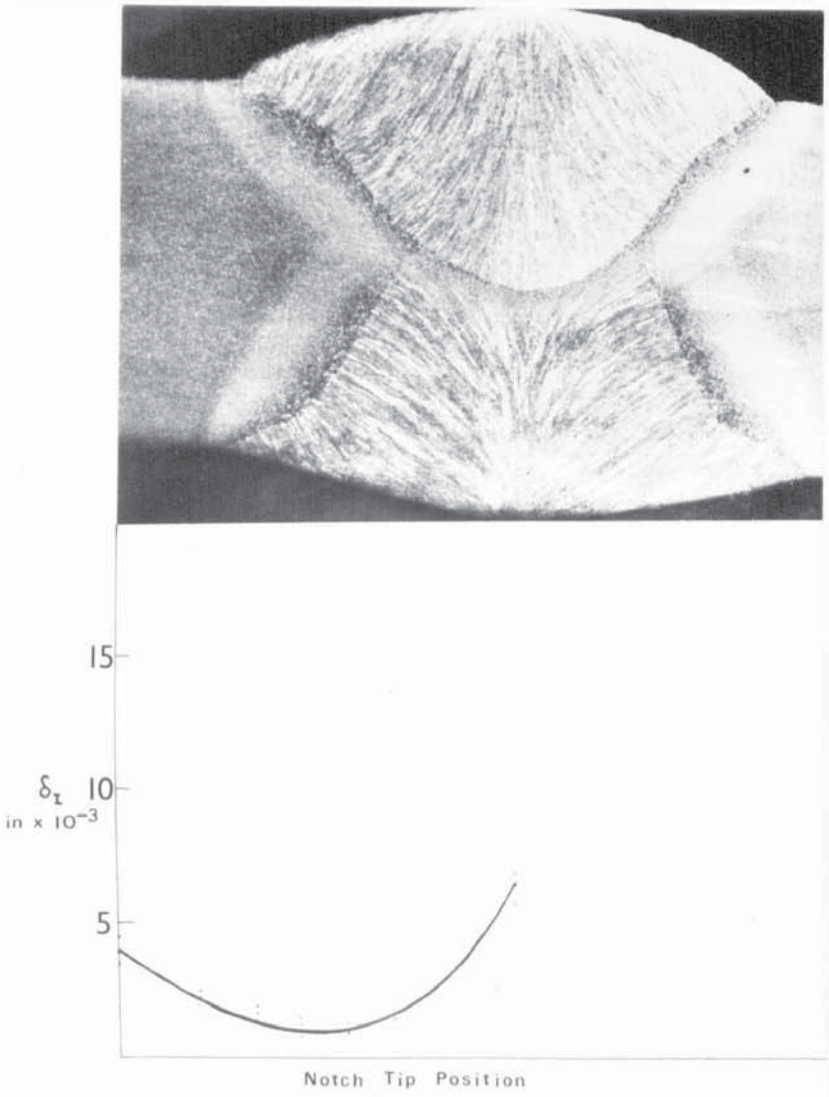

Figure 62

Variation of δ_i with Notch Tip Position in Longitudinal Specimens

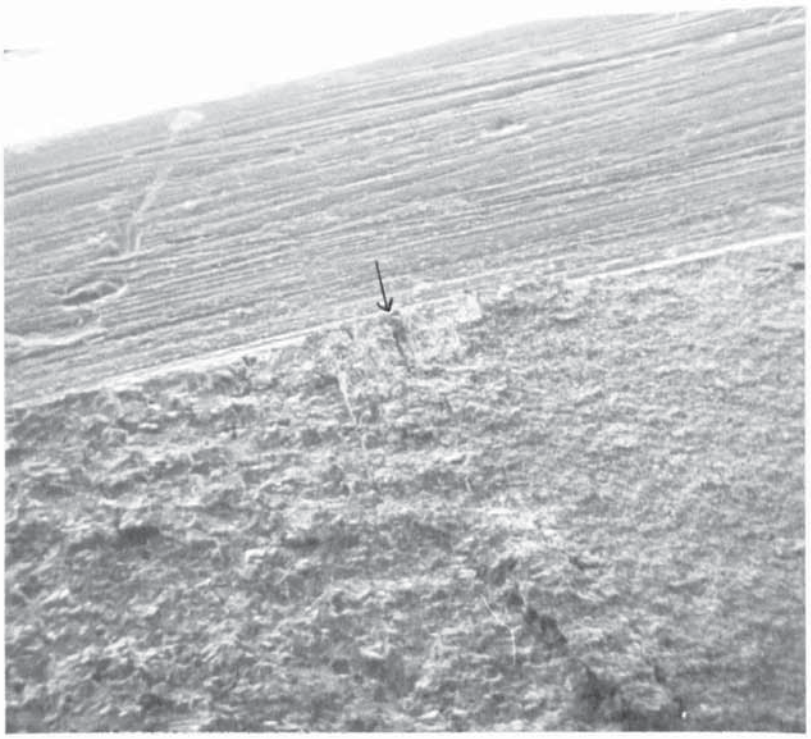

Figure 63 Position of the Initiation of Slow Tearing S.E.M. x 25

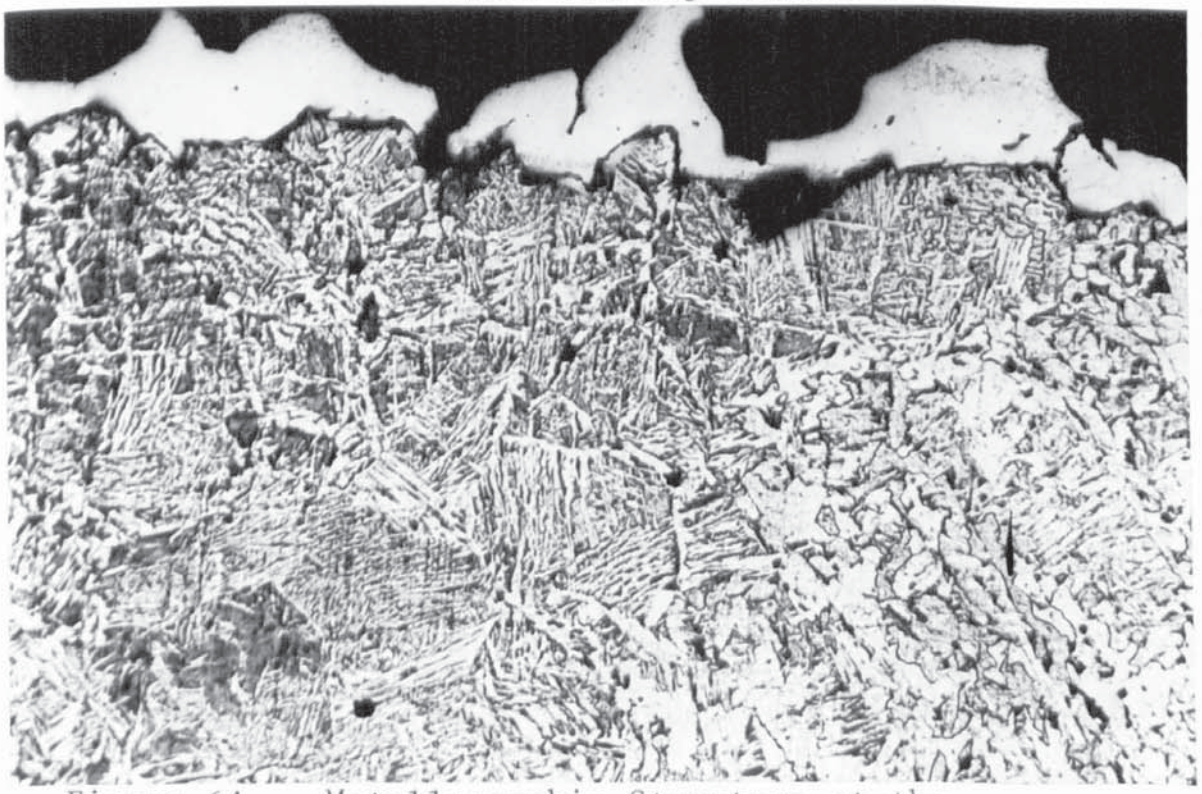

Figure 64 Metallographic Structure at the Position of Crack Initiation x 400

Figure 65 Variation of δ_i with Notch Tip Position through Thickness Specimens

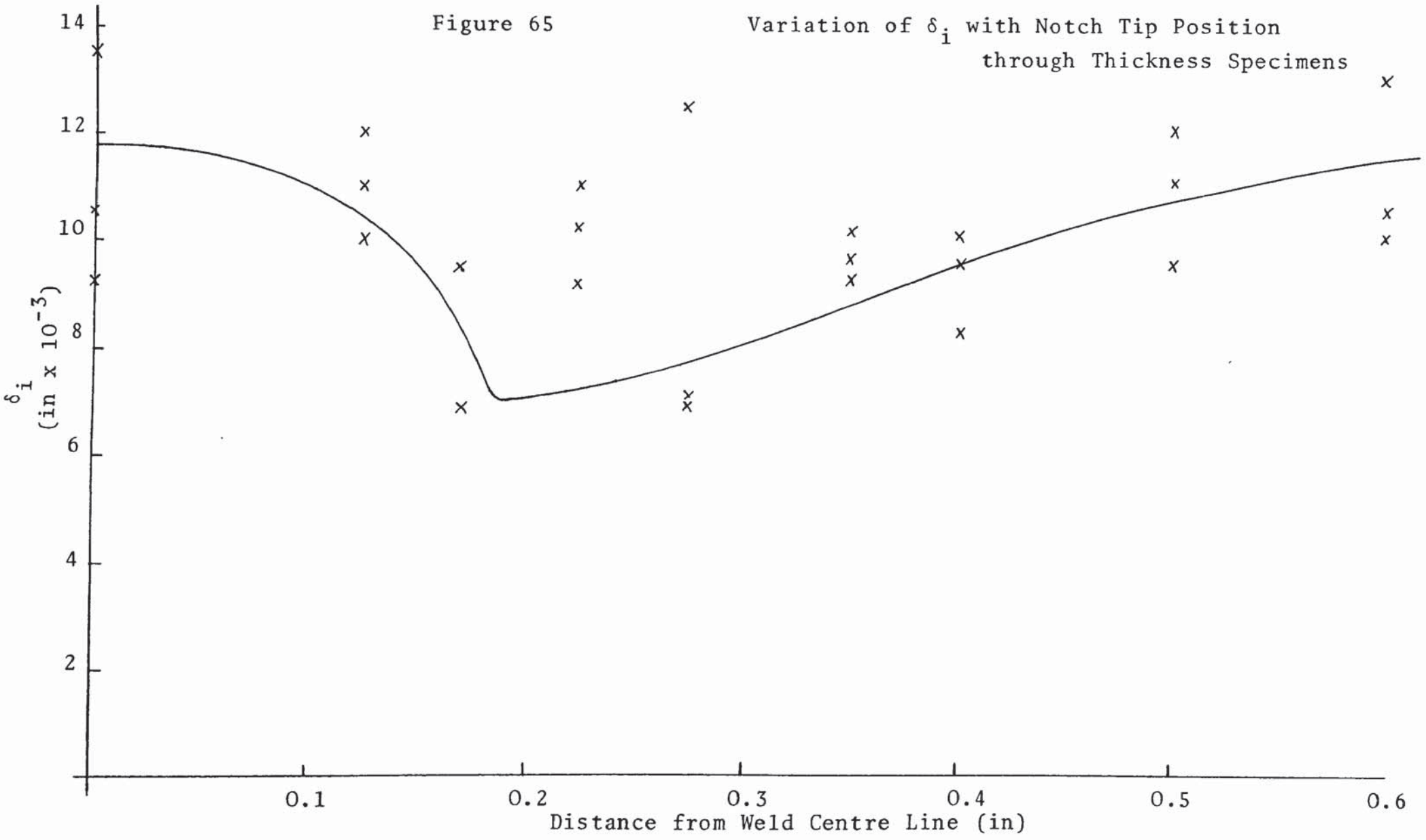

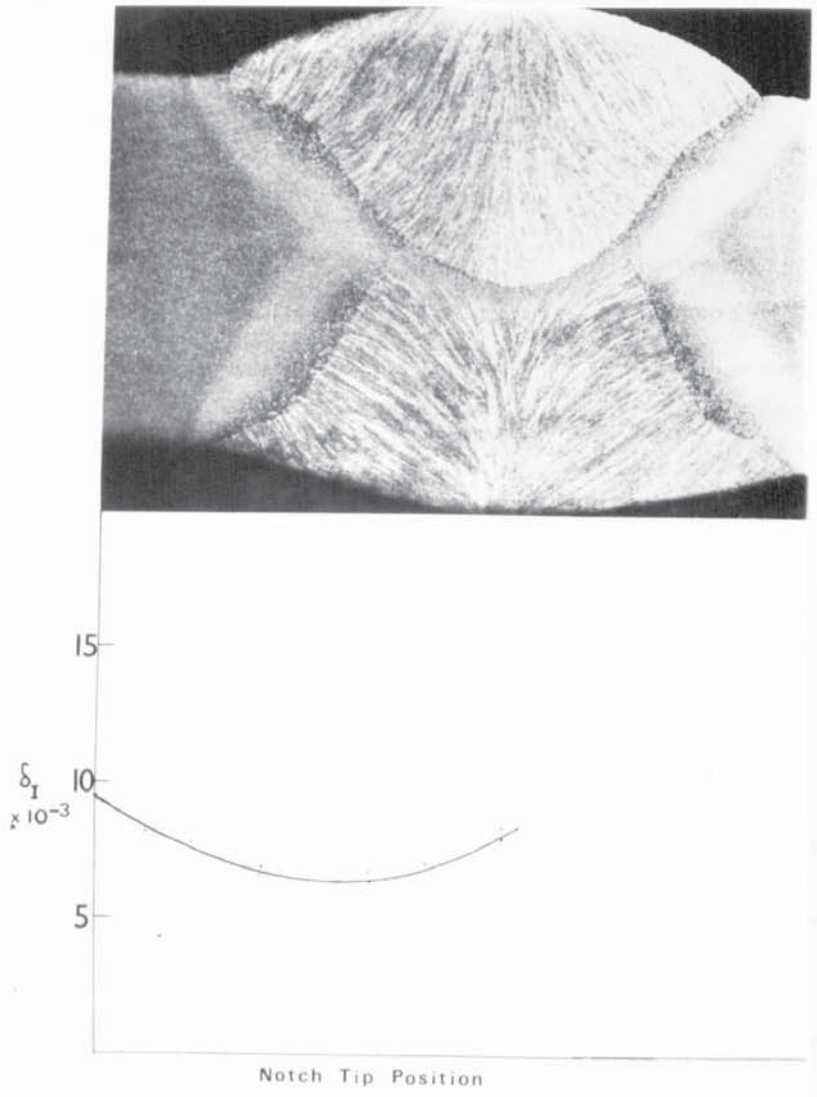

Figure 66

Variation of δ_i with Notch Tip Position in Through-Thickness Specimens

The series of specimens supplied by the Gas Council did not show the decrease in toughness noted on the other specimens. The results shown in Figure 67 tend to indicate a slight increase in toughness across the H.A.Z. from parent plate towards the weld metal, but certainly no decrease in toughness was noted at the fusion boundary.

Analysis of the plate material from these Gas Council specimens showed 0.18% C and 1.21% Mn both elements being much lower than those in the plate used for the main part of the experimental work.

The initial results from the experiments on the effect of cracks approaching welds at angles are presented in Figures 68-69 where it can be seen that on both C.T.S. and bend specimens the cracks turn to follow the line of the H.A.Z. up to an angle of approximately 70^{o}. Metallographic examination of the crack paths showed that the cracks in this situation run in parent plate material and not as might be expected in the brittle region of the H.A.Z.

The second part of the experiment on the shape of the plastic zones in the situation of the angled crack showed that the plastic zone is deformed away from the normal and also spreads into the parent plate material to a greater extent. This effect is shown in Figures 70-72, Figure 70 shows the case of the crack initially parallel to the weld while in Figure 71 and 72 the crack was initially at 30^{o} and 60^{o} to the weld bead respectively.

Figure 67 Variation of δ_i with Notch Tip Position
Gas Council Longitudinal Specimens

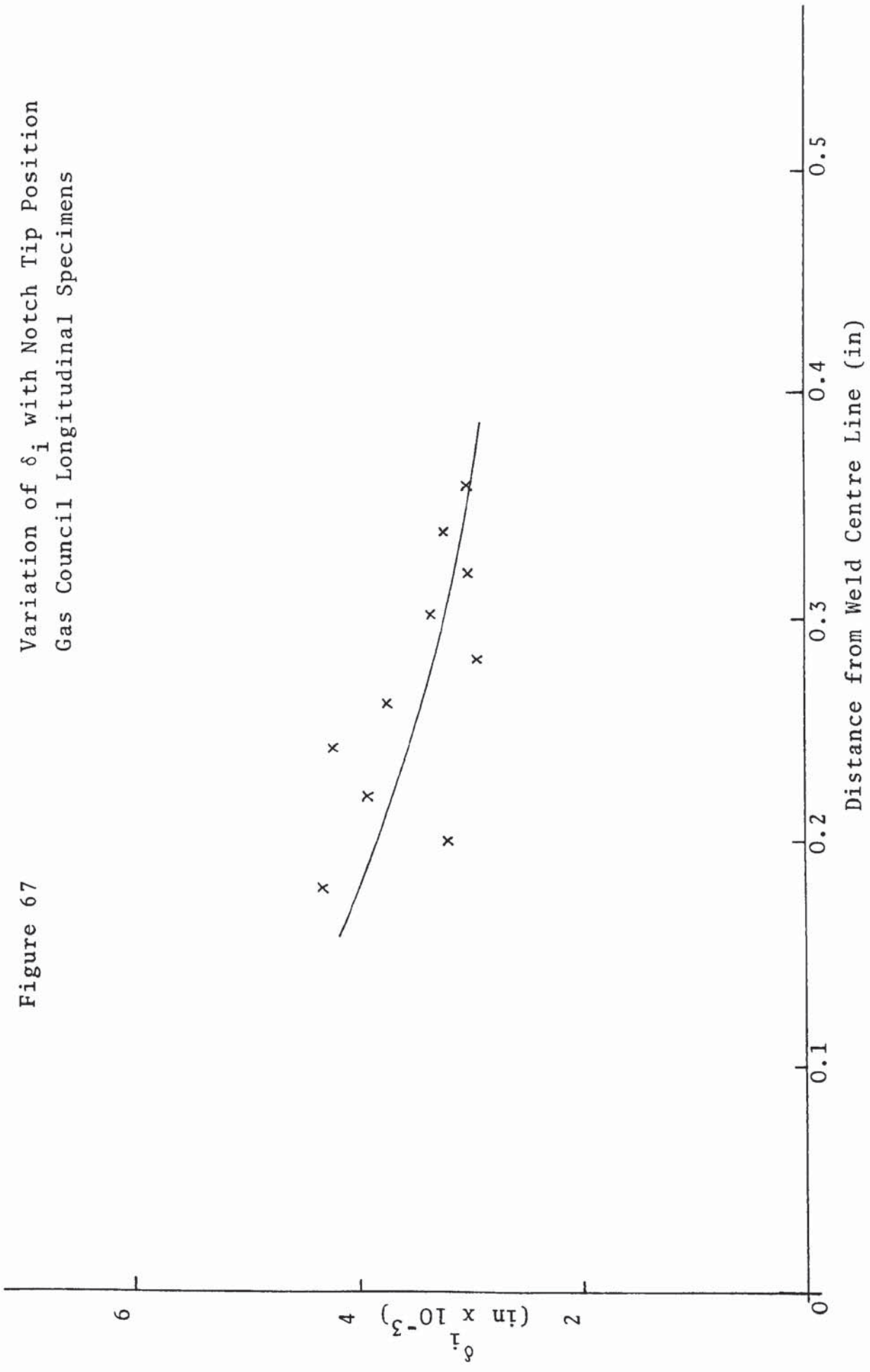

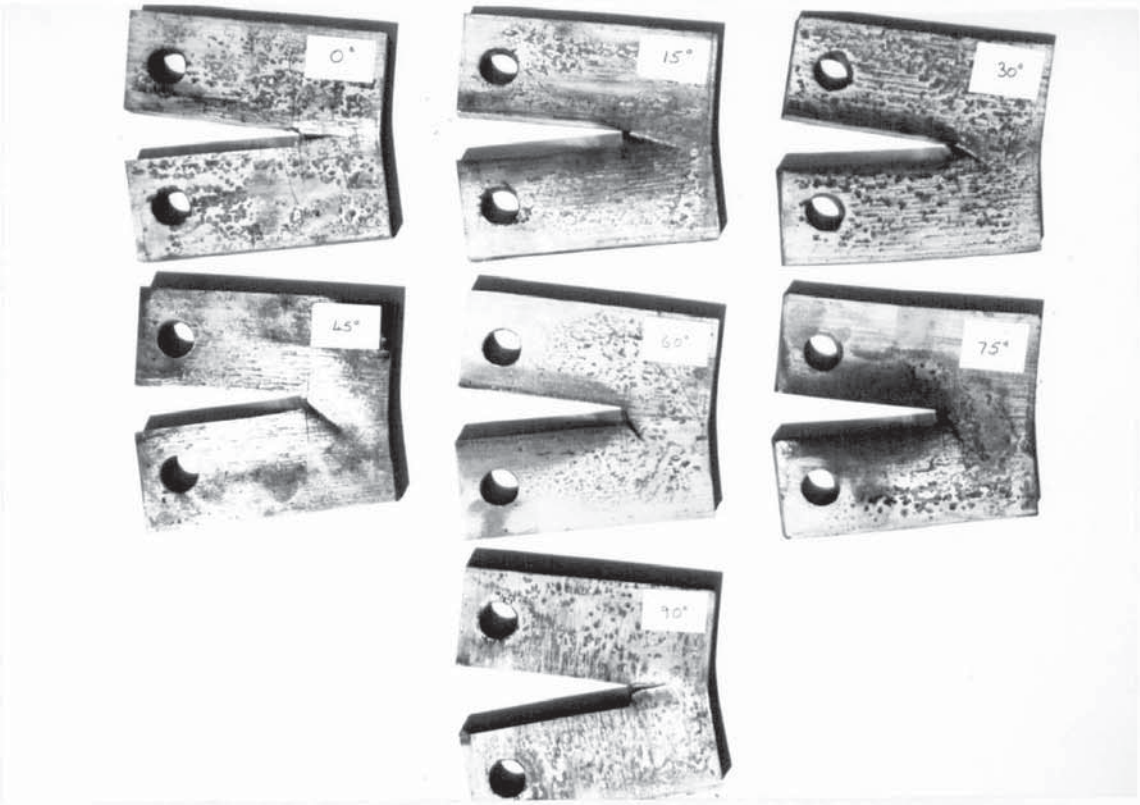

Figure 68 Effect of Weld Angle on Crack Direction in C.T.S. Specimens

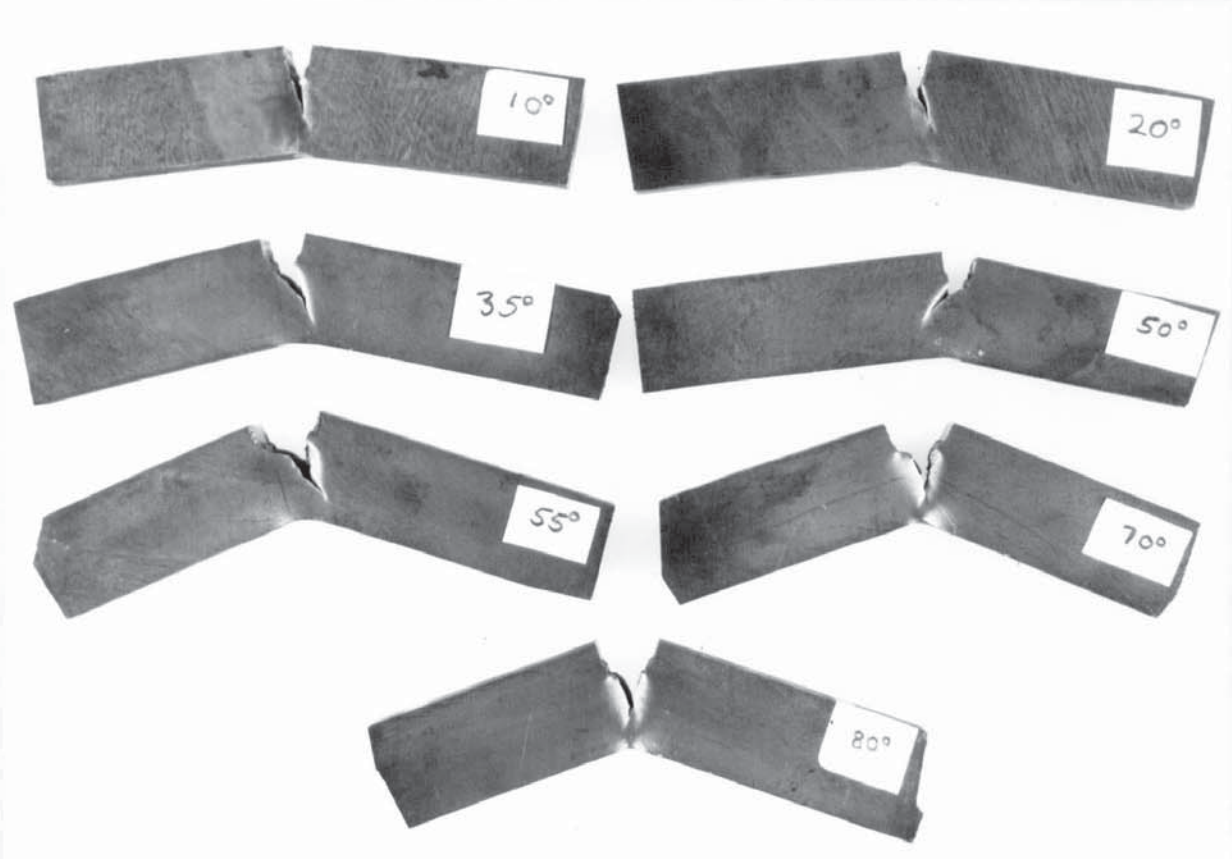

Figure 69 Effect of Weld Angle on Crack Direction in Bend Specimens

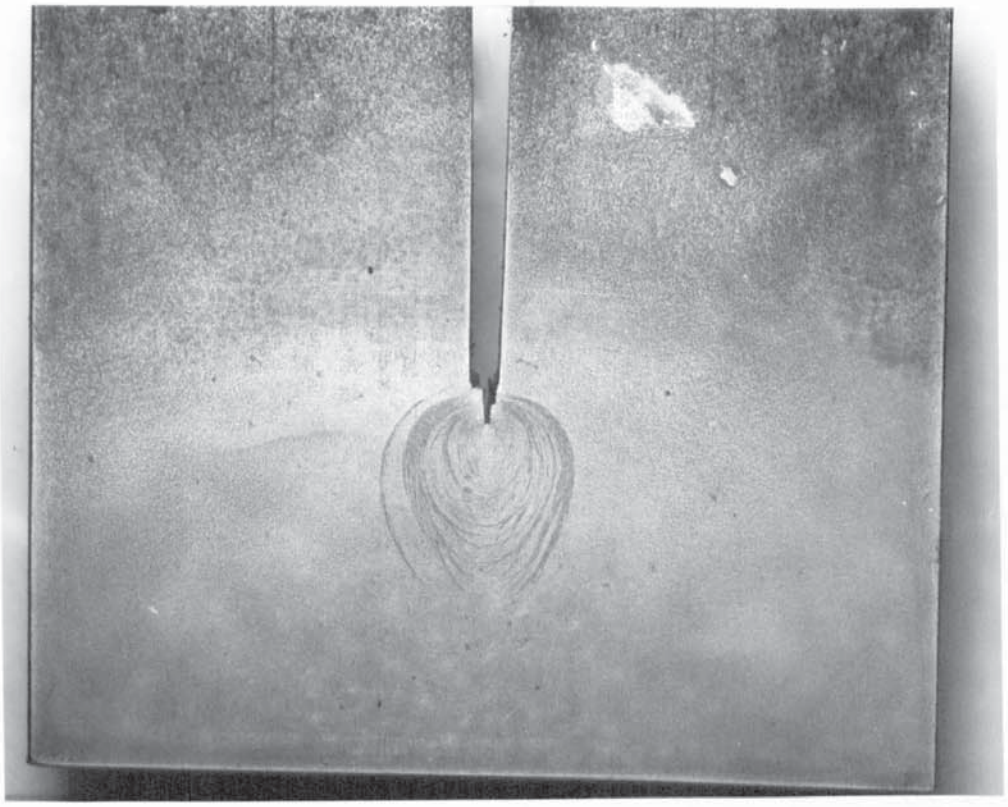

Figure 70 Plastic Zone Shape
Weld Angle 0^{o}

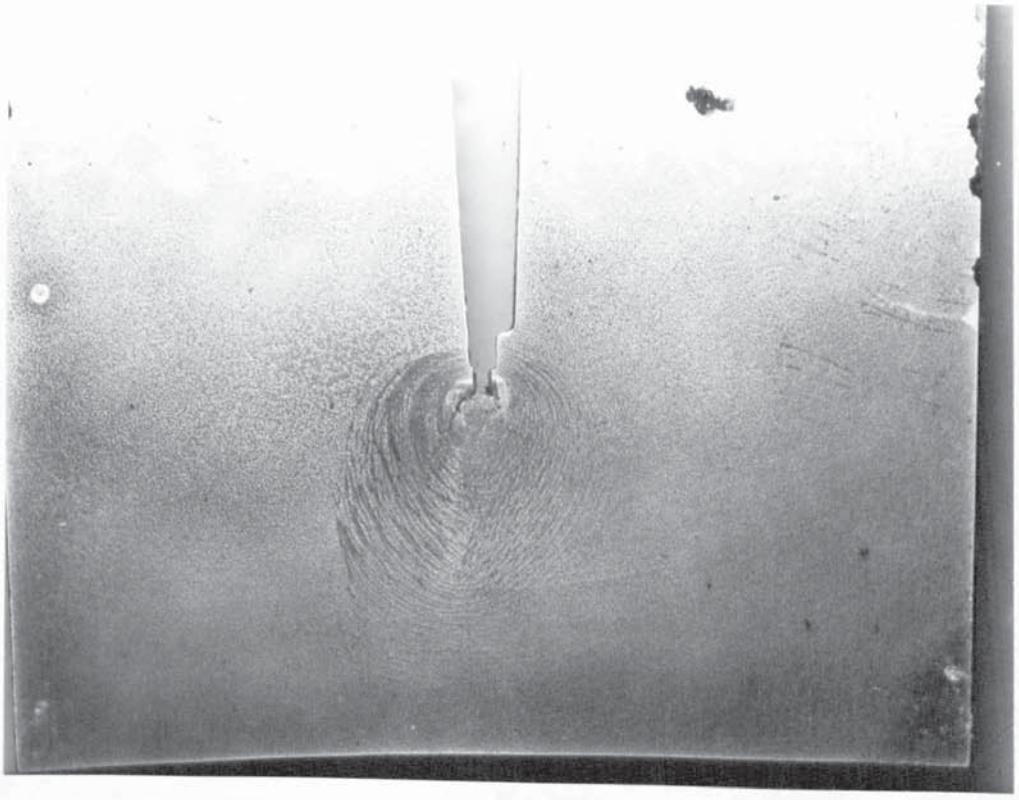

Figure 71 Plastic Zone Shape
Weld Angle 30^{o}

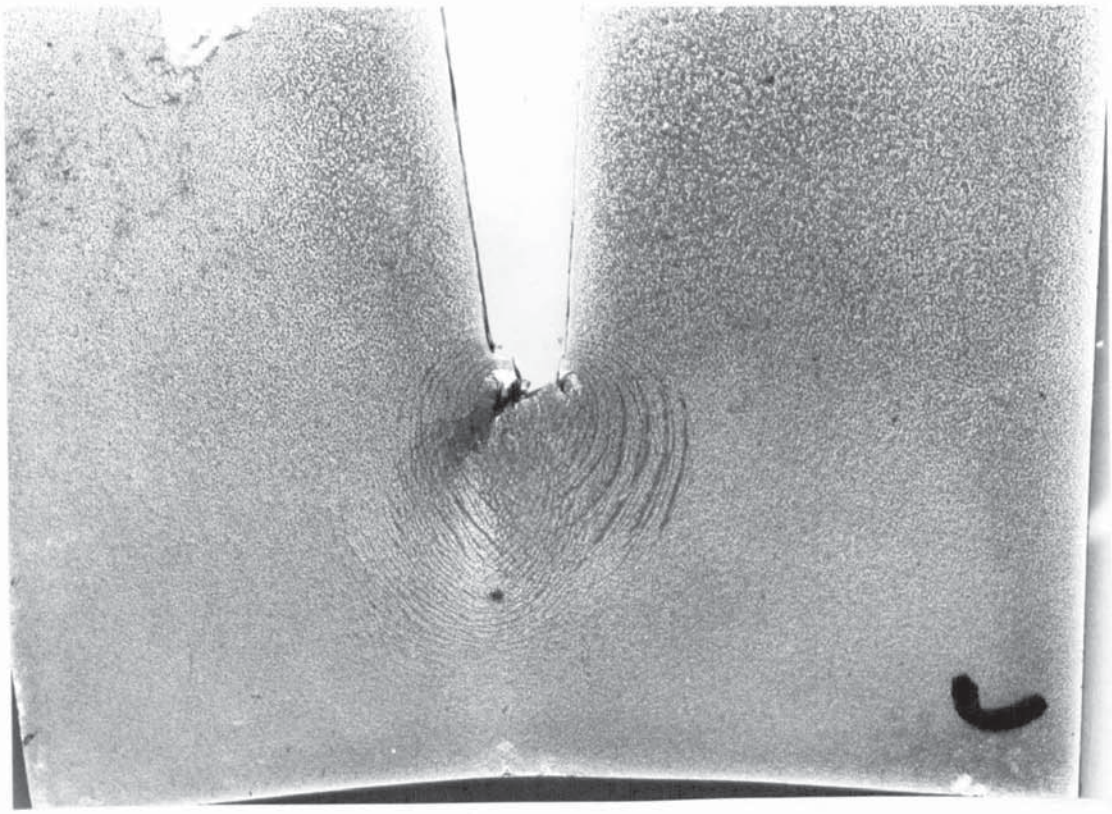

Figure 72 Plastic Zone Shape
Weld Angle 60^{o}

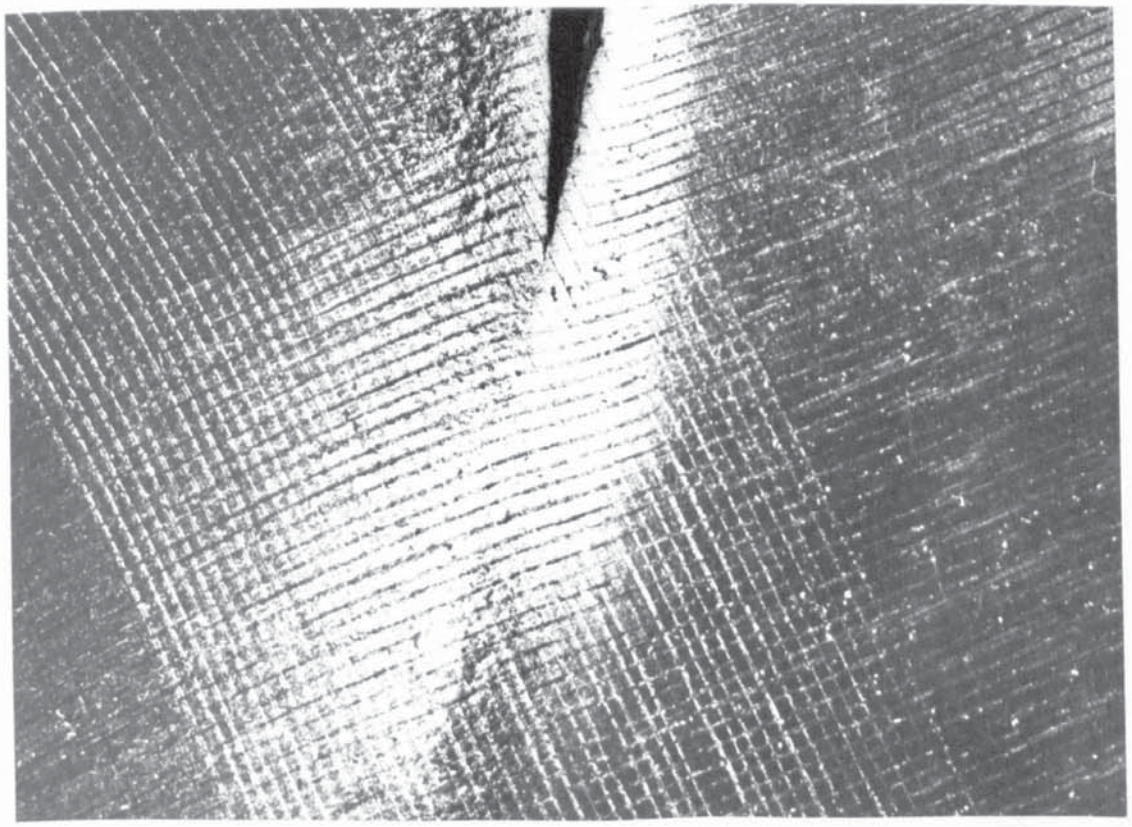

Figure 73 δ_I and δ_{II} at the Tip of an Arrested Crack, Weld Angle 50^{o}

The measurement of both the opening mode C.O.D. δ_I and the sliding mode C.O.D. δ_{II} at arrest at the crack tip in the situation of the angled crack was made via grids scribed on the specimen surface. The occurrence of these two modes of crack tip displacement is demonstrated quite conclusively by Figure 73.

The results from the series of angled specimens of the values of δ_I and δ_{II} are listed in Table XIII. The relationship between the two deformation modes was not proved conclusively to be either of the type described by Wu[63] or that described by Erdogan and Sih[62]. The equations from both of these theories modified to C.O.D. terms can be fitted to the results with almost the same degree of correlation as shown in Figure 74. The question of which relationship fits best could only be resolved by the measurement of a δ_{II_c} for the material which is extremely difficult experimentally.

The experiment on the proof of the validity of the equation:

$$G_c = \sigma_y \delta_c$$

proved fairly conclusive. G_c being calculated via $\sigma_y \delta_c$ and also by the method of Stonesifer and Smith[40]. K values were calculated by these methods over a range of specimens some of which had been used in other experiments and some which had been specially prepared for this experiment. The results are shown in Figure 75

Table XIII

EFFECT OF ANGLE ON OPENING AND SLIDING MODE C.O.D.s.

Angle (^{o})	Opening Mode C.O.D. δ_I (in x 10^{-3})	Sliding Mode C.O.D. δ_{II} (in x 10^{-3})
0	4.0	0
10	4.0	0
20	3.75	0.25
25	3.0	1.0
30	3.0	1.25
35	2.5	2.0
40	2.5	2.0
50	2.0	3.0
60	1.5	3.5
60	1.0	4.0
70	1.0	5.0

Relationship between δ_I and δ_{II} for X-52

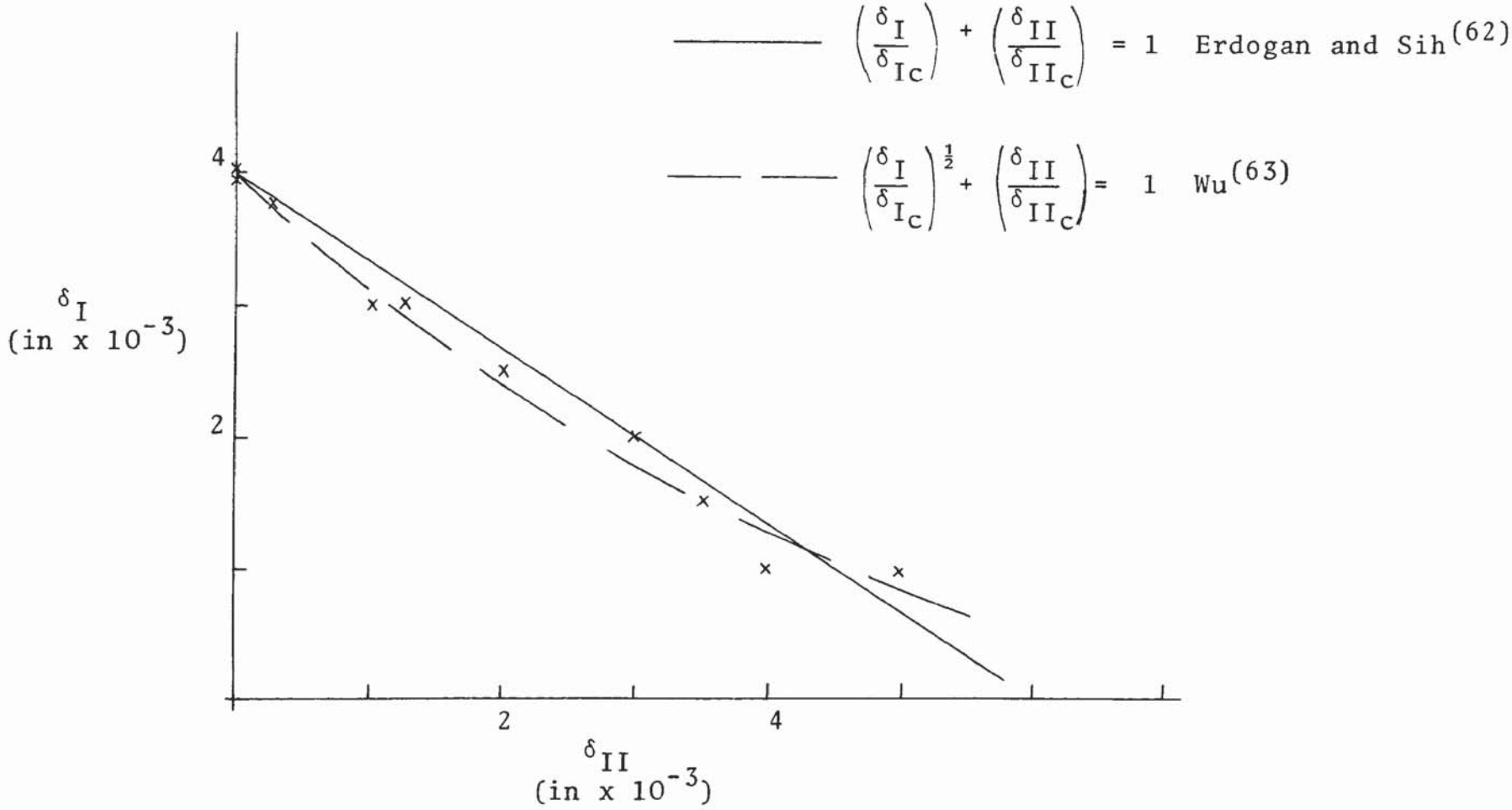

Figure 74

Comparison of Estimates of K_{I_c}

Figure 75

and a statistical analysis showed that the results fit the straight line at 45^{o} very well, thus confirming the validity of the equations linking L.E.F.M. and General Yield fracture mechanics, provided that the technique of Stonesifer and Smith is accepted as reasonable.

Further verification of the links between L.E.F.M. and G.Y.F.M. was obtained by measuring the radius of the plastic zone at the initiation of cracking by using Stresscoat Laquer. On a series of X-52 C.T.S. test pieces an average plastic zone size of 0.5 inches was measured at crack initiation.

Using the equation:

$$\frac{K_I^2}{2\pi\sigma_y^2} = r_y$$

$$K_I = 88\text{Ksi}\sqrt{\text{in}}$$

Whilst using $G_c = \sigma_y \delta_c$ and $K^2 = EG$

$$K_I = 87\text{Ksi}\sqrt{\text{in}}$$

Alternatively the size of the plastic zone can be used to calculate the C.O.D. occurring at the time of measurement, using the equation:

$$r_y = \frac{\delta E}{2\pi\sigma_y}$$

which assumes the relationship $G_c = \sigma_y \delta_c$

This gives a δ of 5×10^{-3} inch at crack initiation which is reasonably close to the values actually measured.

The studies of crack initiation and growth in the various structures examined was begun by investigating the parent plate material. As can be seen from Figures 33-35, there is pronounced fibre texture in the X-52 plate and in a longitudinal bend specimen the fibres will be arranged as shown in Figure 76. Such a specimen was tested until cracking had occurred and was then unloaded and sectioned at 45^{o} across the notch.

From Figures 77-79 it can be seen that failure is initiated by fracture or decohesion of the pearlite fibres causing void formation, these voids then link up by ductile necking of the ferrite lamellae to form a crack, Figure 80. The ductile necking of the ferrite lamellae gives a fibrous appearance to the final fracture as in Figure 81. These last two figures were obtained from a completely broken specimen of the same series as the unloaded specimen.

The grain refined H.A.Z. alternatively showed a slightly more devious crack path than the parent plate material, Figure 82, but the fracture surface appeared much less ductile with very shallow dimples, Figure 83.

The Widmanstätten H.A.Z. crack path appeared to follow the line of the ferrite needles within the prior austenite grains as shown in Figures 84 and 85. The fracture surface Figure 86 showed very little indication of ductility.

Finally, the weld metal showed a meandering crack path with large numbers of voids ahead of and around the crack tip Figure 87, and a typical completely ductile fracture surface Figure 88.

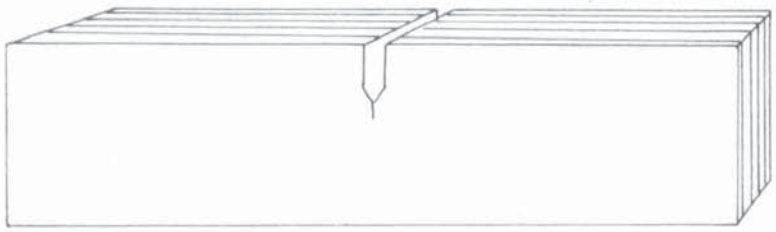

Figure 76 Schematic Arrangement of Lamellae in a Bend Specimen

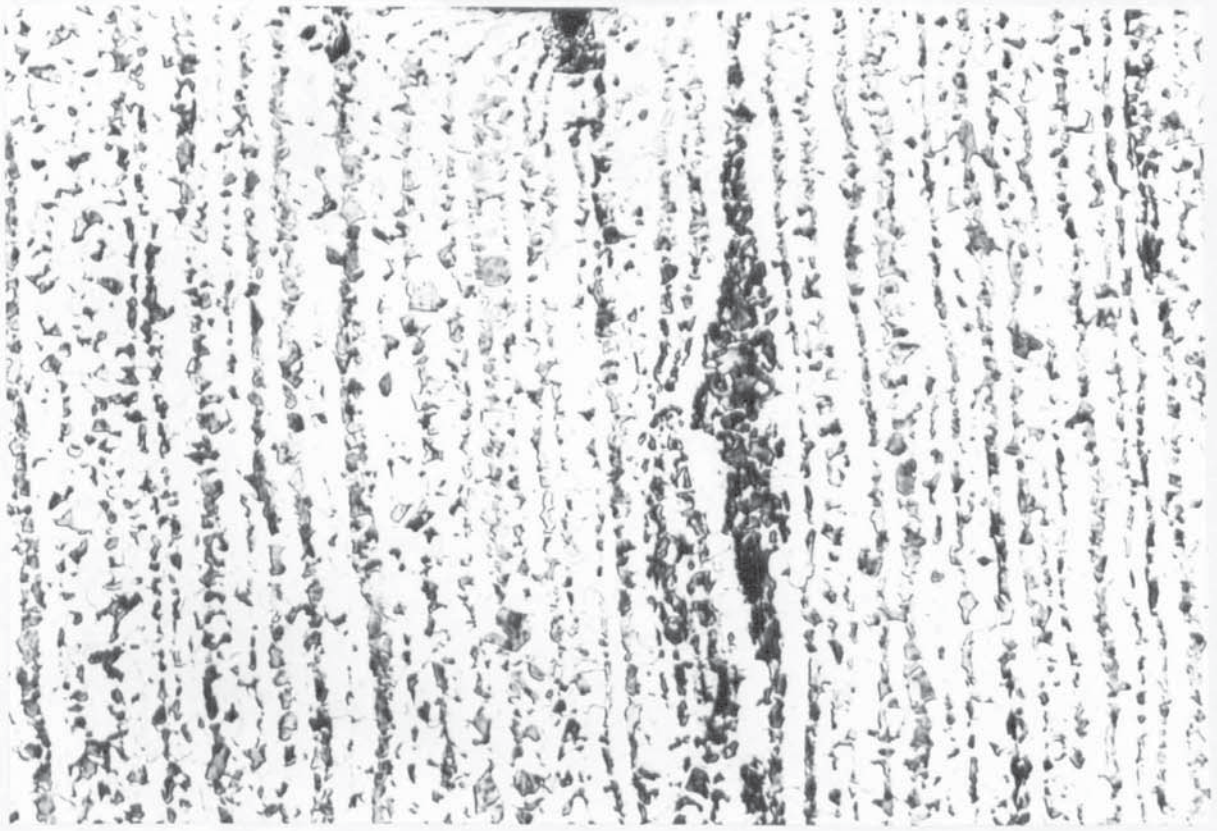

Figure 77 Crack Initiation in Parent Plate x 100

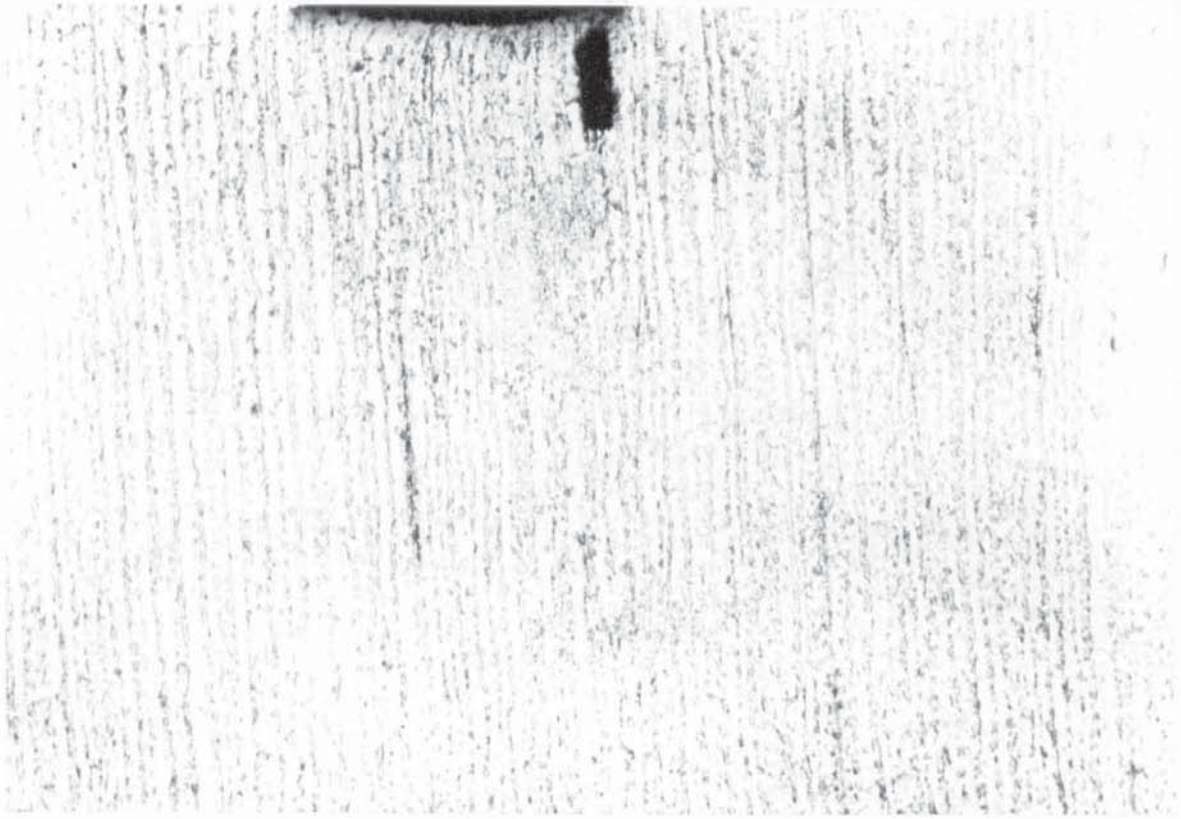

Figure 78 Linking of Crack and Notch Tip x 50

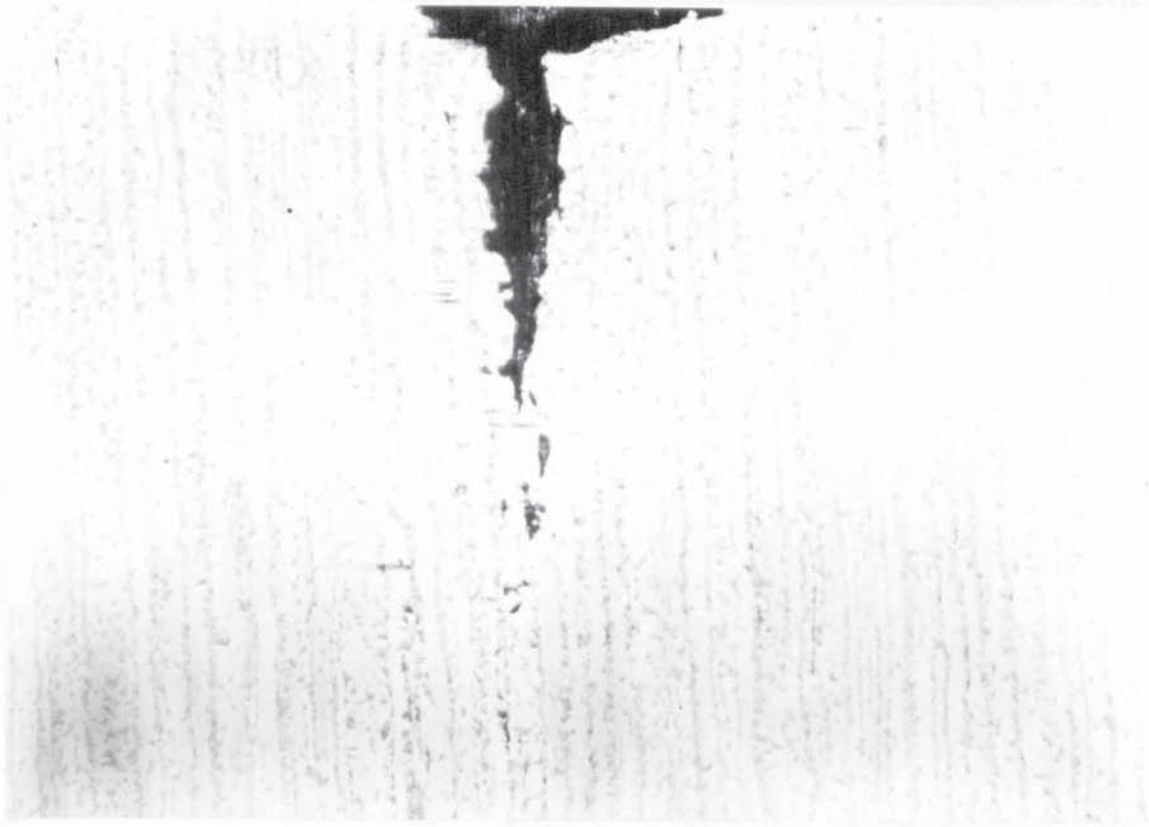

Figure 79 Growing Crack x 50

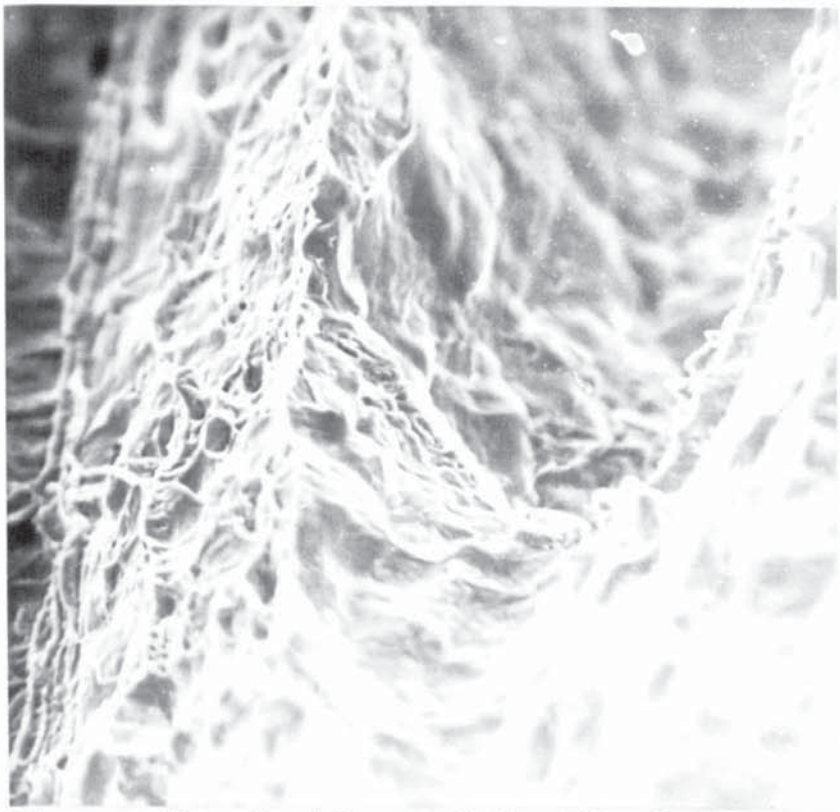

Figure 80 Necking and Ductile Rupture in Ferrite S.E.M. x 470

Figure 81 Final Fracture Appearance of Parent Plate Material S.E.M. x 21

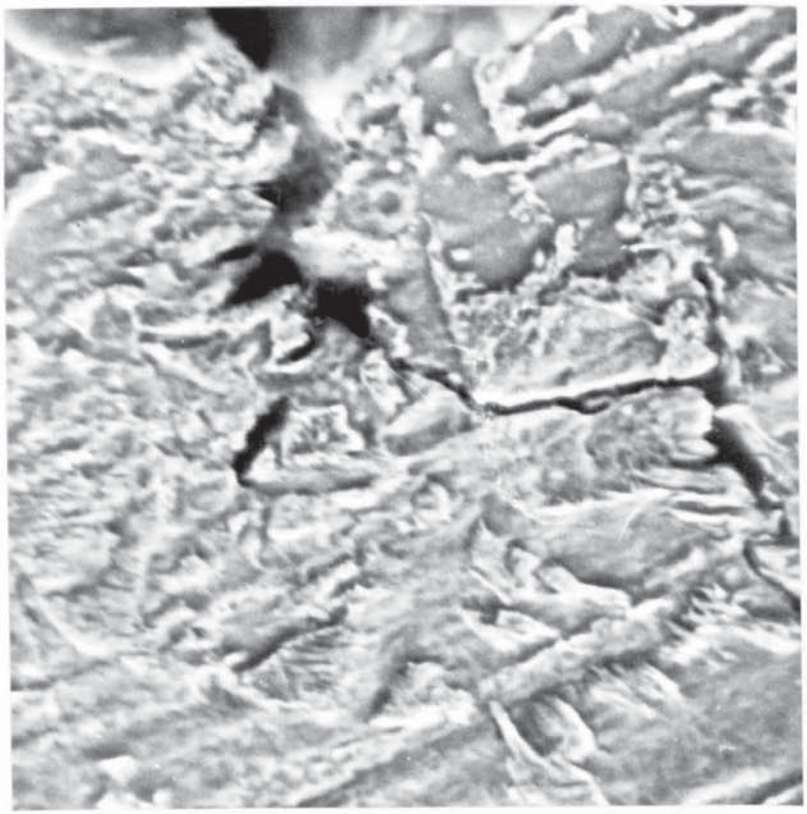

Figure 82 Crack Path in Grain Refined Region S.E.M. x 1700

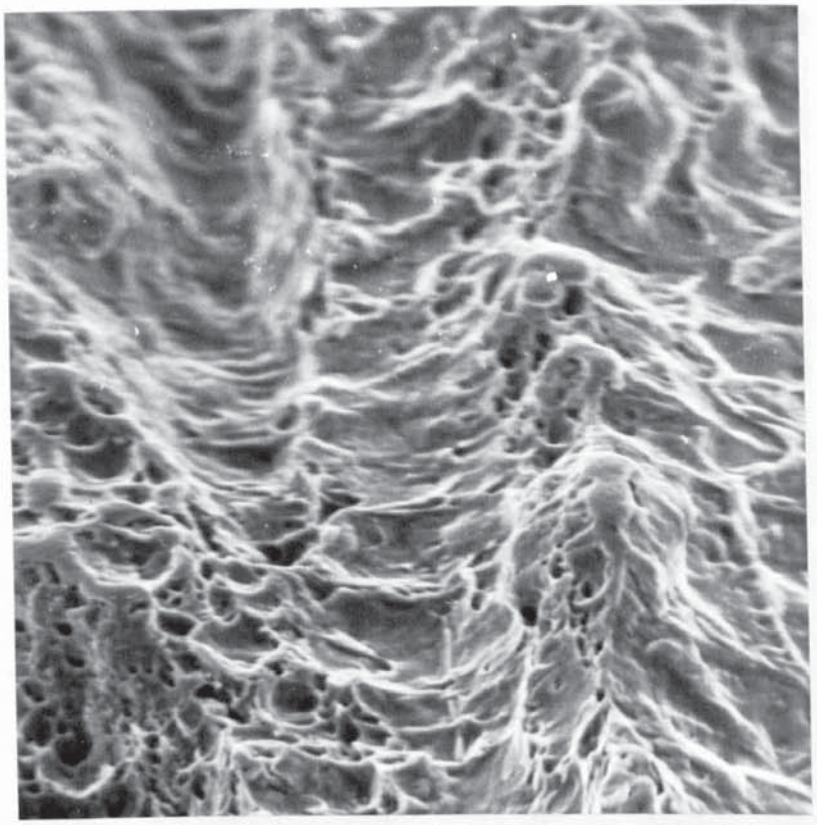

Figure 83 Fracture Surface in Grain Refined Region S.E.M. x 1100

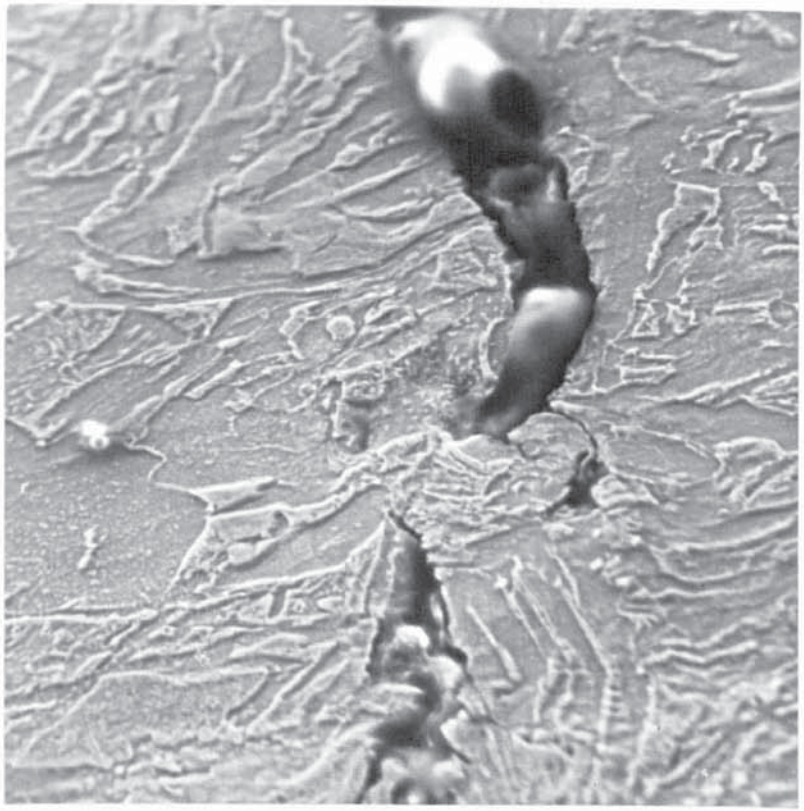

Figure 84 Crack Path in Widmanstätten Region S.E.M. x 850

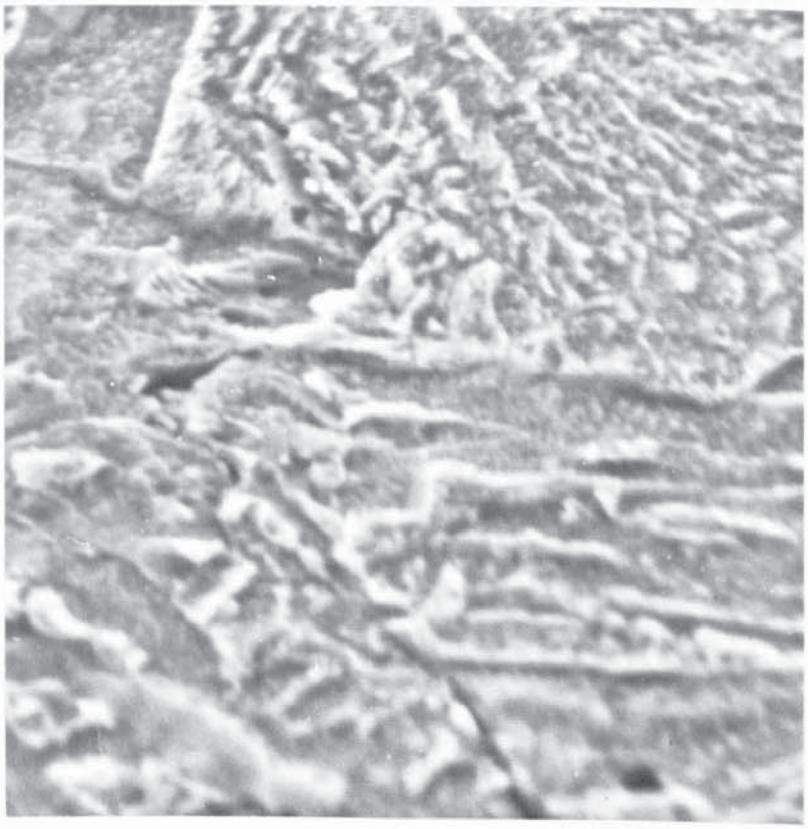

Figure 85 Crack Path in Widmanstätten Region S.E.M. x 3500

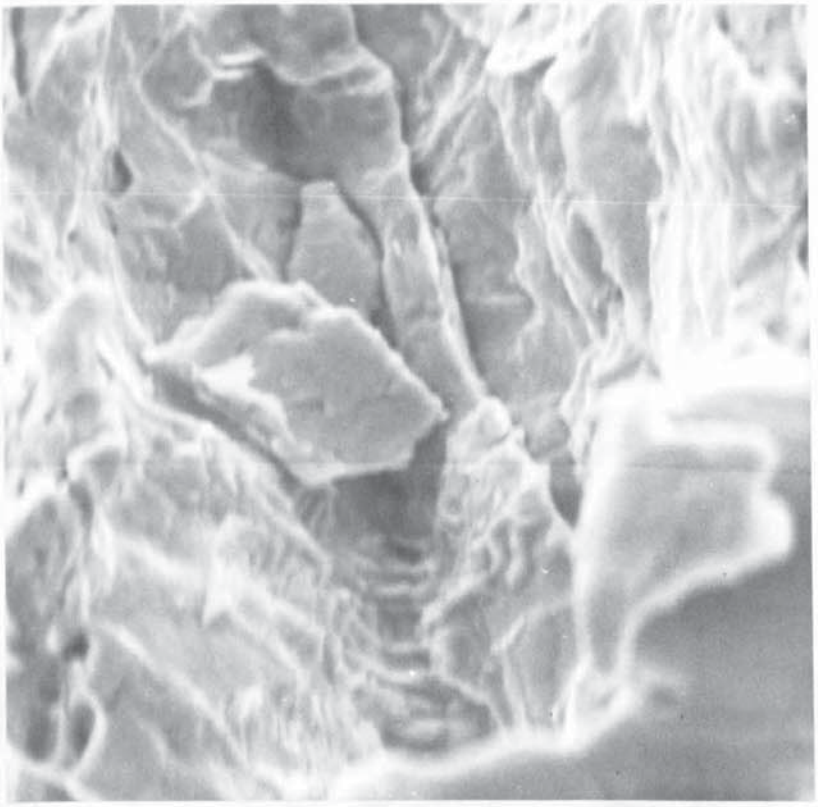

Figure 86 Fracture Surface Widmanstätten Region S.E.M. x2000

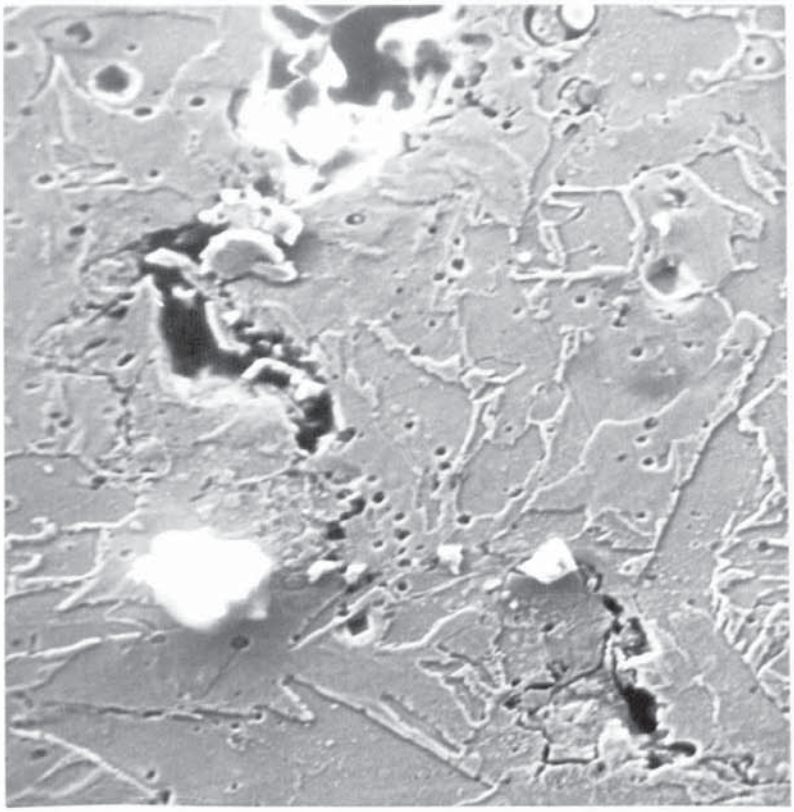

Figure 87 Crack Path in Weld Metal Region S.E.M. x 750

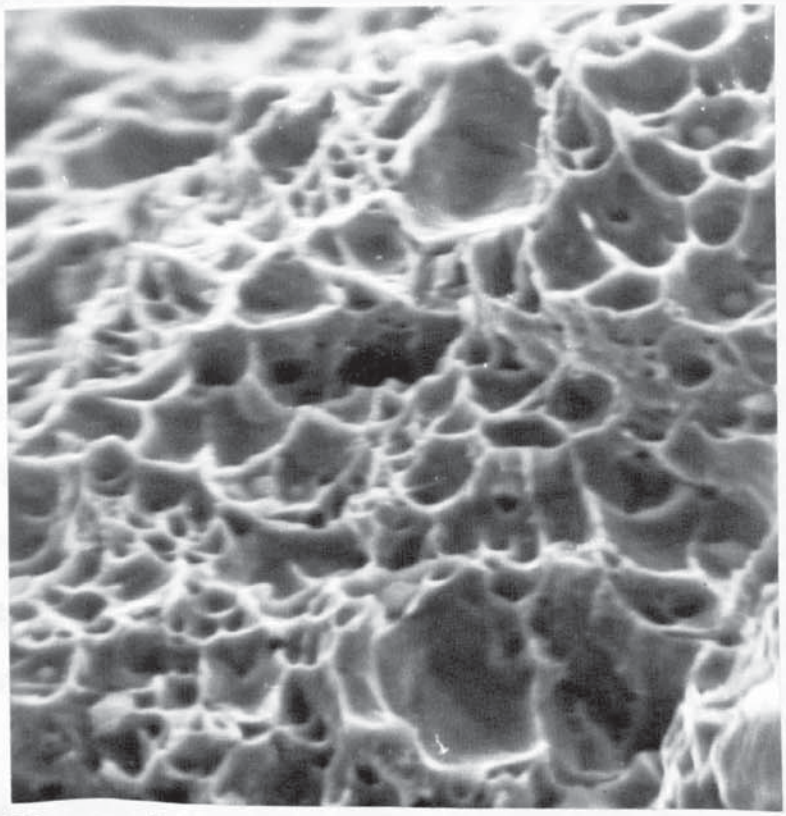

Figure 88 Fracture Surface Weld Metal Region S.E.M. x 2300

6. DISCUSSION

Material

The X-52 material studied in the main part of this work is one of the steels bought in quantity by the Gas Council for pipeline. The purchase price of X-52 is approximately £70 per ton as plate and £100 per ton as finished pipe. These prices are higher than would be paid for equivalent British Specification steels such as B.S. 4360. The extra cost is entailed because the A.P.I./Gas Council specification contains a toughness requirement based on the drop weight tear test[3] which it is felt eliminates the possibility of long brittle failures. The major part of the present work has been therefore to examine the possibility of crack initiation in regions of low toughness.

The analysis of the plate which was supplied to the A.P.I. 5LX-52 specification shows a manganese content in excess of the specified level. It is generally known[98] that the weldability of high yield strength steels decreases with an increase in the percentage of carbon and other alloying elements. The effect of carbon is the most important but the effect of manganese, nickel, chromium etc. is to enhance the problem and produce hard weld junctions.

It is probable that the steel used in the present investigation is the furthest out of specification that might be used for actual pipe. The results therefore will provide a useful guide to the extremes

in properties that could be expected.

The tensile properties measured on the as received plate are also lower than specified but this is quite normal since the cold work involved in the pipe manufacturing process raises the yield stress to the required minimum level.

The gross mechanical fibering observed metallographically in the as received plate is likely to affect the toughness of the material. When cracks propagate in a direction corresponding to a longitudinal crack running down a pipe, the fibering will tend to divide the crack in the manner proposed by Almond et al[92] and discussed in the review of the literature. Similarly cracks which grow through the thickness are likely to be arrested to some extent by each ferrite lamella.

The micro-hardness traverses on the as received plate showed no residual stresses likely to affect the toughness of the material. There is almost certain to be quite high residual stress in the finished pipe however. These residual stresses will arise because of the manufacturing process where the plate is bent and welded into tube and then cold expanded by 2% to ensure roundness. These complex stresses will make the task of estimating the actual load on a crack in service very difficult, but some estimates will be discussed later in the section dealing with the application of the results.

Toughness Measurement Techniques

It was seen from the literature review that the only reasonable technique available is that of crack opening displacement. Unfortunately when the project was begun there was considerable doubt surrounding a number of aspects of the technique.

The first of these points of question was the technique of measuring the crack opening displacement. The clip gauge method was advocated as simple and direct. All attempts to obtain a linear relationship between clip gauge C.O.D. and crack tip C.O.D. were unsuccessful in the present work. In all the specimens tested, the relationship proved to be a parabolic function, different for each specimen geometry.

These findings were confirmed by the study on the effect of distance from the crack tip on the C.O.D. value, this was found to be non-linear and of a complex form. It was therefore not surprising that a straight line equation linking δ_{CG} to δ_t did not fit the observed results.

Recent unpublished work[30] on the relationship between clip gauge and notch tip C.O.D. does in fact take the curved portion of the relationship into account. It is probable therefore that the technique could have been used if this latest data had been available when the work was begun.

Since a linear relationship had not been established it was decided that the only way to determine the crack tip C.O.D. accurately was to measure the C.O.D. at the crack tip. The paddle 'codmeter' would have been an ideal instrument to develop and use but it unfortunately cannot be used on fatigue pre-cracked specimens, although it eventually transpired that fatigue pre-cracking was not necessary in this particular case. The photographic calibration method was therefore chosen and the actual crack tip displacement was correlated with specimen deflection. It was first thought that the specimen deflection would have to be measured in terms of cross-head movement, but tests showed that the cross-head and the Instron chart operated at the same time with very little lag and it was decided to calibrate the crack tip C.O.D. against distance on the chart. These calibrations were then all performed at fixed cross head and chart speeds, of 0.02cm/min and 1 cm/min respectively and all subsequent tests were carried out using these conditions.

A number of errors could occur using the photographic calibration method and it might be argued that a similar calibration would have enabled the clip gauge technique to have been applied. The two major sources of error in the photographic technique would seem to be that the C.O.D. might vary between the surface and centre of a specimen and that the effect of the loading pins bedding into

the specimen could produce erroneous results. As far as could be determined, there was no variation of C.O.D. between the surface and the centre of a specimen and this is supported by earlier work[19]. The extent of plastic indentation by the loading pins was relatively slight and since, as far as could be determined, the amount of indentation was the same on all specimens it was considered that no real error was involved.

The final choice of photographic calibration instead of the clip gauge technique was made because the use of the photographic method eliminated the clip gauge and its associated electronic equipment. This removed a possible source of error due to electronic malfunction and making the experimental arrangement simpler. No clip gauge calibration is required before testing and once the original photographic calibrations have been performed and checked, the actual test procedure becomes one that could be incorporated into most test houses.

Determination of a Critical C.O.D.

Having developed a technique of measuring the C.O.D. it was then necessary to make a decision on what point on the load/displacement curve was to be taken as the critical event in the fracture process. In the recent past the critical event had been taken as the attainment of maximum load and the C.O.D. for this point had been measured as the critical C.O.D.

Reasonable correlation was established using this method between the critical C.O.D. on flawed tubes and small laboratory notch bend specimens but the correlation was only accurate if the amount of plasticity occurring before fracture was small[26].

The maximum load C.O.D. probably coincides with the critical event when the plastic zone size is small but does not when there is extensive plasticity. It had been shown[43] that the maximum load C.O.D. varied with specimen size even when the thickness was held constant, but the C.O.D. for the first appearance of a surface crack gave a seemingly more constant value of the critical C.O.D. It was therefore apparent that a more sophisticated definition of the critical C.O.D. was required if this quantity was to represent a true material property.

It was decided to extend the idea of a critical C.O.D. associated with the appearance of a surface crack to the point where the critical C.O.D. was taken as the C.O.D. for the initiation of any crack at the notch root. The various techniques available for monitoring the initiation of such cracking were discussed in the literature survey and the ultrasonic technique used was described in the section on experimental procedures.

Measuring the initiation of cracking C.O.D., δ_i provided a means of determining a critical C.O.D. which was independent of specimen geometry and specimen type, provided that the thickness of the

specimens remained the same. This was clearly demonstrated by the experiments on bend and C.T.S. specimens with widely varying a/w ratios and also on the subsized bend specimens. All these specimens gave closely comparable results for δ_i.

The accuracy of the ultrasonic method was proved by the results using the destructive technique developed by Knott and Smith[48]. Both techniques giving comparable measures of δ_i. The ultrasonic technique is however to be preferred over the destructive technique because of time and cost. The destructive technique required a series of test pieces to establish a value of δ_i where this can be achieved using only one specimen and the ultrasonic method.

The results of the experiments on the effect of notch acuity on the value of δ_i using both the ultrasonic and destructive techniques showed that the δ_i value was the same for fatigue cracked and 0.008 inch slotted specimens. This observation is the same as that made by Thornton[38] but opposed to that of Knott and Smith[48]. This would tend to indicate that the sensitivity of δ_i to notch sharpness is material dependent. Further it is reasonable to suppose that a notch ductile material such as X-52 would be likely to exhibit less sensitivity than other materials.

The findings of the notch acuity experiment had considerable experimental significance in that it enabled specimens to be tested containing 0.008 inch slots in place of fatigue cracks. The production of specimens was consequently much greater and the position of the notch tip could be arranged to a greater degree of accuracy than a fatigue crack which tends to choose its own path.

Using subsized specimens the δ_i value was found to be the same as that on the standard type of specimen This is reasonable since δ_i is here being advanced as a material constant. Furthermore the two designs of specimens used predominantely, namely ½ inch thick x 1 inch deep and 4 inch span with an a/w ratio of 0.5 and ½ inch thick x ½ inch deep and 2 inch span with an a/w ratio again of 0.5 are those now recommended[30] as the two to be used in practice.

The experiment on the effect of reducing specimen thickness showed that the as received material failed in an ostensibly plane stress manner, there being only a very small variation between δ_i in 0.5 inch thick specimens and 0.1 inch thick specimens. The variation being from 0.004 inch to 0.005 inch respectively. This is consistent with the fractography of the parent plate material which was shown to fail as multiple plane stress ferrite lamellae. The parent plate was also found to be insensitive to temperature between room temperature and -50°C and from past work[5] it was

expected that the worst part of the H.A.Z. would similarly be unaffected by temperature down to $-20^{o}C$. Since the minimum operating temperature of pipelines is in the region of $+10^{o}C$ it seemed reasonable to conduct tests only at room temperature since the production of a C.O.D. transition curve with temperature would serve no useful purpose as far as operating conditions are concerned. It would seem that the presentation of C.O.D. data as a C.O.D./Temperature transition can only be useful in specific situations where there is a very wide range of operating temperature. This is unlikely in a great many structures. The best approach would seem to be to obtain sufficiently accurate data to enable safe operation in the worst conditions; this in Britain is unlikely to be at temperatures lower than $-20^{o}C$.

The use of the δ_i technique proved sufficiently sensitive to toughness variation as was shown in the experiment on the effect of plate direction on toughness. The differences in toughness with orientation were observed very clearly. The results of this experiment are also in agreement with some of the predictions of Almond et al[92] who, working on models of lamellar material, postulated that laminates which tend to arrest or divide a crack will increase the toughness of a material. The longitudinal and transverse cracking directions in the X-52 plate examined in this work correspond to a crack dividing type of structure

while the through-thickness cracking direction is of the crack arrester type. The through-thickness and transverse directions both showed increased toughness over the longitudinal direction. While the increase in toughness in the through-thickness direction would be predicted by the Almond et al model, that in the transverse direction would not and other factors must evidently be taken into account. The cause of the increase in toughness in the transverse direction against that in the longitudinal direction is probably associated with the manner in which the inclusions are arranged in the material.

Compared to previously accepted results for C.O.D. values in low alloy steels the results obtained in this work are very low. For this reason it is possible that the technique may be uneconomic in practice, since large specimens and consequently structures can sustain quite large amounts of slow crack growth before crack instability is reached[58]. The way in which specimen size can affect instability is shown in Figures 46 and 47, specimens with large a/w ratios, therefore small uncut ligaments, reach crack instability i.e. maximum load at or very near to the point of crack initiation. Specimens with large uncut ligaments withstand slow tearing and do not reach crack instability until long after crack initiation.

In general therefore it would seem that a less conservative measure of the critical C.O.D. must be determined if this parameter is to be used in economic design. A move towards a more realistic but less rigorous value of δ_c has been made by Elliott et al[99] who measure δ_c as the C.O.D. occurring at the onset of macroscopic tearing, measured by potential drop methods. However, in the specific case of pipelines any leak constitutes a highly dangerous failure. The large full wall defects to which the application of the δ_i measurement would appear uneconomic would be removed during inspection or observed during hydraulic pressure test. Small partial wall defects could however remain and such defects can be assessed accurately using the δ_i technique. Recent work[58] has shown that leakage from a partial wall defect, i.e. the break through of the defect, occurs very close to the point of crack initiation. Consequently the values measured in the present work will be directly applicable to pipelines and can in this context be termed failure C.O.D.'s

It was concluded from the work on as received material that the techniques developed gave post general yield fracture toughness values which were fundamental material properties. Furthermore the techniques were considered sensitive to changes in material toughness and could be applied directly to pipes. It was then considered that the methods could be used to assess the affect of welding on material toughness in order to detect any possible embrittlement.

Measurement of the Toughness of Welded Material

The welding conditions used to produce test welds for the study on weld metal and heat affected zone toughness were the optimum that could be produced under laboratory conditions. As far as could be determined the heat flow conditions and H.A.Z. widths were theoretically the same in both the test plates and real pipes. This was justified by the metallography which showed that although the actual shape of the weld beads produced in the laboratory differed in some cases from those on pipes, the H.A.Z. widths were the same and the hardness values across the weld and H.A.Z. were also comparable. The test conditions also produced sound welds as shown by unnotched bend tests.

Microhardness traverses across the weldments revealed possible areas of embrittlement on the fusion boundary of the weld in the second pass H.A.Z. This area consisted of a Widmanstätten structure containing very coarse acicular ferrite and it was decided to examine this region very carefully.

It was found possible to obtain values of δ_i for each different metallurgical structure across the joint since the cracks were observed to grow from the centre of the specimen thickness. Thus crack initiation could be monitored in whichever structure occurred at the centre of a specimen. This had not previously been

possible with double-vee weld joints, because critical C.O.D. had been measured at the maximum load point and at maximum load the crack front covered a range of structures thus giving an average value of toughness. To measure the toughness of individual zones in the past has necessitated changing the joint geometry to for example, a K preparation. This could lead to errors because of different heat flow conditions. Alternatively thermal simulation of weld conditions has been used to produce test specimens containing a large volume of structure corresponding to a specific part of the H.A.Z. Such simulations have at times produced erroneous results[71] and it is obviously much better to test welds as close to those that will be used in service as possible.

The values of δ_i across the weldments with the specimen notch in the longitudinal and through-thickness directions showed a minimum toughness coinciding with the Widmanstätten H.A.Z. The toughness of the Widmanstätten region was only one half of that of the parent plate material in both directions. The weld metal itself was the region of highest toughness in the weldment. The yield strength of the weld metal was very close to that of the parent plate material so that the increase in toughness over the parent plate cannot be attributed to undermatching. The probable reason for the high toughness in the weld metal is the metallographic structure of finely

dispersed carbides in ferrite which produces a classical ductile failure by dimple rupture.

The welded specimens supplied by the Gas Council showed no significant variation in toughness across the H.A.Z. and this is probably due to the lower carbon and manganese contents of the plate.

The plate supplied to the University was believed by the supplier to be X-52 but was however slightly outside the permissible chemical analysis specification. Similarly such plate could be made into pipe and used in service. For this reason the experimental results obtained can be used to calculate the smallest possible defect sizes that would be likely to cause leakage at service pressures.

Fractography

Examination of fracture surfaces from different structures of the weldment supported the results on the variation of toughness between parent plate, H.A.Z. and weld metal. The zone of low toughness at the fusion boundary showed extremely shallow, low ductility dimples as compared to the parent plate material. The weld metal, which has the highest toughness, showed a fully ductile dimple fracture surface.

The fracture process which gives rise to the fracture surface observed in the parent plate material was discussed in the results section. Briefly, delamination of the structure along the pearlite-rich bands, and ductile necking of the ferrite, produce the

fibrous fracture appearance. The ferrite fails by dimple rupture, voids forming around second phase particles, followed by necking between the voids.

In the lower toughness, grain refined region of the H.A.Z., the dimples observed were much shallower because of reduced ductility. Fracture surfaces in the Widmanstätten H.A.Z. showed very little ductility, and contained flat facets resembling cleavage. Examples of this type of fracture surface have in the past been referred to as quasi-cleavage[86].

The weld metal as stated earlier showed a classical ductile dimple fracture surface. As in the case of the ferrite in the parent plate, voids are formed around the many carbides in the weld deposit. This is followed by substantial necking of the ferrite leading to void coalescense and the formation of a dimpled surface.

All these observations were in agreement with the variation of toughness across the weldment.

Angled Weld Studies

After the assessment of the toughness of the welded joint in X-52, the effect of welds at angles to advancing cracks was studied. This work, simulating the case of spiral welded pipe, showed that such cracks turned to follow the line of the weld up to an angle of approximately 70^{o}. At angles greater than this the crack proceededacross the weld. This angle of 70^{o} is greater than that in spiral welded pipe, where the angle

between the weld and the pipe centre-line is approximately 60^{o}. This tends to indicate that a fracture in such a pipe would follow the weld rather than travel longitudinally.

Metallographic studies showed that in the situation where the crack turned to follow the line of the weld, the crack did not run in the most brittle region as might be expected but in parent plate material some distance from the weld H.A.Z. The reason for the crack turning to take this line is thought to be due to a distortion of the plastic zone as has been suggested by Richards[66]. The plastic zone was observed to spread further into the soft parent plate material than the harder H.A.Z., thus producing a plastic zone approximately distributed about an axis parallel to the weld. The crack path then tended to follow the new axis of the plastic zone and travel parallel to the weld, away from the centre-line of the specimen. These observations confirmed similar observations by Richards and also permitted an untried field of general yield fracture mechanics to be examined.

On taking a line parallel to the weld the crack moved away from the line of maximum force in the specimen and the crack tip experienced an additional shear stress, the size of this shear increasing with the angle from the specimen centre-line. In this situation the crack tip should have experienced an opening and a sliding mode of deformation, Mode I and Mode II in linear elastic fracture mechanics

notation. The fact that this does occur was clearly demonstrated on arrested cracks and the values of C.O.D. in the opening mode δ_I and shear mode δ_{II} were measured on arrested cracks. The actual values measured can be questioned because of the inaccuracy of the surface grid method used and the measurement of the displacements at the tips of arrested cracks. The measurements are however believed to be reasonably close to the absolute values and can in any case adequately describe the form of the relationship between δ_I and δ_{II}.

The only previous theoretical work in this area has been for the onset of cracking by Wu[63] and Erdogan and Sih[62] who measured K_I and K_{II} stress intensification factors on brittle non-metallic materials. Both the laws postulated by these two sources were converted to C.O.D. terms using the relationship $G = \sigma_y \delta$. The results from the present work then fitted both equations equally closely. Until further work is undertaken, it would seem reasonable therefore to express the relationship between δ_I and δ_{II} as conservatively as possible. The relationship would then be the general yield adaptation of the Erdogan and Sih equation

$$\left(\frac{\delta_I}{\delta_{I_c}}\right) + \left(\frac{\delta_{II}}{\delta_{II_c}}\right) = 1$$

Calculation of Critical Defect Sizes

The small series of experiments performed to test the validity of the link between linear elastic and general yielding fracture mechanics, added further evidence to the firm belief that the two approaches are interchangeable. Since the two approaches are interchangeable and because K_c values are more readily applicable[50] to the assessment of actual structures than C.O.D. data it seems reasonable to convert the δ_i values to K_c values when attempting to assess the performance of pipes. Furthermore it would be impossible to use the C.O.D. data directly to assess the significance of H.A.Z. defects because the high values of σ/σ_y involved invalidate the equations currently available.

In order to use the calculated K_c values to determine critical flaw sizes in pipes at service pressure it is necessary to specify certain conditions. Firstly an estimate must be made of the stress that a defect would have to withstand. In a simple situation this would be taken as the applied stress. However, in the case of a welded joint, Cottrell[52] has shown that the residual stresses can reach yield point magnitude. Therefore in order to make a safe estimate of the critical size of a defect in the region of a weld, it would seem reasonable to use a stress equal to the yield stress plus the applied stress in the calculations.

The region of the weld H.A.Z. is the most likely position for defects to be situated[100]. This region is prone to toe-cracking, undercutting and other forms of weld defects and is the most difficult to examine by non-destructive testing. The region of the weld is also the most important because critical defects in the region away from the weld are much larger because of the lower stresses and higher toughness in the parent plate.

The critical size of a partial wall defect can be calculated using the equation[50].

$$\left(\frac{a}{Q}\right)_c = \frac{1}{1.21\pi} \left(\frac{K_c}{\sigma_y}\right)^2$$

the terms of which were described earlier.

The lowest value of toughness measured in the through-thickness direction, i.e. the direction in which a partial wall defect will grow to cause failure, was a δ_i of 0.006 inch. This is equivalent to a K_c of approximately 95 Ksi$\sqrt{in}$

Putting σ_a equal to the yield stress plus the applied stress σ_a = 77 Ksi

Taking a value of Q = 1 i.e. an aspect ratio of 10:1

$$a_c = 0.40 \text{ inch}$$

This defines a critical flaw in these conditions as an ellipsoidal crack 0.40 inch deep x 4.0 inch long. At maximum working stress this size of defect could propagate through the wall and cause leakage.

In the tougher region of the pipe unaffected by welding the stresses are lower consequently critical defect sizes are much larger. Defects likely to cause failure in this region are full wall thickness approximately 8 inches long, calculated from the equation[101].

$$a_c = \frac{1}{\pi}\left(\frac{K_c}{\sigma}\right)^2 - \frac{1}{2\pi}\left(\frac{K_c}{\sigma_y}\right)^2$$

This makes detection far more certain and would probably prevent test pressurization of the pipe if they were not eliminated during inspection. It would seem therefore that even the smallest estimate of critical longitudinal defects i.e. those situated in the low toughness, highly stressed H.A.Z. are fairly large 0.4 inch deep x 4 inch long and it would be thought that they could be easily detected during inspection.

The work on angled cracks shows that a crack at an angle to the maximum stress, the hoop stress, will require a smaller opening mode C.O.D. to cause failure. The reduction in δ_I required for failure will depend on the proportion of sliding mode C.O.D., δ_{II}, acting on the crack tip. Furthermore when a crack exists at an angle to the pipe centre-line, the stress at the crack tip although only a component of the hoop stress will be augmented by a component of the longitudinal stress. This makes calculation of the exact δ_I required for failure difficult but it might easily be half that

required in the longitudinal crack situation. In such a case if the defect were an elliptical surface flaw its critical size would be 0.2 inch deep x 2 inch long. This would be somewhat more difficult to locate close to a weld but ought to be easily within modern non-destructive testing capability.

7. CONCLUSIONS

It is concluded that:

1. The concept of C.O.D. as a measure of the fracture toughness of ductile material is accurate provided that the critical C.O.D. is taken at the point of crack initiation. This being the only point at which a δ_c can be measured which is a material constant.

2. The application of δ_i to the majority of structures can be considered to be uneconomically pessimistic, but in the specific case of partial wall defects in pipes, it can be used to postulate practical failure conditions precisely.

3. The use of a clip gauge to measure the crack tip C.O.D. via calibration, proved unsuccessful in this work and could lead to erroneous results if used on other similar materials. Until the new equations relating notch tip C.O.D. to clip gauge C.O.D. have been verified and become widely known, the only technique that can at present be recommended for measuring low C.O.D.'s is the photographic method since this gives direct values of crack tip C.O.D. and can also be used on fatigue cracked specimens.

4. In materials having carbon and manganese contents near to the upper limits of the A.P.I. 5LX-52 specification it is possible to obtain an embrittled zone at the fusion boundary of the pipe longitudinal seam weld. Lowering the maximum permissible carbon and manganese levels would reduce and possibly eliminate this problem.

5. In ductile material the relationship between the opening mode C.O.D. δ_I and the sliding mode C.O.D. δ_{II}, can be treated within the limits of the available results as being of the form

$$\left(\frac{\delta_I}{\delta_{I_c}}\right) + \left(\frac{\delta_{II}}{\delta_{II_c}}\right) = 1$$

6. The critical size for a partial wall defect in the fusion boundary of the weld, is approximately 0.4 inch deep x 4.0 inch long, at maximum operating pressure, provided that it lies in a longitudinal direction. This size of defect ought to be easily detected and the pipe therefore rejected.

7. If a crack lies at an angle to the longitudinal direction of the pipe it is possible for a shear displacement at its tip, δ_{II}, to exist. In this situation the necessary δ_I for failure is reduced and the critical defect size is therefore smaller.

8. ACKNOWLEDGEMENTS

The author would like to thank Dr. J.T. Barnby for his guidance and helpful discussion during the course of this work, and to gratefully acknowledge the financial support of the Gas Council.
He would also thank his wife for her encouragement and understanding during the past three years.

9. APPENDIX

Specimen Design

In using the compact tension specimen to examine the effect of a/w on δ_i with the value of a fixed, a flaw was found in the design of these specimens. As was shown in Figure 25, (Page 79), in specimens with a/w ratios less than approximately 0.5 the crack path was unstable. This instability of the crack path had been noted earlier by Cotterell[95] who used linear elastic stress analysis to design specimens in which it did not occur, this approach however seemed to meet with little success.

It was considered that an approach to the problem could be made using simple strength of materials, assuming that the stress in the main body of the specimen tended to run the crack in the desired direction whilst that in the arms tended to cause the crack to run off at 90^{o} to the normal. A simple model of the specimen was taken as shown in Figure 89.

The arms can be considered as built-in cantilever beams and as such the stress tending to run the crack at 90^{o} to the desired direction can be computed as follows:

$$\sigma_A = y. \frac{12}{BH3}. M.$$

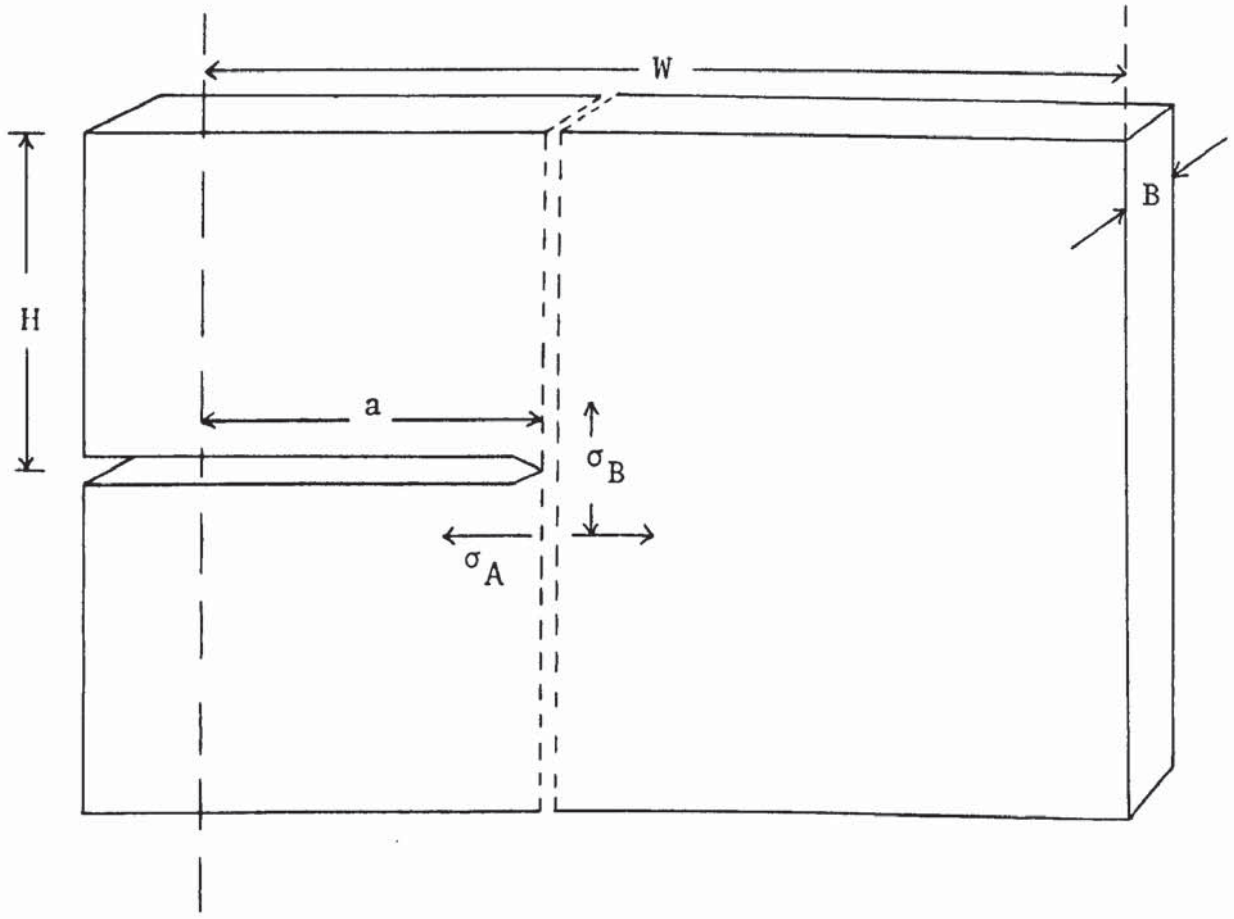

Figure 89

Model of Compact Tension Specimen
Used in Design Analysis

Where σ_A is the stress in the arms tending to run the crack at 90^o to the normal, y is the distance to the neutral axis namely H/2, B the specimen thickness, H the half specimen height and M the modulus.

$$\text{Thus} \quad \sigma_A = \frac{H}{2} \cdot \frac{12}{BH^3} \cdot P. \; a$$

Where P is the applied load and a the crack length.

$$\therefore \quad \sigma_A = \frac{6P}{BH^2} \cdot a$$

Thus for a specimen with fixed, H, W and B the change in arm stress with crack length can be calculated for a given value of P and the relationship will be a straight line.

Similarly the stress in the body section of the specimen can be computed, assuming that this stress, the stress tending to run the crack along the axis of the specimen, is composed of the stress developed from the bending of the uncut section plus the tensile stress developed from the applied load.

$$\text{Thus} \quad \sigma_{Body} = \sigma_{Bending} + \sigma_{Tensile}$$

$$\sigma_{Bending} = \frac{(W-a)}{2} \; M. \; \frac{12}{B(W-a)^3}$$

$$\sigma_{Tensile} = \frac{P}{B(W-a)}$$

$$\sigma_B = \frac{6P\left[a + \frac{(W-a)}{2}\right]}{B(W-a)^2} + \frac{P}{B(W-a)}$$

If again all variables other than a are held constant the relationship between body stress and crack length can be computed.

The two equations for arm stress and body stress are shown superimposed in Figure 90 from which it can be seen that there is a "cross-over" point after which the stress in the uncut section of the specimen is always higher than that developed in the arms.

This simple analysis was refined by the inclusion of appropriate stress concentration factors[102] into the equations

$$\sigma_A = \frac{6P}{BH2}\, a \times 1.5$$

$$\sigma_B = \frac{6P\left[a + \frac{(W-a)}{2}\right]}{B(W-a)^2} \times 2.3 + \frac{P}{B(W-a)} \times 2$$

From these equations graphs as in Figure 90 were drawn for a model specimen ½ inch thick, with a W of 6 inches and H 2 inches. Perspex specimens of these dimentions were produced with crack lengths bounding the predicted transition area and these were found to fail in accordance with the graphical predictions.

Shortly after this analysis was completed Cotterell published another paper[96] using a similar strength of materials approach to predict the crack path in this type of specimen.

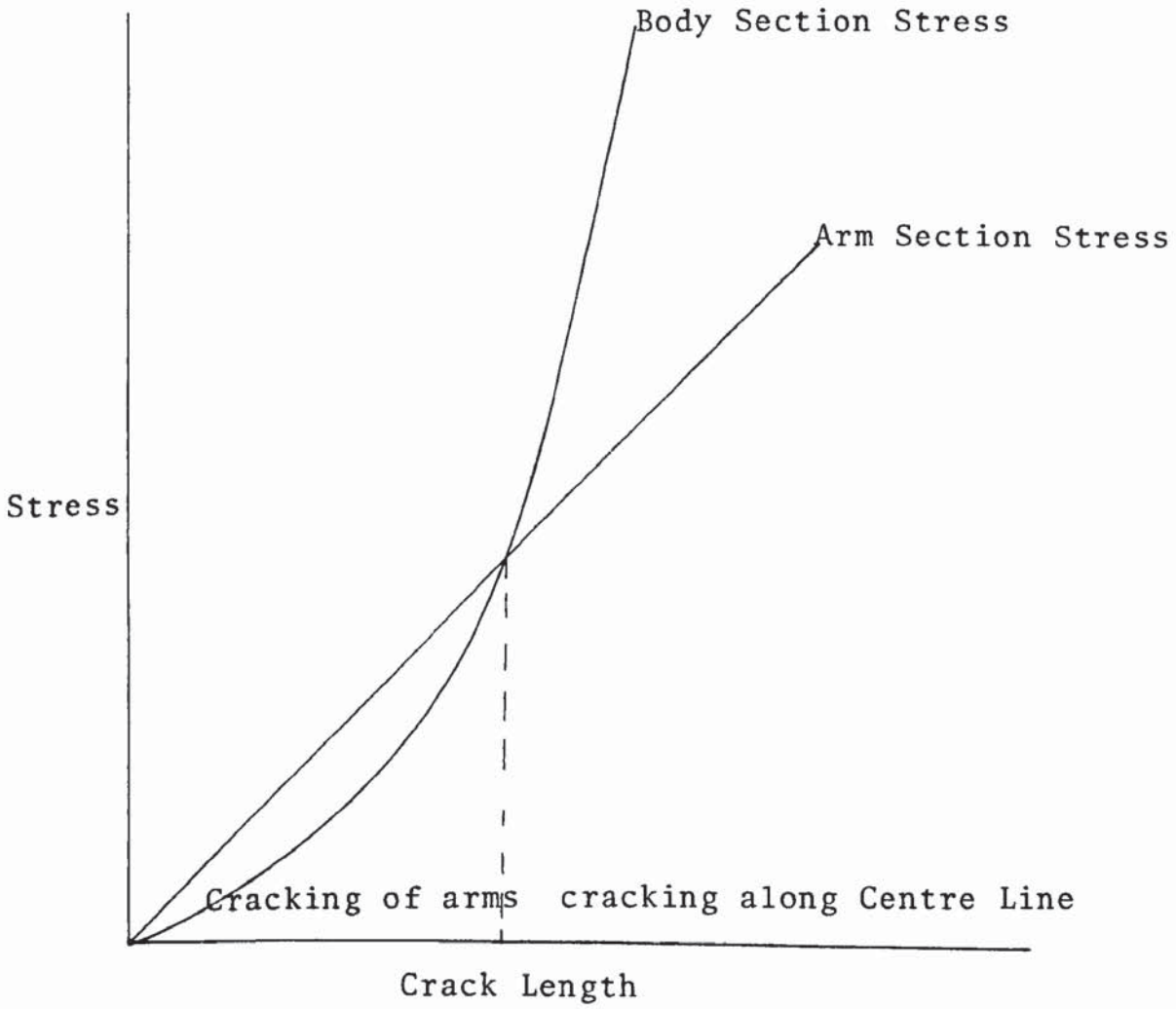

Figure 90

Relationships between Arm Section and Body Section Stresses and Crack Length

10. REFERENCES

1.	American Petroleum Institute	A.P.I. Std. 5LX 15th Edition March 1968
2.	Mc. Clure, G.M., Duffy, A.R. and Eiber, R.J.	Trans A.S.M.E. 1965, 87B, 265-278
3.	Symposium on Linepipe Research	Dallas (Nov. 1965) A.G.A. Cat. No. L,30,000
4.	4th Symposium on Linepipe Research	Dallas (Nov. 1969) A.G.A. Cat. No. L,30,075
5.	Fearnehough, G.D., Haddrill, D.M. and Weiner, R.T.	J. West of Scotland I.S.I. 1970, 77, 70-86
6.	Griffith, A.A.	Phil. Trans. Roy. Soc. 1920, A221, 163-198
7.	Inglis, C.E.	Trans. Inst. Naval Arch 1913, 55, I, 219-230
8.	Orowan, E.	Rep. Prog. Phys. 1948-49, 12, 185-232
9.	Orowan, E.	"Fracture" 147-160 1959, New York, Wiley and Son.
10.	Irwin, G.R.	U.S. Naval Research Lab. Rep. N.R.L. 4763.1956
11.	Westergaard, H.M.	J. Applied. Mech 1939, 61, 6, A49-A53
12.	American Society for Testing and Materials	"Plane Strain Crack Toughness Testing of High Strength Metallic Materials" 1967, Philadelphia, A.S.T.M.
13.	Wells, A.A.	Proc. Crack Propagation Symp. Cranfield, 1961, 1, 210-230
14.	Cottrell, A.H.	"Steels for Reactor Pressure Circuits" 281-296, 1960, I.S.I.
15.	Bilby, B.A., Cottrell, A.H. and Swinden, K.H.	Proc. Roy. Soc. 1963, A272, 304-314
16.	Wells, A.A.	Brit. Weld. Journ 1963, 10, 563-570
17.	Irwin, G.R.	App. Mech. 1957, 24, 361-364

18.	Wells, A.A.	Eng. Frac. Mech. 1969, 1, 3, 399-410
19.	Burdekin, F.M. and Stone, D.E.W.	Journ. Strain Analysis 1966, 1, 2, 145-153
20.	Barenblatt, G.I.	Adv. Applied Mech. 1962, 7, 55-129
21.	Dugdale, D.S.	Journ. Mech. Phys. Solids 1960, 8, 2, 100-104
22.	Bilby, B.A., Cottrell A.H. Smith, E. and Swinden, K.H.	Proc. Roy. Soc. 1964 A279, 1-9
23.	Dixon, J.R. and Strannigan, J.S.	J. Mech. Eng. Sci. 1964, 6, 2, 132-136
24.	Gerberick, W.W.	Proc. Soc. Exp. Stress Analysis 1964, 21, 2, 335-344
25.	Pilkington, R.	"Crack Opening Displacement Measurements at Evelated Temperature" C.E.G.B. Report RD/L/N75/70
26.	Fearnehough, G.D. and Watkins. B.	Int. Journ. Fracture Mech. 1968, 4, 3, 233-243
27.	Nicholls, R.W., Burdekin, F.M., Cowan, A., Elliott, D. and Ingham, T.	"Practical Fracture Mechanics for Structural Steels" F1-F13, 1969, Lon. U.K.A.E.A. with Chapman and Hall.
28.	Elliott, D. and May, M.J.	"The Effect of Position on Measurement of C.O.D." BISRA Open Report MG/C/47/69
29.	Elliott, D. and May, M.J.	"C.O.D. Inferred from Plasticity Phenomena" BISRA Open Report MG/C/86/68
30.	Barnby, J.T.	Private Communication
31.	Strawley, J.E., Swedlow, J.L. and Roberts, E.	Int. Journ. Fracture Mech. 1970, 6, 441-444
32	Wells, A.A.	Private Communication
33.	Wells, A.A. and McBride, F.H.	Canadian. Met Quart. 1965, 6, 4, 347-368

34.	Burdekin, F.M., Dawes, M.G., Archer, G.L., Bonomo, F. and Egan, G.R.	Brit. Weld. Journ. 1968, 15, 590-600
35.	Dawes, M.G.	Brit. Weld. Journ. 1968, 15, 563-570
36.	Parry, G.W. and Mills, R.G.	Journ. Strain Analysis 1968, 3, 3, 159-162
37.	Saunders, G.G. and Dolby, R.E.	Brit. Weld. Journ. 1968, 15, 230-240
38.	Thornton, D.V.	Eng. Fracture Mech. 1970, 2, 125-143
39.	Marcal, P.V. and King, J.P.	Int. Journ. Mech. Sci. 1967, 9, 143-155
40.	Stonesifer, S.R. and Smith, H.L.	U.S. Naval Research Lab. N.R.L. Report 7053 April 1970.
41.	Kies, J.A., Smith, H.L. and Stonesifer, F.R.	U.S. Naval Research Lab. NRL Report 6917 Sept. 1969.
42.	Cowan, A. and Kirby, N.	"Practical Fracture Mechanics for Structural Steels" D1-D27, 1969, London. U.K.A.E.A. with Chapman and Hall.
43.	Harrison, T.C. and Fearnehough, G.D.	Int. Journ. Fracture Mech. 1969, 5, 3, 348-349.
44.	Knott, J.F.	J.I.S.I. 1967, 205, 288-291.
45.	Johnson, H.H.	Materials, Research and Standards 1965, 5, 442-445.
46.	Jones, M.H. and Brown, W.F.	Materials, Research and Standards 1964, 4, 3, 120-129.
47.	Clarke, W.J. and Ceschini, L.J.	Materials Evaluation 1969, 27, 180-184
48.	Knott, J.F. and Smith, R.F.	"Practical Application of Fracture Mechanics to Pressure Vessel Technology" I. Mech. E. ConF. London. 1971
49.	American Society for Testing and Materials.	Materials, Research and Stds. 1964, 4, 3, 107-119.

50.	Tiffany, C.F. and Masters J.N.	"Fracture Toughness Testing and its Applications" 249-277 1965, Philadelphia, A.S.T.M.
51	Goodier, J.M. and Field, F.A.	"Fracture of Solids" 103-118, 1963, New Yort, Gordon and Breach.
52.	Cottrell, C.L.M.	Brit. Weld. Journ. 1968, 15, 262-267.
53.	Irvine, W.H., Quirk, A. and Bevitt, E.	Journ. Brit. Nvc. Energy Soc. 1964, 3, 31-48.
54.	Follas, E.S.	Int. Journ. Fracture Mech. 1965, 1, 104-113
55.	Parry, G.W. and Lazeri, L.	Eng. Fracture Mech. 1969, 1, 519-537
56.	Wells, A.A.	Brit. Weld. Journ. 1968, 15, 221-229
57.	Cowan, A. and Kirby, N.	Trans. A.S.M.E. 1970, 92B, 1, 79-85
58	Fearnehough, G.D., Lees, G.M., Lowes, J.M. and Weiner, R.T.	"Practical Application of Fracture Mechanics to Pressure Vessel Technology" I. Mech.E. Conf. London 1971.
59	Hahn, G.T. Sarrate, M. and Rosenfield, A.R.	Int. Journ. Fracture Mech. 1969, 5, 3, 187-210
60.	Burdekin, F.M. and Taylor, T.E.	J. Mech. Engng. Sci. 1969, 11, 5, 486-497
61.	Broek, D.	"Aerospace Proceedings" 2, 811-835, 1966, London, Macmillan.
62.	Erdogan, F. and Sih, G.C.	Trans. A.S.M.E. 1963, 85D, 519-527
63.	Wu, E.M.	Trans A.S.M.E. 1967, 34E, 967-974
64.	Pook, L.P.	"The Effect of Crack Angle on Fracture Toughness" N.E.L. Reprot No. 449.
65.	Dowse, K.R. and Richards, C.E.	Met. Trans. 1971, 2, 2, 599-603.

66. Richards, C.E. "The Influence of Material Properties on Fatigue Crack Propagation as Demonstrated by Experiments on Silicon Iron" C.E.G.B. Report RD/L/R1679

67. Archer, G.L. "The Fracture Toughness in the H.A.Z.'s of C-Mn Steel and a Low Alloy Steel" Welding Institute Report E/32/69.

68. Nippes, E.F. and Savage, W.F. Welding Journ. 1949, 28, 11, 534s-546s.

69. Widgery, D.J. Met. Construction and Brit. Weld. Journ. 1969, 1, 328-332

70. Watkins, B., Vaughan, H.G. and Lees, G.M. Brit. Weld. Journ. 1966, 13, 350-356.

71. Dolby, R.E. and Widgery, D.J. "The Simulation of H.A.Z. Microstructures". Welding Institute Report M/52/70.

72 Dolby, R.E. "Fracture Toughness Comparison of Weld H.A.Z. and Simulated Microstructures" Welding Institute Report M/53/70.

73. Tipper, C.F. Admiralty Ship Welding Committee Report R3, H.M.S.O., 1948.

74. Robertson, T.S. J.I.S.I., 1953, 175, 361.374.

75. Boyd, G.M. Engineering 1953, 175 65-102.

76. Roberts, D.K. and Wells, A.A. Brit. Weld. Journ. 1954, 1, 553-560

77. Wells, A.A. Welding Journ. 1952, 17,263s-267s.

78. Parker, E.R., Davies, H.E., And Flanigan, A.E. Proc. A.S.T.M. 1946, 46, 1159-1169.

79. Plateau, J. , Henry, G. and Crussard, C. Rev. Metall. 1957, 54, 200-216.

80. Rogers, H.C. Trans. A.I.M.E. 1960, 218 498-506.

81.	Rogers, H.C.	Acta. Met. 1959, 7, 750-752.
82.	Puttick, K.E.	Phil. Mag, 1959, 4, 964-969.
83.	Cottrell, A.H.	"Fracture" 20-53, 1959 New York, John Wiley and Sons.
84.	Gurland, J. and Plateau, J.	T.A.S.M. 1963, 56, 442-454.
85.	Crussard, C., Borione, R., Plateau, J., Morillon, Y. and Maratray, F.	J.I.S.I. 1956, 183, 146-177
86.	Beachem, C.D. and Pellous, R.M	"Fracture Toughness Testing and its Applications" 210-244, 1965, Philadelphia, A.S.T.M.
87.	Bastien, P.G.	J.I.S.I. 1957, 187, 281-291.
88.	Soete, W.	Journ. West of Scot. I.S.I. 1952-52, 60, 276-293.
89.	Matton-Sjöberg, P.	Ibid. 180-223.
90.	de Kazinczy, F. and and Backofen, W.A.	T.A.S.M. 1961, 53, 1, 55-73.
91.	Kapadia, B.M., English, A.T. and Backofen, W.A.	T.A.S.M. 1962, 55, 3, 389-398
92.	Almond, E.A., Embury, J.D. and Wright, E.S.	"Interfaces in Composites" 107-129, 1969. Philadelphia, A.S.T.M.
93.	Embury, J.D., Petch, N.J., Wraith, E.A. and Wright, E.S.	T.A.I.M.E. 1967, 239, 114-118.
94.	Almond, E.A. Petch, N.J., Wraith, A.E. and Wright, E.S.	J.I.S.I. 1969, 207, 10 1319-1323.
95.	Cotterell, B.	Int. Journ. Fracture Mech. 1966, 2, 526-533.
96.	Cotterell, B.	Int. Journ. Fracture. Mech. 1970, 6, 189-192.
97.	Kfouri, A.P.	Private Communication.